AD_____

Award Number: DAMD17-98-1-8223

TITLE: Developing Strategies to Block Beta-Catenin Action in Signaling and Cell Adhesion During Carcinogenesis

PRINCIPAL INVESTIGATOR: Mark Peifer, Ph.D.

CONTRACTING ORGANIZATION: University of North Carolina
Chapel Hill, North Carolina 27599-1350

REPORT DATE: July 2001

TYPE OF REPORT: Annual

PREPARED FOR: U.S. Army Medical Research and Materiel Command
Fort Detrick, Maryland 21702-5012

REPORT DOCUMENTATION PAGE

Form Approved
OMB No. 074-0188

1. AGENCY USE ONLY (Leave blank)	2. REPORT DATE	3. REPORT TYPE AND DATES COVERED
	July 2001	Annual (1 Jul 00 - 30 Jun 01)

4. TITLE AND SUBTITLE

Developing Strategies to Block Beta-Catenin Action in Signaling and Cell Adhesion During Carcinogenesis

5. FUNDING NUMBERS

DAMD17-98-1-8223

6. AUTHOR(S)

Mark Peifer, Ph.D.

7. PERFORMING ORGANIZATION NAME(S) AND ADDRESS(ES)

University of North Carolina
Chapel Hill, North Carolina 27599-1350
E-Mail: peifer@unc.edu

8. PERFORMING ORGANIZATION REPORT NUMBER

9. SPONSORING / MONITORING AGENCY NAME(S) AND ADDRESS(ES)

U.S. Army Medical Research and Materiel Command
Fort Detrick, Maryland 21702-5012

10. SPONSORING / MONITORING AGENCY REPORT NUMBER

11. SUPPLEMENTARY NOTES

Report contains color

12a. DISTRIBUTION / AVAILABILITY STATEMENT

Approved for Public Release; Distribution Unlimited

12b. DISTRIBUTION CODE

13. ABSTRACT ***(Maximum 200 Words)***

To understand cancer, we must first understand normal cell behavior. *Drosophila* Armadillo (Arm) and its human homolog ß-catenin are key players in adhesive junctions and in transduction of Wingless (Wg)/Wnt signals. Our working hypotheses are: 1) Several protein partners compete to bind Arm, and 2) Arm:dTCF activates Wg-responsive genes, while dTCF alone represses the same genes. Aim 1 is to understand how different partners compete with one another for binding Arm. Aim 2 focuses on how Arm and dTCF positively and negatively regulate Wg-responsive genes. In the past year we made significant progress. We used the two-hybrid system to further define the Arm binding site on DE-cadherin and extended our analysis of the effect of point mutations on binding. Our collaborators at the Weizmann Institute completed a parallel analysis in mammalian cells, assessing the ability of cadherin-derived peptides to compete ß-catenin from its endogenous partners. This work was published in Molecular Biology of the Cell. We have also introduced into transgenic flies mutant versions of DE-cadherin which should specifically block Arm or p120catenin binding.

14. SUBJECT TERMS	15. NUMBER OF PAGES
Breast Cancer	59
	16. PRICE CODE

17. SECURITY CLASSIFICATION OF REPORT	18. SECURITY CLASSIFICATION OF THIS PAGE	19. SECURITY CLASSIFICATION OF ABSTRACT	20. LIMITATION OF ABSTRACT
Unclassified	Unclassified	Unclassified	Unlimited

FOREWORD

Opinions, interpretations, conclusions and recommendations are those of the author and are not necessarily endorsed by the U.S. Army.

X Where copyrighted material is quoted, permission has been obtained to use such material.

N/A Where material from documents designated for limited distribution is quoted, permission has been obtained to use the material.

N/A Citations of commercial organizations and trade names in this report do not constitute an official Department of Army endorsement or approval of the products or services of these organizations.

N/A In conducting research using animals, the investigator(s) adhered to the "Guide for the Care and Use of Laboratory Animals," prepared by the Committee on Care and use of Laboratory Animals of the Institute of Laboratory Resources, national Research Council (NIH Publication No. 86-23, Revised 1985).

NP For the protection of human subjects, the investigator(s) adhered to policies of applicable Federal Law 45 CFR 46.

X In conducting research utilizing recombinant DNA technology, the investigator(s) adhered to current guidelines promulgated by the National Institutes of Health.

X In the conduct of research utilizing recombinant DNA, the investigator(s) adhered to the NIH Guidelines for Research Involving Recombinant DNA Molecules.

N/A In the conduct of research involving hazardous organisms, the investigator(s) adhered to the CDC-NIH Guide for Biosafety in Microbiological and Biomedical Laboratories.

Mark Ryder 6/16/01

PI - Signature Date

Table of Contents

(5) Introduction:

To understand abnormal cell behavior in cancer, we must first understand normal cell behavior. We focus on *Drosophila* Armadillo (Arm); Arm and its human homolog ß-catenin are critical for normal embryonic development (reviewed in Peifer, 1997). Both are key players in two separable biological processes: 1) They are components of cell-cell adhesive junctions, and 2) they act in transduction of Wingless/Wnt (Wg/Wnt) family cell-cell signals. Mutations in ß-catenin or its regulators are early steps in colon cancer and melanoma (reviewed in (Peifer and Polakis, 2000). We use the fruit fly as our model, combining classical and molecular genetics with cell biology and biochemistry. We take advantage of the speed and ease of the fly system and of its synergy with vertebrate cell biology. As one avenue to reveal Arm's roles in adherens junctions and transduction of Wg signal, we are identifying and examining the function of proteins with which Arm physically and/or functionally interacts. Our goal is to precisely define Arm/ß-catenin's dual roles, ultimately allowing the design of drugs inhibiting oncogenic ß-catenin. Our working hypotheses are: 1) Several protein partners compete to bind to the same site on Arm; the affinity of Arm for different partners is adjusted via phosphorylation of these partners, and 2) The Arm:dTCF complex activates Wg-responsive genes; dTCF represses the same genes in the absence of Arm. We will integrate approaches at all levels from combinatorial chemistry to studying gene function in intact animals, using fruit flies to carry out a functional genomics approach to understanding Arm function, and then transferring this knowledge directly to the mammalian system. Our first Aim is to understand how different partners interact with and compete with one another for binding Arm, and how phosphorylation regulates this. Our second Aim focuses on how the Arm and its partner dTCF positively and negatively regulate Wg responsive genes.

Specific Aim 1. Identify the sequence determinants mediating the binding of Armadillo/ß-catenin's protein partners to Armadillo/ß-catenin.

Specific Aim 2. Explore the mechanism of action of dTCF, a Wg/Wnt effector.

(6) Body:

This award is a combined IDEA Award and Career Development Award. The IDEA component ends this year, while the CDA continues for another year. In the three years of the IDEA Award, we made significant progress on both of our Specific Aims, which we have outlined below.

Aim 1.

Our statement of work stated:
Year 1
1. Minimize interacting regions of all three partners and begin mutagenesis.
2. Carry out two-hybrid screen for random peptides that interact with Arm.
3. Mutagenize & test in two-hybrid system potential phosphorylation sites.

Year 2
4. Complete mutational analysis of Arm targets in two hybrid system and test peptides in vivo.
5. Mutate potential phosphorylation sites in peptide models and test effects of GSK.

Year 3
6. Mutate regions required for Arm binding in the context of intact targets, reintroduce into flies and test for biological function.
7. Introduce peptides into cultured mammalian cells and test ability to bind ß-catenin and block its function.

NOTE: Much of the work described in this section was recently published in a paper from our lab in Molecular Biology of the Cell (Simcha et al., 2001)—below we refer to Figures in this paper, which is included in the Appendix.

We previously found that dAPC, DE-cadherin , and dTCF all can bind to a ~260 amino acid fragment comprising Arm's Arm repeats 3-8 (Pai et al., 1996; van de Wetering et al., 1997) McCartney et al., 1999). In the first two years of work under this grant, we minimized the region of the DE-cadherin cytoplasmic tail required for Arm binding, defined a 22 amino acid region that was sufficient, using the yeast two-hybrid system as an assay (task 1 in the statement of work; Fig. 1 of Simcha et al., (2001) in Appendix). We also defined two different 34 amino acid portions of dAPC2, containing a single 15 amino acid repeat or a single 20 amino acid repeat, as sufficient for binding Arm (McCartney et al., 1999). Because such small regions were sufficient, we have not

pursued screening for random peptides that bound Arm (task 2).

We further extended these observations by beginning to examine the sequence requirements for Arm binding, beginning our examination by focusing on the DE-cadherin target. We based these experiments on both the enrichment of acidic amino acids in all of the targets of Arm, and on a slight but intriguing sequence similarity between Arm's partners. In particular, the motif SLSSL is conserved in APC and cadherin. This is of special interest because vertebrate E-cadherin and APC are phosphorylated in this region, most likely on these serines. In APC, phosphorylation of these serines by GSK-3 enhances ß-catenin binding (Rubinfeld et al., 1996). In E-cadherin, serines in the region are phosphorylated by an unknown kinase; mutation of the serines to alanine blocks ß-catenin binding (Stappert and Kemler, 1994) . We thus made an extensive series of site-directed mutations of conserved residues (focusing in particular on acidic amino acids and on serines) within the minimal Arm binding region, including a small deletion and clustered point mutations (as outlined in tasks 1,3, and 4 of the statement of work; Fig. 5 of Simcha et al., (2001) in Appendix). These tests were initiated in year two and completed in the last year. To our surprise, many of these mutations do not block binding to Arm when tested in the context of the full length cadherin tail. This suggests that multiple points of contact may underlie binding and that changes in individual contact sites may not be sufficient to block the interaction. However, the more extensive changes do abolish binding, and some of the lesser changes reduce binding detectably, beginning to reveal key residues (Fig. 5 of Simcha et al., (2001) in Appendix).

To supplement this work using the yeast two-hybrid system, we are carrying out a collaboration with Avri Ben'Zeev of the Weizmann Institute in Israel. We provided a series of mutant cadherin constructs which they then tested in cultured mammalian cells, using a series of assays which they have developed for examining the ability of the E-cadherin cytoplasmic tail to block ß-catenin action (Sadot et al., 1998). They began this analysis in year two and have completed it in year 3. They have tested both our wild-type and mutant DE-cadherin constructs for their ability to bind to ß-catenin in mammalian cells, when expressed as GFP-fusion proteins (tasks 4,5, and 7). They examined the localization of these fusion proteins, their ability to block destruction of endogenous ß-catenin (by competing for ß-catenin binding with APC), their ability to block activation by the ß-catenin-TCF/LEF complex (by competing for ß-catenin binding with TCF/LEF), and their ability to block adherens junction formation (by competing for ß-catenin binding with-cadherin).

The results of these assays were quite revealing. First, we found that slightly longer portions of DE-cadherin are required in mammalian cells than are required in yeast, suggesting that competition with endogenous partners increases the stringency of the binding reaction Fig. 2-4 of Simcha et al., (2001) in Appendix). Second, we found that the effect of mutations was roughly parallel in yeast and in mammalian cells (with one exception), although all mutations tended to have a stronger effect in mammalian cells, likely due to competition with endogenous partners (Fig. 5-6 of Simcha et al., (2001) in Appendix). The exception was also quite revealing. While mutation of potential phosphorylation sites had little effect in yeast (Fig. 5 of Simcha et al., (2001) in Appendix), it resulted in striking reduction in binding in mammalian cells (Fig. 6 of Simcha et al., (2001) in Appendix), strongly supporting the idea that binding is normally regulated by phosphorylation (similar results were obtained by Lickert et al., (2000)). Finally, we found that different partners differ in their sensitivity to blockage by the cadherin peptide. The ß-catenin-TCF?LEF interaction is most sensitive to disruption, while the ß-catenin-E-cadherin interaction is least sensitive. The results of all of this work, both in yeast and in mammalian cells, were recently published in Molecular Biology of the Cell (Simcha et al., 2001), and the work from our lab in this paper was funded entirely by this IDEA Award. A copy is included in the Appendix, where the details of the methods used, the results, and their interpretation can be found.

While this manuscript was in preparation, a paper appeared that allowed us to carry our analysis to an even higher level. This paper reported the use of X-ray crystallography to solve the structure of a complex of *Xenopus* ß-catenin and Tcf3 (Graham et al., 2000). This thus revealed in atomic resolution how ß-catenin binds one of its partners. The authors also created a speculative model for how E-cadherin might bind ß-catenin. Using our mutagenesis data, we evaluated and extended this model, creating a detailed prediction of how E-cadherin might interact with its partner (Fig. 7 of Simcha et al., (2001) in Appendix). This model was subsequently tested by the recent publication of the structure of complex of ß-catenin and E-cadherin, also solved by X-ray crystallography (Huber and Weis, 2001). This will allow a further refinement of our understanding of how ß-catenin binds diverse partners. Together, the crystal structure, our studies, and other mutagenesis studies of ß-catenin's interaction with its partners (e.g., von Kries et al., 2000) will provide pharmaceutical companies with the insights they need to begin the rational design of inhibitors of interactions of ß-

catenin and its partners, which might have therapeutic value in cancer or other diseases.

With this information in hand, we have now turned our attention using what we learned about the interaction of Arm and DE-cadherin to blocking particular interactions of E-cadherin and its catenin partners, and examining the consequences of this in vivo. Cadherins directly interact with at least two different cytoplasmic partners, Arm and the distantly related protein p120catenin. In work funded by other sources, we have employed a similar strategy to that described above to define the p120 catenin-binding site of the DE-cadherin tail (Lu et al., 1999). We found that fly p120catenin binds to the juxta-membrane region, similar to its mammalian partners (Thoreson et al., 2000; Yap et al., 1998). We then mutagenized the DE-cadherin tail and found clustered point mutations that block p120catenin binding in yeast. We have now introduced mutations that block Arm binding, defined by our work described above, and mutations that block p120catenin binding, into the intact DE-cadherin gene (Task 6 of the Statement of Work). Three of the four mutants, along with a wild-type control, have been introduced into flies. We are now beginning to test the effects of over-expressing these constructs in a wild-type background and asking whether they can rescue animals mutant for DE-cadherin, in collaboration with Ulrich Tepass of the University of Toronto.

Aim 2. Armadillo:dTCF, a bipartite transcription factor

Year 1

1. Construct, introduce into flies and begin to test effects of *arm* mutants with C-termini replaced with known activation and repression domains.
2. Examine genetic interactions between *gro*, *wg* ,*arm* and *dTCF* mutations

Year 2

3. Complete analysis of *arm* -activation and repression domain fusions and initiate mutagenesis of Arm's C-terminus.
4. Examine physical interaction between Gro and dTCF in vitro and in vivo; Construct, introduce into flies and begin to test mutant forms of dTCF unable to bind Gro.

Year 3

5. Complete analysis of phenotypic consequences of mutations in Arm's C-terminus. Complete analyzing phenotype of mutant forms of dTCF unable to bind Gro.
6. Analyze the effects of mutant Arm constructs in cultured normal and transformed mammalian breast and colon epithelial cells.

In the three years of the IDEA Award, we made significant progress in our work on the role of Arm and dTCF in regulating Wg/Wnt responsive genes. As reported in the first annual report, in the first year, we explored in detail genetic and molecular interactions between *gro*, *wg* ,*arm* and *dTCF* (task 2 and 4 above)– this work was a collaboration with the labs of Amy Bejsovec at Northwestern and Hans Clevers at Utrecht. These data, together with a parallel analysis of the interaction between Groucho homologs and TCF/LEF proteins in mammalian cells, demonstrated that TCF proteins play a dual role in the regulation of Wg/Wnt target genes. In the absence of Wg/Wnt signaling, they act together with the co-repressor Groucho to repress Wg/Wnt responsive genes. The rise in Arm levels triggered by Wingless signaling converts this repressor into an activator, leading to the expression of Wg-target genes. This work was published in Nature (Cavallo et al., 1998); reprint included in first year).

In year two, we explored in more detail the role of Arm's C-terminus in Wg signaling (Tasks 1,3, and 5 of the Statement of Work). We found that C-terminally truncated mutant Armadillo has a deficit in Wg signaling activity, even when corrected for reduced protein levels. However, we also found that Armadillo proteins lacking all or part of the C-terminus retain some signaling ability if overexpressed, and that mutants lacking different portions of the C-terminal domain differ in their level of signaling ability. Finally, we found that the C-terminus plays a role in Armadillo protein stability in response to Wingless signal, and that the C-terminal domain can physically interact with the Arm repeat region. These data suggest that the C-terminal domain plays a complex role in Wingless signaling, and that Armadillo recruits the transcriptional machinery via multiple contact sites, which act in an additive fashion. These data were published in Genetics, with partial support from the IDEA Award (Cox et al., 1999); reprint included last year). While this work was underway, others examined the consequences of replacing the C-terminus of ß-catenin with the Engrailed repressor domain (Tasks 1 and 3 of Statement of Work), and showed that, as we had hypothesized, this repressed Wnt target genes (Montross et al., 2000). Two other groups delineated activation domains in ß-catenin and showed that a heterologous transactivator could mimic the properties of ß-catenin's C-terminus (Hsu et al., 1998; Vleminckx et al., 1999)

Career Development Award

The Career Development Award component of this grant pays a substantial portion of my salary (i.e., the PI, Mark Peifer). This has substantially reduced the amount of time I have to devote to teaching and service, and has thus allowed me to focus on research, both that funded by the Army and other research ongoing in my lab. I have thus acknowledged this support in additional publications produced during this period, which are listed in Section 8, and included reprints (where available) in the Appendix.

(7) Key research accomplishments for the entire 3 years.

a) A 22 amino acid piece of DE-cadherin is sufficient for Armadillo binding in the yeast two-hybrid system.
b) Clusters of 3-4 point mutations in conserved sequence motifs in DE-cadherin do not block Armadillo binding in the two hybrid system, while a subset of more extensive amino acid substitutions in this region do so.
c) The minimal cadherin peptides can compete for interaction with ß-catenin in vivo, displacing its endogenous partners.
d) The effect of mutations in the core binding region parallels that assessed in yeast, with one exception.
e) In general, the requirements for interaction with ß-catenin were more stringent in mammalian cells, where endogenous partners are present, than in yeast, where they are absent, suggesting that competition between partners likely regulates complex formation in vivo.
f) Mutation of known phosphorylation sites in De-cadherin dramatically reduces binding in mammalian cells, while it had little effect on binding in yeast, suggesting that phosphorylation regulates binding in vivo.
g) Our mutagenesis studies, combined with the crystal structure of the ß-catenin:TCF complex, allowed us to make a prediction of the structure of the ß-catenin:E-cadherin complex.
h) Binding to TCF/LEF is more easily competed than that to APC/Axin, and both are more easily competed than binding to E-cadherin.
i) Groucho binds dTCF
j) Groucho acts as a dTCF co-repressor in vivo, repressing Wingless-responsive genes and thus shaping pattern of the embryonic segment.
k) Armadillo's C-terminus plays multiple roles in Armadillo function.

(8) Reportable outcomes for the last year.

New publications in the last year supported in part by the IDEA grant:

Simcha, I., Kirkpatrick, C., Sadot, E., Shtutman, M. Polevoy, G., Geiger, B., Peifer, M., and Ben-Ze'ev, A. (2001). Cadherin Sequences that Inhibit ß-catenin Signaling: a Study in Yeast and Mammalian Cells. Molecular Biology of the Cell 12: 1177-88. (copy included in appendix).

New publications in the last year acknowledging partial salary support for Mark Peifer via the CDA:

Loureiro, J.J., Akong, K., Cayirlioglu, P., Baltus, A.E., DiAntonio, A., and Peifer, M. Activated Armadillo/ß-catenin does not play a general role in cell migration and process extension in *Drosophila*. Developmental Biology 235: 33-44 (reprint not yet available).

Tepass, U., Truong, K., Godt, D., Ikura, M., Peifer, M. (2000). Cadherins in embryonic and neural morphogenesis.. Nature Reviews: Molecular Cell Biology1: 91-100 (reprint included in the Appendix).

McCartney, B.M., McEwen, D.G., Grevengoed,, E., Maddox, P., Bejsovec, A., Peifer, M. (2001)*Drosophila* APC2 and Armadillo participate in tethering mitotic spindles to cortical actin. Nature Cell Biology, in press (reprint not yet available).

Publications from the previous year acknowledging partial salary support for Mark Peifer via the CDA for which reprints are now included:

McEwen, D.G., Cox, R.T., and Peifer, M. (2000). The canonical Wg and JNK signaling cascades collaborate to promote both dorsal closure and ventral patterning. Development 127, 3607-3617. (reprint included in appendix).

Cox, R.T., McEwen, D.G., Myster, D.G., Duronio, R.J., Loureiro, J., and Peifer, M. (2000). A screen for mutations that suppress the phenotype of *Drosophila armadillo*, the ß-catenin homolog. Genetics 155, 1725-1740. (reprint included in appendix).

Degrees supported by this grant

1. Ph.D. awarded to Dr. Robert Cavallo, December 1999, entitled "New partners for Armadillo in signal transduction and cell adhesion". A portion of the work in this thesis was supported by the IDEA Award.
2. M.S. awarded to Mr. Gordon Polevoy, April 2001, entitled "Mechanisms of Armadillo's roles in signaling and adhesion." Virtually all of the work in this thesis was supported by the IDEA Award.

Presentations by Mark Peifer discussing this work.

"Cell adhesion, signal transduction and cancer: the Armadillo Connection.", "Signaling by Adhesion Receptors" Gordon Conference, Newport RI July, 2000.

"Cell adhesion, signal transduction and cancer: the Armadillo Connection", The 17th Whitehead Symposium, "Molecular Machines" Whitehead Institute and MIT, Boston MA, October 2000

"Cell adhesion, signal transduction and cancer: the Armadillo Connection", The British Societies for Cell and Developmental Biology—Joint Spring meeting, "Cell and Tissue Morphogenesis" Brighton, UNITED KINGDOM, April 2001

"Cell adhesion, signal transduction and cancer: the Armadillo Connection", The 25th Annual Lineberger Comprehensive Cancer Center Symposium, "Regulatory Mechanisms in Human Cancer" Chapel Hill NC, April 2001

"Cell adhesion, signal transduction, and cancer: the Armadillo Connection". Laboratory of Molecular Carcinogenesis, NIEHS/NIH, RTP NC October, 2000

"Cell adhesion, signal transduction, and cancer: the Armadillo Connection". Memorial Sloan-Kettering Cancer Center, New York NY December, 2000

"Cell adhesion, signal transduction, and cancer: the Armadillo Connection". Department of Molecular Biology, Princeton University, Princeton NJ February 2001

"Cell adhesion, signal transduction, and cancer: the Armadillo Connection". Division of Biology, University of California at San Diego, La Jolla, CA, May 2001

(9) Conclusions.

We made significant progress on each of the specific aims. In carrying out Aim 1, we examined in detail the binding of DE-cadherin to Arm/ß-catenin, identifying a very small region that is sufficient for binding in the yeast two-hybrid system and identifying within that region the key amino acids required for binding. We completed an analysis of binding of wild-type and mutant peptides in mammalian cells, in collaboration with our colleagues at the Weizmann Institute. This work was published in Molecular Biology of the Cell. These data should provide a basis for understanding the interaction between the protein product of the oncogene ß-catenin and its mammalian partners in both normal development and physiology, and during oncogenesis.

In carrying out Aim 2, we found that dTCF plays a dual role in Wingless/Wnt signaling. We had previously shown that it acts together with Arm to activate Wingless target genes. In work funded in part by this grant, we found that in the absence of Arm, dTCF forms a complex with the co-repressor Groucho, and together they repress Wingless target genes. This work was published in Nature. We also examined the role of the C-terminus of Arm, which we had hypothesized acted as a transcriptional activation domain. We found that it plays a more complex role in Arm function. The C-terminus can be divided into two regions, which contribute in an additive way to Arm's role as an activator of Wingless signaling. It also appears to regulate the stability of Arm. This work was published in Genetics. Subsequent work by others has confirmed the relevance of our results for mammalian ß-catenin. Understanding the mechanism by which Wnt target genes are repressed will provide insight into the normal and abnormal regulation of the genes responsible for oncogenesis in tumors resulting from activation of the Wnt pathway.

(10) References.

Cavallo, R. A., Cox, R. T., Moline, M. M., Roose, J., Polevoy, G. A., Clevers, H., Peifer, M. and Bejsovec, A. (1998). *Drosophila* TCF and Groucho interact to repress Wingless signaling activity. *Nature* 395, 604-608.

Cox, R. T., Pai, L.-M., Kirkpatrick, C., Stein, J. and Peifer, M. (1999). Roles of the C-terminus of Armadillo in Wingless signaling in *Drosophila. Genetics* 153, 319-332.
Graham, T. A., Weaver, C., Mao, F., Kimelman, D. and Xu, W. (2000). Crystal Structure of a beta-Catenin/Tcf Complex. *Cell* 103, 885-896.
Hsu, S. C., Galceran, J. and Grosschedl, R. (1998). Modulation of transcriptional regulation by LEF-1 in response to Wnt-1 signaling and association with ß-catenin. *Mol. Cell. Biol.* 18, 4807-4818.
Huber, A. H. and Weis, W. I. (2001). The structure of the beta-catenin/E-cadherin complex and the molecular basis of diverse ligand recognition by beta-catenin. *Cell* 105, 391-402.
Lickert, H., Bauer, A., Kemler, R. and Stappert, J. (2000). Casein kinase II phosphorylation of E-cadherin increases E-cadherin/ß-catenin interaction and strengthens cell adhesion. *J. Biol. Chem.* 275, 5090-5095.
Lu, Q., Paredes, M., Medina, M., Zhou, J., Cavallo, R., Peifer, M., Orecchio, L. and Kosik, K. (1999). δ-catenin, an adhesive junction associated protein which promotes cell scattering. *J. Cell Biol.* 144, 519-532.
McCartney, B. M., Dierick, H. A., Kirkpatrick, C., Moline, M. M., Baas, A., Peifer, M. and Bejsovec, A. (1999). *Drosophila* APC2 is a cytoskeletally-associated protein
that regulates Wingless signaling in the embryonic epidermis. *J. Cell Biol.* 146, 1303-1318.
Montross, W. T., Ji, H. and McCrea, P. D. (2000). A ß-catenin/engrailed chimera selectively suppresses Wnt signaling. *J. Cell Sci.* 113, 1759-1770.
Pai, L.-M., Kirkpatrick, C., Blanton, J., Oda, H., Takeichi, M. and Peifer, M. (1996). *Drosophila* α-catenin and E-cadherin bind to distinct regions of *Drosophila* Armadillo. *J. Biol. Chem.* 271, 32411-32420.
Peifer, M. (1997). ß-catenin as oncogene: the smoking gun. *Science* 275, 1752-1753.
Peifer, M. and Polakis, P. (2000). Wnt signaling in oncogenesis and embryogenesis-- A look outside the nucleus. *Science* 287, 1606-1609.
Rubinfeld, B., Albert, I., Porfiri, E., Fiol, C., Munemitsu, S. and Polakis, P. (1996). Binding of GSK-ß to the APC/ß-catenin complex and regulation of complex assembly. *Science* 272, 1023-1026.
Sadot, E., Simcha, I., Iwai, K., Ciechanover, A., Geiger, B. and Ben-Ze'ev, A. (2000). Differential interaction of plakoglobin and beta-catenin with the ubiquitin-proteasome system. *Oncogene* 19, 1992-2001.
Sadot, E., Simcha, I., Shtutman, M., Ben-Ze'ev, A. and Geiger, B. (1998). Inhibition of beta-catenin-mediated transactivation by cadherin derivatives. *Proc. Nat. Acad. Sci. USA* 95, 15339-44.
Simcha, I., Kirkpatrick, C., Sadot, E., Shtutman, M., Polevoy, G., Geiger, B., Peifer, M. and Ben-Ze'ev, A. (2001). Cadherin Sequences That Inhibit beta-Catenin Signaling: A Study in Yeast and Mammalian Cells. *Mol. Biol. Cell* 12, 1177-88.
Stappert, J. and Kemler, R. (1994). A short core region of E-cadherin is essential for catenin binding and is highly phosphorylated. *Cell Adhesion Commun.* 2, 319-327.
Thoreson, M. A., Anastasiadis, P. Z., Daniel, J. M., Ireton, R. C., Wheelock, M. J., Johnson, K. R., Hummingbird, D. K. and Reynolds, A. B. (2000). Selective uncoupling of p120(ctn) from E-cadherin disrupts strong adhesion. *J. Cell Biol.* 148, 189-202.
van de Wetering, M., Cavallo, R., Dooijes, D., van Beest, M., van Es, J., Loureiro, J., Ypma, A., Hursh, D., Jones, T., Bejsovec, A. et al. (1997). Armadillo co-activates transcription driven by the product of the *Drosophila* segment polarity gene *dTCF. Cell* 88, 789-799.
Vleminckx, K., Kemler, R. and Hecht, A. (1999). The C-terminal transactivation domain of ß-catenin is necessary and sufficient for signaling by the LEF-1/ßcatenin complex in *Xenopus laevis. Mech. Dev.* 81, 65-74.
von Kries, J. P., Winbeck, G., Asbrand, C., Schwarz-Romond, T., Sochnikova, N., Dell'Oro, A., Behrens, J. and Birchmeier, W. (2000). Hot spots in beta-catenin for interactions with LEF-1, conductin and APC. *Nat. Struct. Biol.* 7, 800-7.
Yap, A. S., Niessen, C. M. and Gumbiner, B. M. (1998). The juxtamembrane region of the cadherin cytoplasmic tail supports lateral clustering, adhesive strengthening, and interaction with p120ctn. *J. Cell Biol.* 141, 779-789.

Appendix —Reprints of publications supported in part by this grant

Publications supported in part by the IDEA grant:

Simcha, I., Kirkpatrick, C., Sadot, E., Shtutman, M. Polevoy, G., Geiger, B., Peifer, M., and Ben-Ze'ev, A. (2001). Cadherin Sequences that Inhibit ß-catenin Signaling: a Study in Yeast and Mammalian Cells. Molecular Biology of the Cell 12: 1177-88 (reprint included in the Appendix).

Publications acknowledging partial salary support for Mark Peifer via the CDA:

Tepass, U., Truong, K., Godt, D., Ikura, M., Peifer, M. (2000). Cadherins in embryonic and neural morphogenesis.. Nature Reviews: Molecular Cell Biology1: 91-100 (reprint included in the Appendix).

Publications from the previous year acknowledging partial salary support for Mark Peifer via the CDA for which reprints are now included:

McEwen, D.G., Cox, R.T., and Peifer, M. (2000). The canonical Wg and JNK signaling cascades collaborate to promote both dorsal closure and ventral patterning. Development 127, 3607-3617. (reprint included in appendix).

Cox, R.T., McEwen, D.G., Myster, D.G., Duronio, R.J., Loureiro, J., and Peifer, M. (2000). A screen for mutations that suppress the phenotype of *Drosophila armadillo*, the ß-catenin homolog. Genetics 155, 1725-1740. (reprint included in appendix).

Molecular Biology of the Cell
Vol. 12, 1177–1188, April 2001

Cadherin Sequences That Inhibit β-Catenin Signaling: A Study in Yeast and Mammalian Cells

Inbal Simcha,*† Catherine Kirkpatrick,† Einat Sadot,* Michael Shtutman,* Gordon Polevoy,‖ Benjamin Geiger,* Mark Peifer,‡‖¶# and Avri Ben-Ze'ev*#

*Department of Molecular Cell Biology, Weizmann Institute of Science, Rehovot, Israel, 76100; ‡Department of Biology, ‖Curriculum in Genetics and Molecular Biology, and ¶Lineberger Comprehensive Cancer Center, University of North Carolina, Chapel Hill, North Carolina 27599-3280; and §Department of Genetics, Cell Biology and Development, University of Minnesota, Minneapolis, Minnesota 55455

Submitted November 6, 2000; Revised January 19, 2001; Accepted January 30, 2001
Monitoring Editor: Joan S. Brugge

Drosophila Armadillo and its mammalian homologue β-catenin are scaffolding proteins involved in the assembly of multiprotein complexes with diverse biological roles. They mediate adherens junction assembly, thus determining tissue architecture, and also transduce Wnt/Wingless intercellular signals, which regulate embryonic cell fates and, if inappropriately activated, contribute to tumorigenesis. To learn more about Armadillo/β-catenin's scaffolding function, we examined in detail its interaction with one of its protein targets, cadherin. We utilized two assay systems: the yeast two-hybrid system to study cadherin binding in the absence of Armadillo/β-catenin's other protein partners, and mammalian cells where interactions were assessed in their presence. We found that segments of the cadherin cytoplasmic tail as small as 23 amino acids bind Armadillo or β-catenin in yeast, whereas a slightly longer region is required for binding in mammalian cells. We used mutagenesis to identify critical amino acids required for cadherin interaction with Armadillo/β-catenin. Expression of such short cadherin sequences in mammalian cells did not affect adherens junctions but effectively inhibited β-catenin–mediated signaling. This suggests that the interaction between β-catenin and T cell factor family transcription factors is a sensitive target for disruption, making the use of analogues of these cadherin derivatives a potentially useful means to suppress tumor progression.

INTRODUCTION

Vertebrate β-catenin and its *Drosophila* homologue Armadillo (Arm) play critical roles in both cell adhesion and signal transduction (reviewed by Gumbiner, 1996; Willert and Nusse, 1998). These proteins are key effectors of Wingless (Wg)/Wnt signal transduction, interacting with DNA-binding proteins of the TCF/LEF family to form bipartite transcription factors that activate Wnt responsive genes (reviewed by Wodarz and Nusse, 1998). β-Catenin and Arm are also core components of the cadherin-catenin complex, which mediates cell-cell adhesion at adherens junctions and connects these junctions to the actin cytoskeleton (reviewed by Ben-Ze'ev and Geiger, 1998; Provost and Rimm, 1999). These quite distinct biological functions of β-catenin/Arm most probably rest on a similar biochemical role: β-catenin/Arm mediates assembly of multiprotein complexes. Thus, in adherens junctions, it simultaneously binds cadherins and α-catenin, whereas in the nucleus it links TCF/LEF proteins to the basal transcriptional machinery (reviewed by Zhurinsky *et al.*, 2000a).

In addition to these roles in normal development and physiology, β-catenin is also a critical target in the development of a variety of human tumors (reviewed by Peifer and Polakis, 2000). In normal cells, β-catenin/Arm's role in signal transduction is kept off by targeting the protein for rapid proteolytic destruction. β-Catenin/Arm is targeted for destruction by a multiprotein complex, which includes two scaffolding proteins, APC and axin/conductin, and a kinase, GSK3β. Assembly of this complex leads to phosphorylation of β-catenin/Arm, and its subsequent ubiquitination and destruction. If this complex is disrupted by mutations in either APC (reviewed by Peifer and Polakis, 2000) or axin/conductin (Liu *et al.*, 2000; Satoh *et al.*, 2000) the Wnt pathway is activated. This can lead to cell proliferation and tumor initiation. Finally, β-catenin binds to a diverse set of other proteins, including the presenilins, the epidermal growth factor (EGF) receptor, the actin-binding protein fas-

† These authors contributed equally to this work.
# Corresponding authors. E-mail addresses: avri.ben-zeev@weizmann.ac.il (A.B.-Z.); peifer@unc.edu (M.P.).

cin, and the transcription factor Teashirt (reviewed by Zhurinsky *et al.*, 2000a). In most of these cases, the function of the interaction remains a mystery.

To understand the roles β-catenin/Arm plays in embryonic development and oncogenesis, we must understand in detail how it functions as a scaffold. Furthermore, if we understood in molecular detail how β-catenin/Arm binds to individual partners, we might be able to use this information to design inhibitors that could interfere with β-catenin's interaction with individual partners. For example, a specific inhibitor of the β-catenin/TCF interaction might hold promise as a therapeutic agent in colorectal and other types of cancer. β-Catenin/Arm protein is composed of a series of protein-protein interaction motifs that allow it to function as a scaffold. The N-terminal domain contains the binding site for α-catenin, as well as phosphorylation sites recognized by GSK3β, whereas the C terminus contains the transcriptional activation domain and the binding site for Teashirt (reviewed by Zhurinsky *et al.*, 2000a). The central two thirds of β-catenin/Arm is composed of twelve 42-amino acid Arm repeats. Many partners bind to this region, including TCF/LEF, cadherins, APC, and axin. Because these latter partners play key roles in cell adhesion, Wnt signaling, or the destruction complex, their interactions with β-catenin/Arm have been studied in some detail. These studies examined which regions of β-catenin/Arm are sufficient for binding to the partner and also which region of the partners are sufficient for binding to β-catenin/Arm. In each case, the minimum region of the partner that is sufficient for interaction with β-catenin/Arm is relatively small. The minimal fragments thus far tested range from 70 amino acids for mammalian E- or N-cadherin (Sadot *et al.*, 1998), 41 amino acids for *Drosophila* E-cadherin (DE-cadherin; Pai *et al.*, 1996), 31 amino acids for *Drosophila* APC2 (McCartney *et al.*, 1999), 17 amino acids for mammalian LEF-1 (von Kries *et al.*, 2000), and 25 amino acids for human axin (Nakamura *et al.*, 1998).

When the interacting regions of cadherins, TCF/LEF, and APC are aligned, there is only modest sequence similarity, although all are rich in acidic amino acids and serines. Phosphorylation of these serines, as is thought to happen in APC (Rubinfeld *et al.*, 1996), axin (Jho *et al.*, 1999) and cadherin (Stappert and Kemler, 1994; Lickert *et al.*, 2000), would increase the net negative charge further. This charge distribution is intriguing in light of the structure of β-catenin (Huber *et al.*, 1997). The Arm repeats form a superhelix, with a large groove on the surface lined by basic amino acids. In another Arm repeat protein, the nuclear localization signal receptor, the nuclear localization signal peptide binds in an extended conformation in the groove (Conti *et al.*, 1998).

Previous mutational studies of β-catenin/Arm partners have begun to define the sequence requirements for binding. Mutation of three conserved serines in one of the 20-amino acid β-catenin-binding sites of human APC reduced the ability of the mutated fragment to down-regulate β-catenin levels, suggesting reduced binding to β-catenin (Rubinfeld *et al.*, 1997). Clustered point mutations in LEF-1 (Hsu *et al.*, 1998; von Kries *et al.*, 2000) and TCF4 (Omer *et al.*, 1999) identified critical amino acids that are either required for binding or contribute to it. Mutational analysis of the β-catenin-binding site in E-cadherin focused on a series of serine residues that are phosphorylated in vivo (Stappert and Kemler, 1994; Lickert *et al.*, 2000). Mutation of individual serines had a modest effect on binding, whereas mutation of all eight conserved serines abolished binding in vivo.

These data suggest a testable model for the interaction between β-catenin/Arm and its partners, in which charge-based and other interactions mediate the binding between the Arm repeats of β-catenin/Arm and short regions of its partner proteins, potentially binding as extended peptides in the basic Arm repeat groove. Here, we test this model for the interaction between β-catenin/Arm and its partners, by carrying out a detailed analysis of the sequence requirements for interaction between cadherins and β-catenin/Arm.

MATERIALS AND METHODS

Cadherin Constructs and Yeast Two-Hybrid Experiments

The Arm R1–12 construct in pCK2 was described by Pai *et al.* (1996; it was previously called Arm R1–13, but the subsequent crystal structure of β-catenin led to reassessment of repeat number and boundaries). Similar constructs containing Arm repeats 2–10 (ArmR2–10: amino acids 177–596) and the corresponding fragments of mouse β-catenin (R1–12: amino acids 119–708; R2–10: amino acids 169–583) were generated for this work. DE-cadherin fragments were generated by polymerase chain reaction (PCR) with flanking *Bam*HI and *Eco*RI restriction sites and cloned into pCK4 (Pai *et al.*, 1996). The amino acids included in each fragment are diagrammed in Figure 1, A and B. All constructs included a stop codon after the final amino acid of DE-cadherin. All clones were sequenced in their entirety to confirm their sequence. The DE-cadherin mutants (DEC) were generated by a two-step PCR procedure. Primers for each strand containing the desired mutant sequence were used in two separate PCR reactions with flanking primers to amplify the N- and C-terminal portions of the DE-cadherin cytoplasmic domain. Products from these two reactions were mixed and used as a template for another PCR reaction containing only the flanking primers. This reaction generated a full-length DE-cadherin cytoplasmic domain with flanking *Bam*HI and *Eco*RI sites containing the desired mutations, which was cloned into pCK4. Mutation DECM2 was introduced into the smaller DEC30 fragment by amplifying the relevant portion of the longer mutant clone with DEC30 primers. All mutations were confirmed by sequencing and are diagrammed in Figure 6A. Two-hybrid assays were performed as described by Pai *et al.* (1996). Arm or β-catenin fragments were fused to the LexA DNA-binding domain in pCK2, and DE-cadherin fragments were fused to the Gal4 activation domain in pCK4. The two plasmids were transformed simultaneously into the yeast strain L40. β-Galactosidase values are the averages from duplicate assays performed on at least three independent transformants.

Cell Lines and Transfections

Chinese hamster ovary (CHO), 293T and MDCK cells were maintained in DMEM with 10% calf serum. Transient transfections with *Drosophila* E-cadherin (DEC) constructs were carried out using the calcium phosphate precipitation method with 293T cells and by Lipofectamine (GIBCO, Grand Island, NY) with CHO cells. For recloning the various mutant DEC sequences from the pCK4 plasmid into the pEGFP-C1 plasmid (Clontech, Palo Alto, CA), the DEC inserts were amplified by PCR using primers designed to contain pCK4 plasmid sequences (in the HA-tag domain) that were linked to the multicloning site, ACCTAGATCTTACCCATACGATGTTCCAG, and the terminator sequence, CGATGCAC AGTTGAAGTGAACTTGC, downstream of the multicloning site of pCK4. The amplified sequences were excised by *Bgl*II and *Eco*RI digestion and inserted into pEGFP-C1 at the same *Bgl*II/*Eco*RI sites. The green fluorescence protein (GFP) tag was localized at the N terminus of

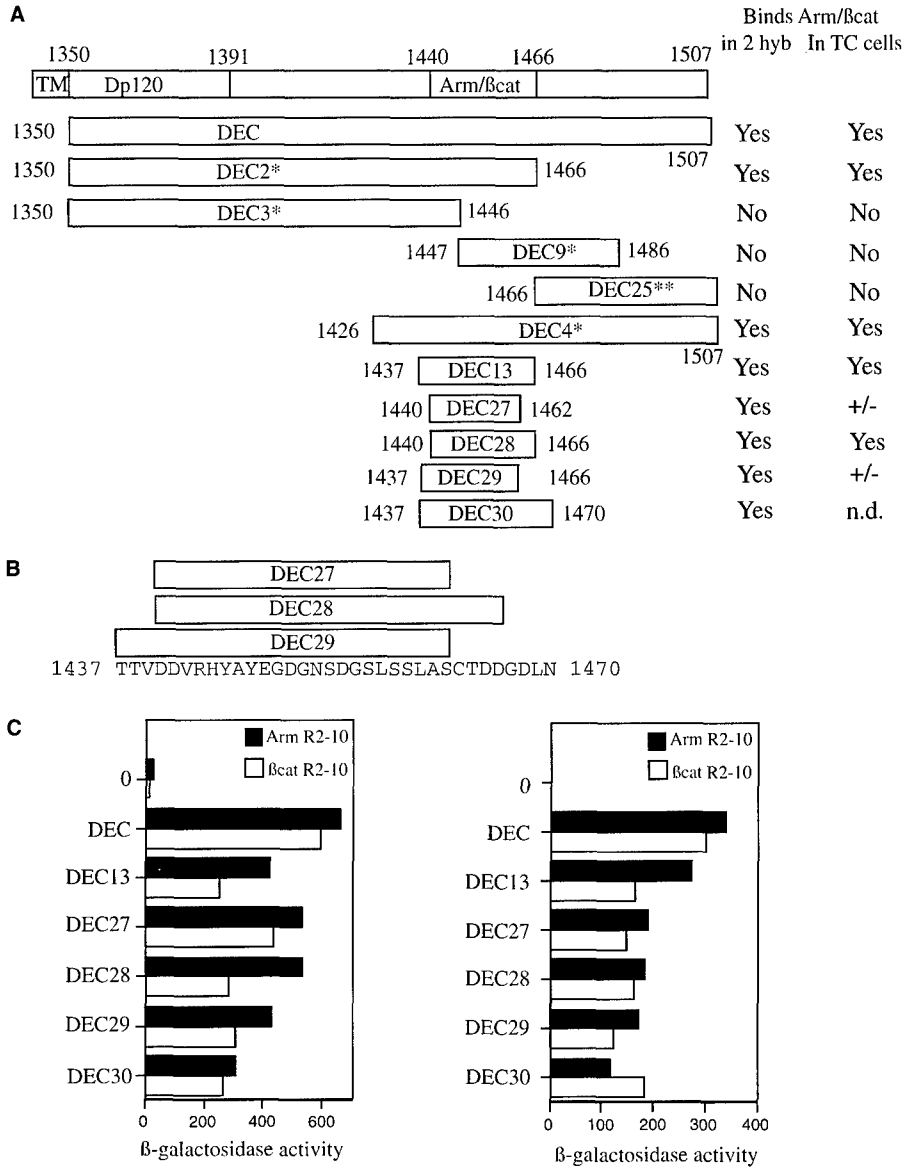

Figure 1. Mapping the minimal binding site on DEC cytoplasmic tail for β-catenin (βcat) and Arm using the yeast two-hybrid (2 hyb) system. (A) Schematic representation of the DEC derivatives used in our analyses, with ability to bind Arm/β-catenin in either yeast or mammalian cells summarized in the right-hand columns. TM, transmembrane; TC, tissue culture. *Data from Pai *et al.* (1996). (B) Sequence of the minimal binding region of DE-cadherin, with the boundaries of the smallest DEC derivatives indicated. (C) All of the DEC derivatives bind to both fragments of Arm and β-catenin in yeast. The full-length DE-cadherin cytoplasmic domain (DEC), or smaller derivatives of DEC (diagrammed in A and B), fused to the Gal4 transcriptional activation domain, were transformed into yeast cells along with portions of Arm or β-catenin fused to the LexA DNA-binding domain. Average β-galactosidase values are shown for each DEC derivative together with the full Arm repeat region of Arm or β-catenin (Arm R1–12 or βcat R1–12, left), or a smaller fragment of the Arm repeat region (Arm R2–10 or βcat R2–10, right). 0, background level of β-galactosidase activity with no DEC fragment fused to Gal4. **DEC 25 was tested against only Arm R1–12. Its β-galactosidase value was 14.4 U, compared with 18.3 U for the negative control.

these DEC constructs. For LEF/TCF-dependent transactivation analysis, cells were transfected with the pCGN-HA expression vector containing the S33Y β-catenin mutant (Shtutman *et al.*, 1999) and the TOPFLASH and FOPFLASH luciferase reporter vectors (van de Wetering *et al.*, 1997), as previously described (Zhurinsky *et al.*, 2000b). A β-galactosidase–expressing vector was cotransfected as an internal control for transfection efficiency. After 24 h, the cells were lysed, and both luciferase and β-galactosidase activities were determined by enzyme assay kits (Promega, Madison, WI). For Western blots and immunoprecipitations, cells were harvested 24 h after transfection and lysed in either Laemmli's sample buffer or immunoprecipitation buffer (see below), respectively.

Immunoblotting and Immunoprecipitation

Equal amounts of total protein from the different transfected cells were separated by SDS-PAGE and subjected to Western blotting using the following antibodies: monoclonal anti-HA (clone 12CA5; Boehringer Mannheim, Indianapolis, IN), polyclonal anti-HA (a gift from M. Oren, Weizmann Institute of Science, Rehovot, Israel), polyclonal anti-β-catenin (Sigma, St. Louis, MO), and monoclonal anti-GFP antibody (Roche Molecular Biochemicals, Burlington, NC). For coimmunoprecipitation, cells transfected with the GFP-DEC constructs and the S33Y β-catenin were lysed in immunoprecipitation buffer containing 20 mM Tris-HCl, pH 8.0, 1% Triton X-100, 140 mM NaCl, 10% glycerol, 1 mM EGTA, 1.5 mM $MgCl_2$, 1 mM dithiothreitol, 1 mM sodium orthovanadate, and 50 μg/ml phenylmethylsulfonyl fluoride. Equal amounts of protein were incubated with 2 μl of polyclonal anti-β-catenin antibody and 20 μl of protein A/G-agarose beads (Santa Cruz Biotechnology, Santa Cruz, CA) for 4 h at 4°C. The beads were washed five times with 20 mM Tris-HCl buffer, pH 8.0, containing 150 mM NaCl and 0.5% Nonidet P-40, and the immune complexes were recovered by boiling in Laemmli's sample buffer and resolved by SDS-PAGE. To detect the coprecipitated GFP-DEC constructs, the blots were incubated with anti-GFP antibody. Blots were developed using the ECL method (Amersham,

Arlington Heights, IL). Autoradiograms were scanned with a GS-700 imaging densitometer (Bio-Rad, Hercules, CA) and quantitated using the FotoLook PS 2.07.2 software. The intensity of the bands was quantitated using the National Institutes of Health image 1.61 software.

Immunofluorescence Microscopy

Cells were cultured on glass coverslips, fixed with 3% paraformaldehyde in phosphate-buffered saline, and permeabilized with 0.5% Triton X-100. Monoclonal or polyclonal antibodies to β-catenin were used to label the endogenous β-catenin. The secondary antibodies were Cy3 goat anti-mouse or anti-rabbit immunoglobulin G (Jackson ImmunoResearch Laboratories, West Grove, PA). The transfected GFP-DEC constructs were detected in the fluorescein isothiocyanate channel. The samples were visualized using an Axiovert S100 microscope (Zeiss, Germany).

RESULTS

Mapping the Minimal Arm/β-Catenin–interacting Region of DE-Cadherin

The binding site for Arm on the DE-cadherin cytoplasmic tail was previously mapped to the C-terminal portion of the cadherin tail (Pai *et al.*, 1996). To determine the minimum region essential for binding, we first used the yeast two-hybrid system to assess binding between the Arm repeat region of both Arm and β-catenin and smaller fragments of the DE-cadherin tail (Figure 1). A series of fragments, ranging in size from 23–34 amino acids, were tested, and all bound both Arm and β-catenin as assessed by the two-hybrid system (Figure 1C).

We then examined whether these minimal binding fragments, when fused to GFP at their N termini, retained the ability to interact with β-catenin in mammalian cells. To do so, we made use of several assays. First, we assessed the ability of the GFP–DE-cadherin tail and its fragments to coimmunoprecipitation with β-catenin (Figure 2A). Second, we tested the ability of these fragments to block the interaction of β-catenin with endogenous LEF/TCF, as measured by their ability to block LEF/TCF-mediated transactivation (Figure 2B). Finally, we assessed the capacity of these fragments to block the interaction of β-catenin with endogenous APC or axin, thus stabilizing β-catenin by blocking its targeting to the proteasome (Figure 2C). These assays generally paralleled the results in the yeast two-hybrid system (Figure 1C). One difference was noted however: whereas DEC28, which is 27 amino acids in length, binds by all three assays to β-catenin (Figures 1), DEC27 and DEC29, the smallest constructs that bound Arm and β-catenin in yeast (Figure 1, A and C), failed to detectably coimmunoprecipitate with β-catenin (Figure 2A) and also failed to block LEF/TCF-mediated gene expression (Figure 2B). DEC27 and DEC29, which are 4 amino acids shorter than DEC28 at their C termini (DEC29 also has three extra N-terminal amino acids), exhibited a reduced ability to stabilize β-catenin, although they retained some activity in this assay (Figure 2C).

A subset of these DEC fragments was also tested for the effect on endogenous β-catenin localization and levels by immunofluorescence (Figure 3). Transfection of the control GFP expression vector into MDCK cells gave a diffuse distribution of GFP in the cytoplasm and the nucleus, without affecting the organization of the endogenous β-catenin in the transfected cells. In contrast, expression of the GFP-tagged DEC tail in these cells (DEC, Figure 3A) resulted in partial disruption of adherens junctions and the accumulation of β-catenin in the cytoplasm and the nuclei (Figure 3B). Expression of the shorter (30 amino acid) cadherin tail fragment DEC13 in MDCK cells (Figure 3C) resulted in the accumulation and diffuse distribution of β-catenin (Figure 3D) but without a detectable effect on its organization in adherens junctions. In contrast, DEC9, which was unable to bind β-catenin in the assays described above (Figures 1 and 2), had no effect on the accumulation or organization of endogenous β-catenin in MDCK cells (Figure 3, E and F). It is noteworthy that DEC13 was positive in Arm/β-catenin binding in the two-hybrid screen (Figure 1, A and B) and by coimmunoprecipitation in mammalian cells (Figure 2A) and effectively protected β-catenin from degradation in 293 cells (Figure 2C). In CHO cells that express only very low levels of N-cadherin (and thus do not form adherens junctions), transfection of DEC (Figure 4A) or DEC13 (Figure 4C) brought about the accumulation of β-catenin in the nuclei of these cells (Figure 4, B and D), whereas DEC9 expression (Figure 4E), as expected, had no effect on the endogenous β-catenin (Figure 4F). The transfection into MDCK cells of DEC27 and DEC29 (Figure 3I), which did not bind to β-catenin in the assays described above (Figures 1 and 2), also had no effect on the subcellular distribution of β-catenin or the organization of adherens junctions (Figure 3J). In contrast, DEC28 (which bound to β-catenin in the two-hybrid assay and coimmunoprecipitation, Figures 1 and 2), when transfected into MDCK cells (Figure 3G), induced the accumulation of the endogenous β-catenin in the cytoplasm and nuclei of these cells (Figure 3H).

Defining Amino Acids Critical for the Arm/β-Catenin–DE-Cadherin Interaction

We next set out to determine which amino acids within the minimal DE-cadherin–binding region were essential for the interaction with Arm and β-catenin. Mammalian β-catenin can bind DE-cadherin both in *Drosophila* (White *et al.*, 1998; Cox *et al.*, 1999) and in cultured mammalian cells (see below), and Arm can also bind mammalian E-cadherin (A. Wodarz and R. Nusse, personal communication). We therefore used the comparison of vertebrate and *Drosophila* cadherins to determine candidate residues that might contribute to binding. Based on comparisons of the Arm-binding regions of cadherin, APC, and TCF family members, we focused on acidic and serine/threonine residues, although we also mutated other conserved amino acids. Although we focused on residues within the minimal binding region, we introduced our mutations in the context of the full-length DE-cadherin tail, thus mimicking the situation in vivo.

We began with three clustered point mutations that each change three or four nearby residues in different regions of the minimal binding site to alanine (Figure 5A). DECM1 altered four conserved serine residues in the center of the minimal binding region, DECM2 altered four conserved amino acids including one acidic residue in the N-terminal part of the minimal binding region, and DECM3 altered three conserved acidic residues (aspartates) in the C-terminal part of the minimal binding region (Figure 5A). Surprisingly, none of these mutations significantly affected binding to the full-length Arm repeat region of either Arm or β-cate-

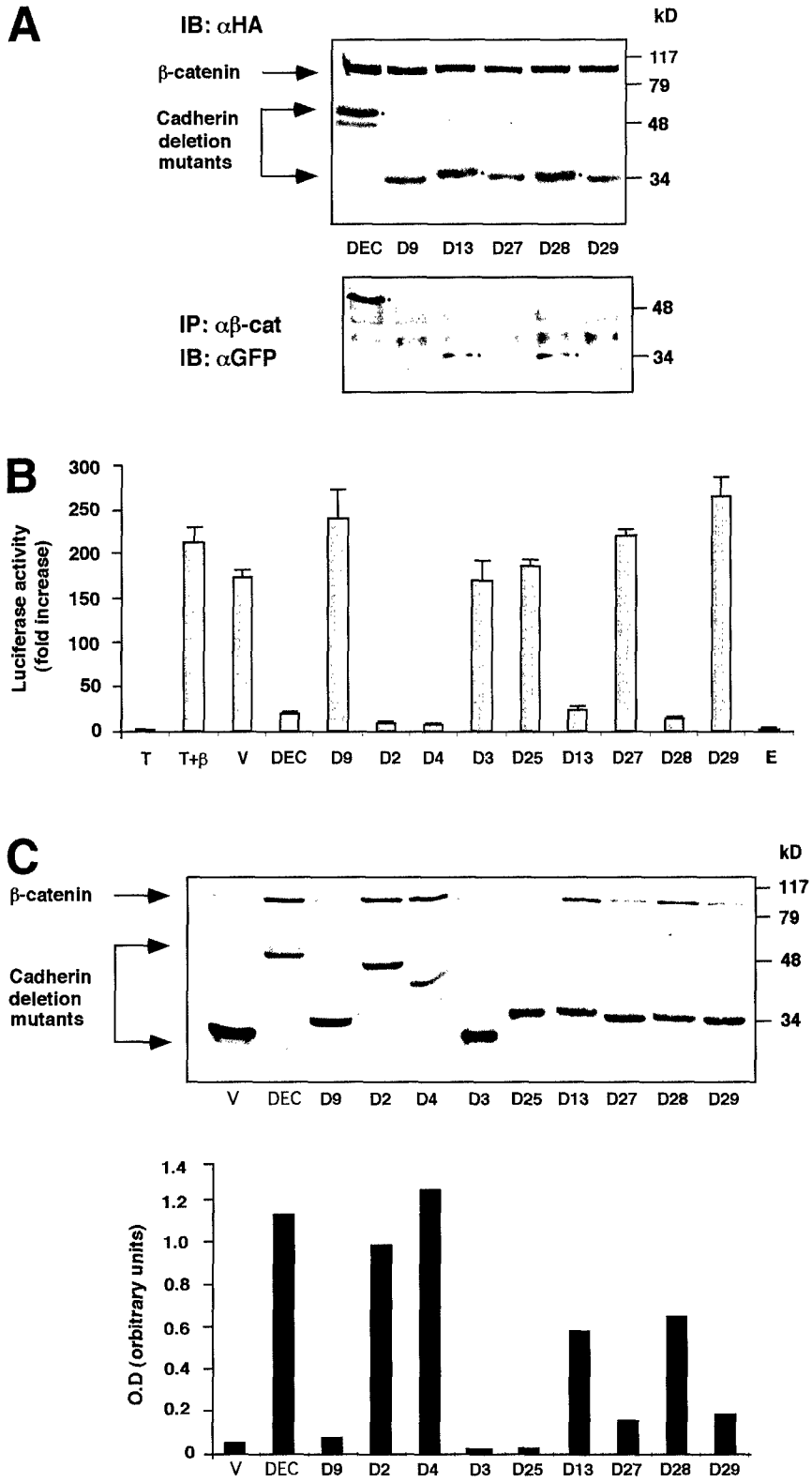

Figure 2. Analysis of the ability of different fragments of the DEC cytoplasmic tail to interact with β-catenin, affect its stability, and inhibit β-catenin–mediated transactivation. (A) The ability of selected GFP-DEC derivatives to coimmunoprecipitate with cotransfected HA-tagged β-catenin was determined by immunoprecipitation (IP) from 293T cells transfected with HA-tagged β-catenin and GFP-tagged DEC constructs with anti-GFP antibody, followed by Western blotting with anti-HA antibody. The total level of transfected β-catenin and DEC constructs was determined by immunoblotting (IB) with anti-HA-antibody. (B) 293T cells were transfected with GFP-tagged derivatives of the DEC cytoplasmic tail (DEC) or the full-length mammalian E-cadherin tail (E), along with β-catenin (β), a LEF/TCF reporter plasmid (T), and Lac Z. Luciferase activity was determined from duplicate plates as fold activation after normalizing for transfection efficiency by measuring β-galactosidase activity. T, cells were transfected with the reporter plasmid alone; V, cells transfected with the reporter plasmid, HA-tagged β-catenin and the GFP-vector used for the construction of the cadherin derivatives. (C) The cadherin derivatives used in B were transfected into CHO cells, and their ability to protect the endogenous β-catenin from degradation was determined by analyzing the level of β-catenin expressed in the DEC mutant-transfected cells by Western blotting with anti-β-catenin antibody. The level of expression of DEC constructs was determined by immunoblotting with an antibody against the GFP tag. Quantitation of the β-catenin level expressed in CHO cells was carried out by normalizing the intensity of the β-catenin bands shown to those of the DEC band for each derivative.

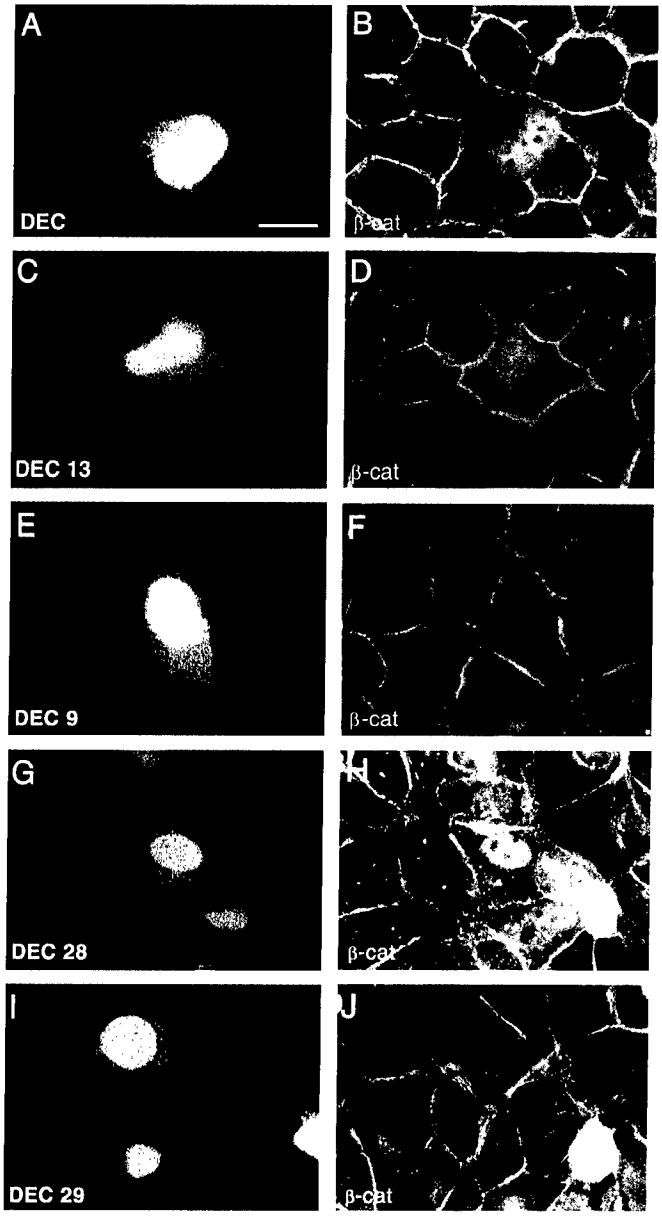

Figure 3. The effect of DEC cytoplasmic domain derivatives on the organization of adherens junctions and subcellular distribution of β-catenin (β-cat). MDCK cells were transfected with various GFP-tagged DEC derivatives (diagrammed in Figure 1, A and B), and the distribution of the GFP-tagged DEC derivatives (A, C, E, G, and I) and of the endogenous β-catenin (B, D, F, H, and J) was determined by double fluorescence microscopy using rhodamine-labeled anti-β-catenin antibody. Bar (in A), 10 μm. Note the reduction in junctional β-catenin in DEC-expressing cells but not in cells transfected with other DEC constructs. Also note that DEC9 and DEC29 do not increase the endogenous β-catenin level, whereas DEC13 does.

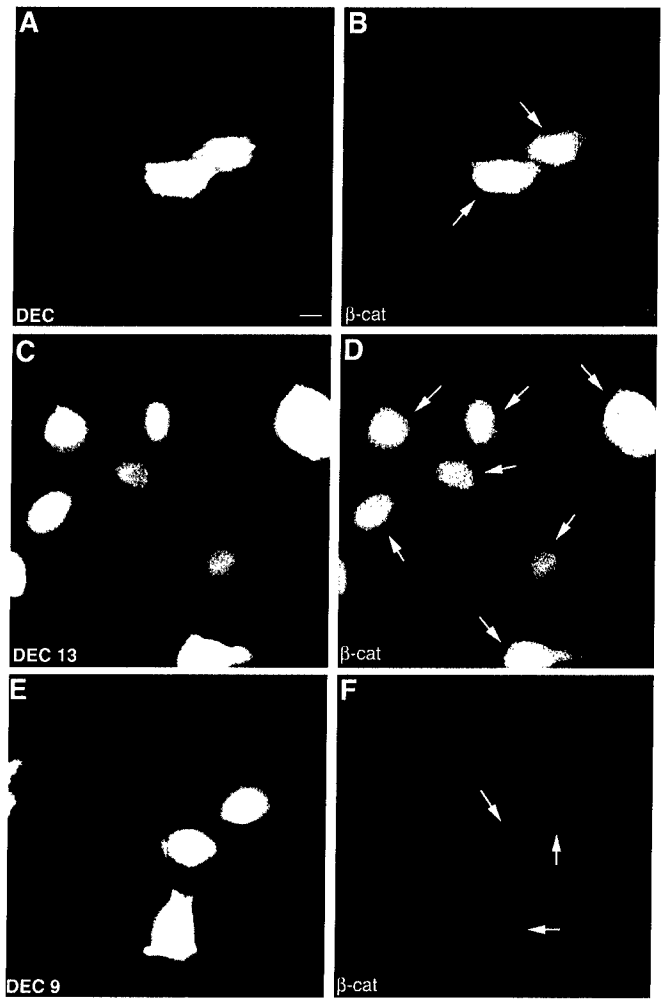

Figure 4. Analysis of the ability of DEC derivatives to increase the level and the accumulation of endogenous β-catenin (β-cat) in the nucleus. Some of the GFP-DEC constructs described in Figure 3 were transfected into CHO cells (A, C, and E), and their ability to elevate the endogenous β-catenin and induce its translocation into the nucleus (B, D, and F) was determined by double fluorescence as described in Figure 3. Bar in (A), 10 μm. The arrows mark the transfected cells. Note that, whereas DEC13 and DEC induced the accumulation of endogenous β-catenin in the nucleus, DEC9 was unable to do so.

nin in the two-hybrid system (Figure 5B, left). Because Arm repeats 3–8 retain the ability to bind several of Arm's partners (Pai *et al.*, 1996), we reasoned that such shorter Arm fragments might be compromised in binding to DE-cadherin derivatives and thus might be more sensitive to mutational changes. We therefore tested the DECM1-DECM3 mutants for their capacity to bind to Arm repeats 2–10 of both Arm and β-catenin (Figure 5B, right). In this assay, there was a substantial reduction in the binding of DECM2 to both Arm and β-catenin, whereas the other two mutations (DECM1 and DECM3) did not substantially affect binding (Figure 5B, right). These data suggested that DECM2 might weaken binding but not enough to be detectable in the context of the full-length DE-cadherin tail binding to the full-length Arm repeat region. Interactions outside the minimal Arm-binding region may normally help stabilize this association and thus could partially compensate for mutations such as DECM2. We therefore introduced the DECM2 mutation into a 34-amino acid peptide centered on the minimal binding region

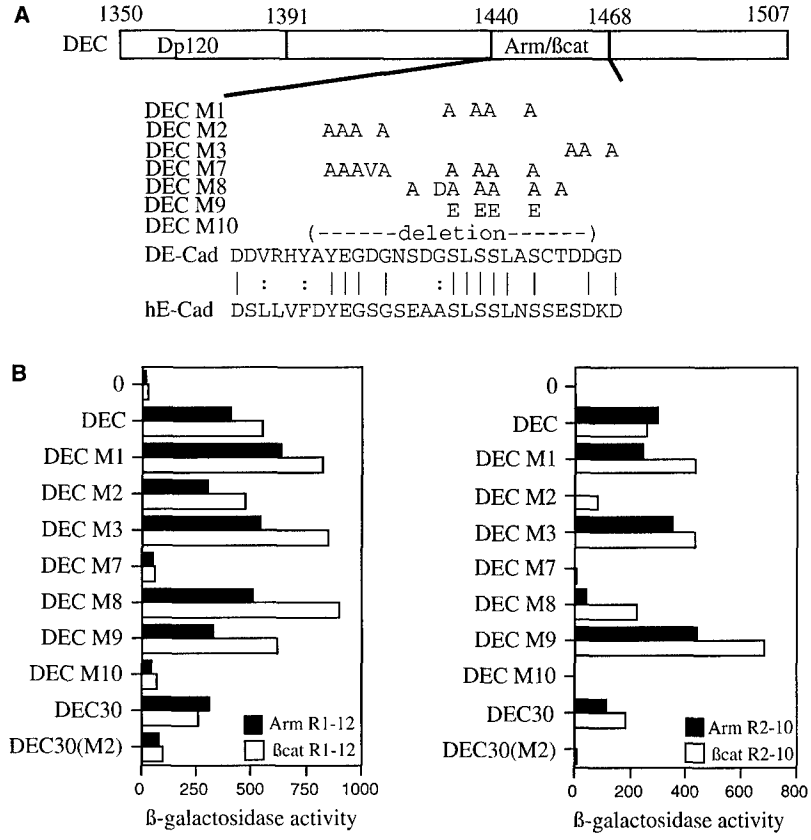

Figure 5. Analysis of the effect of clustered point mutations in the minimal Arm-binding domain of DEC on its ability to bind Arm and β-catenin (βcat) in the yeast two-hybrid system. (A) Diagram of the DEC tail and sequences of the clustered point mutations used in this study, with the sequences of DE-cadherin (DE-Cad) and human E-cadherin (hE-Cad) in the region of the mutations shown below. All mutations were introduced into and analyzed in the context of the full-length cytoplasmic tail. The mutation DECM2 was also tested in the context of a smaller fragment of the cadherin tail (DEC30; Figure 1A)—this derivative is DEC30(M2). (B) The DE-cadherin mutants diagrammed in A were fused to the Gal4 transcription activation domain and transformed into yeast cells together with the full Arm repeat region of Arm or β-catenin (Arm R1–12 or βcat R1–12, left) or a smaller fragment of the Arm repeat region (Arm R2–10 or βcat R2–10, right), fused to the LexA DNA-binding domain. Average β-galactosidase activities are shown.

(DEC30; Figure 1A). In this context (rather than in the full-length DEC tail), the DECM2 mutation essentially abolished binding to even the full-length Arm repeat region (DEC30(M2); Figure 5B).

Next, we tested this same set of mutants for binding to β-catenin in cultured mammalian cells, using the assays described above. Both DECM1 and DECM3 retained substantial ability to block TCF-directed gene expression (Figure 6A), suggesting that they could block binding of β-catenin to TCF family members. All three mutants were reduced in their ability to stabilize β-catenin (Figure 6B), although all appear to retain a small amount of activity in this assay. Finally, the overexpression of DECM3 in MDCK cells (Figure 6C) resulted in the accumulation of β-catenin in the cytoplasm and nuclei of these cells (Figure 6D).

In addition to these mutations, we also analyzed three mutants with more substantial changes in the minimal binding region. Mutant DECM7 combined the changes found in DECM1 and DECM2 and also mutated an additional amino acid, aspartic acid 1450, to valine (Figure 5A). Mutant DECM8 altered all of the serine and threonine residues in the core of the binding site to alanine (Figure 5A) and also altered the semiconserved residue glycine 1455 to aspartic acid. A subset of these residues is a likely target of phosphorylation in vivo (Stappert and Kemler, 1994). Finally, in DECM10, 20 amino acids were deleted in the core of the minimal binding region (Figure 5A). When tested against the full Arm repeat region of Arm or β-catenin in the two-hybrid system, DECM7 and DECM10 were essentially inactive (Figure 5B). In contrast, DECM8 had little effect on binding to the entire Arm repeat region (Figure 5B, left), although it did reduce binding to Arm repeats 2–10 of both Arm and β-catenin (Figure 5B, right). We also analyzed an additional mutant, DECM9, in which four of the conserved serine residues were changed to glutamic acid (Figure 5A). These serine residues are phosphorylated in vivo, and in some cases, this change mimics phosphorylation. DECM9 retained full ability to bind both Arm and β-catenin in the two-hybrid assays (Figure 5B).

We then studied the interaction of this set of mutants with β-catenin in mammalian cells. In this setting, DECM7, DECM8, and DECM10 all abolished interaction completely, losing both the ability to block TCF/LEF-dependent gene expression (Figure 6A) and to stabilize β-catenin (Figure 6B). The expression of M8 in MDCK cells (Figure 6E) had no effect on adherens junctions or on β-catenin organization (Figure 6F). In contrast, DECM9 preserved the capacity to interact with β-catenin, because it very efficiently protected it from degradation (Figure 6C) and inhibited LEF/TCF-directed transactivation (Figure 6A), in line with the two-hybrid assays. This is in striking contrast to DECM1, in which the same serine residues were changed to alanine rather than glutamic acid.

DISCUSSION

β-Catenin/Arm plays key roles in cell-cell adhesion and Wnt signal transduction. Deregulation of these activities

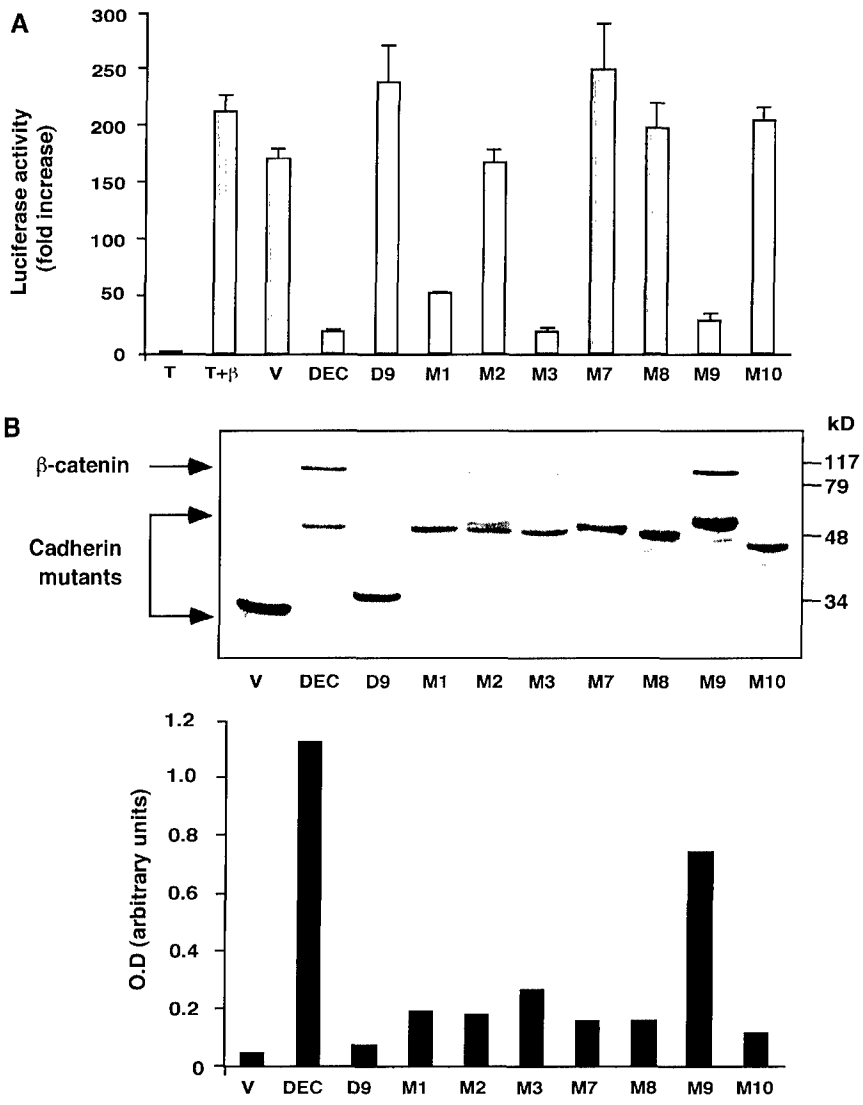

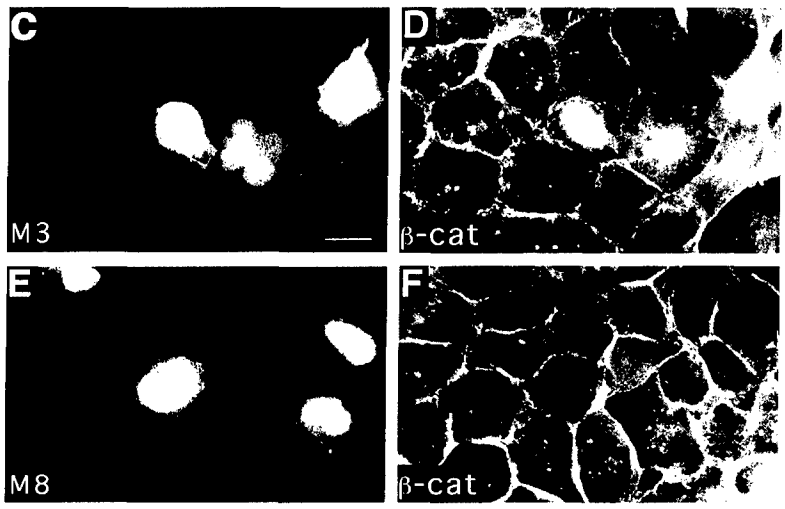

Figure 6. Analysis of the effect of clustered point mutations in the minimal Arm-binding domain of DEC on its capacity to interact with β-catenin, protect it from degradation, inhibit β-catenin/LEF-mediated transactivation, and affect β-catenin organization. (A) The ability of clustered point mutations (diagrammed in Figure 5A) to affect β-catenin/LEF-1–mediated transactivation in 293T cells was examined as described in Figure 2B. (B) The ability to protect β-catenin from degradation was examined in CHO cells, and the levels of β-catenin were quantified as described in Figure 2C. Because the samples were originally analyzed on the same gel with the samples shown in Figure 2C, the control samples (V, DEC, and D9) are shown again. (C–F) MDCK cells were transfected with GFP-tagged DECM3 (C, M3) and DECM8 (E, M8), and the organization of the endogenous β-catenin (β-cat) in the respective samples (D and F) was determined by double fluorescence microscopy. Bar, 10 μm.

can lead to disease. Activation of β-catenin–mediated signaling contributes to a wide variety of human tumors (reviewed by Zhurinsky *et al.*, 2000a), and dysfunction of cadherin-catenin adhesion is involved in cancer metastasis (reviewed by Christofori and Semb, 1999). β-Catenin/Arm mediates these distinct processes by forming a scaffold upon which different multiprotein complexes are assembled. To unravel β-catenin's normal functions and the alterations in its function in disease, a detailed understanding of its interactions with protein partners is required. This might facilitate a rational approach to design inhibitors of these interactions. For example, an effective, specific inhibitor of the β-catenin–TCF interaction might have therapeutic potential in cancers in which Wnt signaling is activated.

We used the cadherin/β-catenin interaction as a model for investigating this question. We previously found that 71 amino acid derivatives of the cytoplasmic tail of vertebrate N- or E-cadherin inhibit β-catenin/TCF-mediated transactivation when introduced into human colon cancer cells (Sadot *et al.*, 1998; Simcha *et al.*, 1998). Moreover, expression of the N-cadherin tail in human colon cancer cells inhibited the elevated transcription of *cyclin D1* (Shtutman *et al.*, 1999), thus potentially suppressing its oncogenic function. In the present study, we analyzed the interaction between DE-cadherin and β-catenin/Arm in detail, using several assays, each of which provided different measures of binding. Using the yeast two-hybrid system, we assessed interaction in the absence of most, if not all, of β-catenin/Arm's normal partners, because yeast lack β-catenin, cadherins, TCFs, APC, and axin. Furthermore, kinases and other proteins that regulate interactions between β-catenin/Arm and its partners, are also likely absent. We also used several assays in mammalian cells, which, in contrast to yeast, possess both a full (or nearly full) complement of β-catenin partners and the normal set of regulatory machinery that modulates the interaction between β-catenin and its partners. This diversity of assays allowed us to discriminate among the binding abilities of cadherin mutants in a more detailed way than was possible in most previous studies of β-catenin/Arm interaction with other partners, which, for the most part, relied on single assays.

Using these assays, we found that quite small fragments of DE-cadherin, including the 23-amino acid DEC27, bind both β-catenin and Arm in yeast. In cultured mammalian cells the criteria for interaction were more stringent. The smallest DE-cadherin peptide that interacted in mammalian cells was DEC28, which is 27 amino acids in length. This difference may reflect the fact that in mammalian cells DEC fragments must compete with endogenous partners for binding—weakened interactions might prevent effective competition. Alternately, it may simply reflect differences in the fusion proteins used in each assay. It is noteworthy, however, that the binding of short DEC fragments, such as DEC28 in mammalian cells, is weaker than binding of the full cytoplasmic tail of DE-cadherin or mammalian E-cadherin, as assessed by their ability to inhibit transcriptional activation by β-catenin (Figure 2B).

Our mutational analysis also revealed critical amino acids in cadherin required for interaction with β-catenin. The β-catenin/Arm-binding site is highly conserved among all classical cadherins. Most of our mutations in conserved residues had parallel effects in yeast and mammalian cells. For example, mutation of three acidic amino acids near the C terminus of the minimal binding region (DECM3) had little effect on either binding in yeast or the ability to block TCF-mediated transactivation, whereas mutation of four more N-terminal conserved residues (DECM2) resulted in a detectable reduction in binding in yeast and a substantial reduction in the ability to block TCF-mediated transactivation. The most extensive mutations, DECM7 and DECM10, completely blocked the binding in all assays.

Surprisingly, the serine residues in the binding site, mutated in DECM1 and DECM8, were largely dispensable for binding in yeast. In contrast, these mutations impaired or eliminated the ability to block TCF-mediated transactivation and to stabilize β-catenin in mammalian cells. One possible explanation for these differential effects is that these serines are phosphorylated in mammalian cells (Stappert and Kemler, 1994; Lickert *et al.*, 2000); this may strengthen binding. Consistent with this possibility, mutation of the four conserved serines to glutamic acid (mutant DECM9), which may mimic phosphorylation, did not block binding to β-catenin in mammalian cells. In fact, DECM9 very effectively protected β-catenin against degradation (Figure 2C), in agreement with recent studies by Lickert *et al.* (2000). If, in yeast, the relevant kinase(s) are absent, mutation of these serines would not affect binding.

While this paper was under review, two studies appeared that complement our data. Graham *et al.* (2000) solved the structure of β-catenin bound to XTcf3, thus revealing in full detail how β-catenin binds to one of its partners. XTcf3 binds in the groove on the surface of β-catenin, with the XTcf3 peptide forming a β-hairpin at its N terminus and an α-helix at its C terminus, with an extended peptide in between. From this structure and parallel mutagenesis of β-catenin, they identified two key charge-charge interactions between β-catenin and the extended XTcf3 peptide and a key hydrophobic interaction of β-catenin with the α-helix of XTcf3. They also assessed the ability of cadherin to bind to their β-catenin mutants and, from this, proposed a model for how cadherins bind β-catenin.

Based on our data, we extended this model, as shown in Figure 7A. In addition to the sequence similarity noted by Graham *et al.* (2000) in the extended peptide region, we suggest a further sequence alignment in the α-helical region. Notably, the three XTcf3 residues, which they identified as critical for interaction with β-catenin, are conserved in diverse cadherins (boxed in Figure 7A). Although the spacing between the extended peptide and the α-helix differs between TCF and cadherins, this region of XTcf3 is disordered in the structure and may form a flexible loop, and if fully extended, the cadherin peptide could span the gap. We also noted a similar, although less striking, alignment of the 20 amino acid repeats of APC and XTcf3, with all three key residues also conserved (Figure 7B).

Our mutational analysis can also be examined in light of this structure (Figure 7A). Mutation DECM2, which has a severe effect on binding, alters four amino acids including a glutamic acid predicted by analogy to XTcf3 to mediate

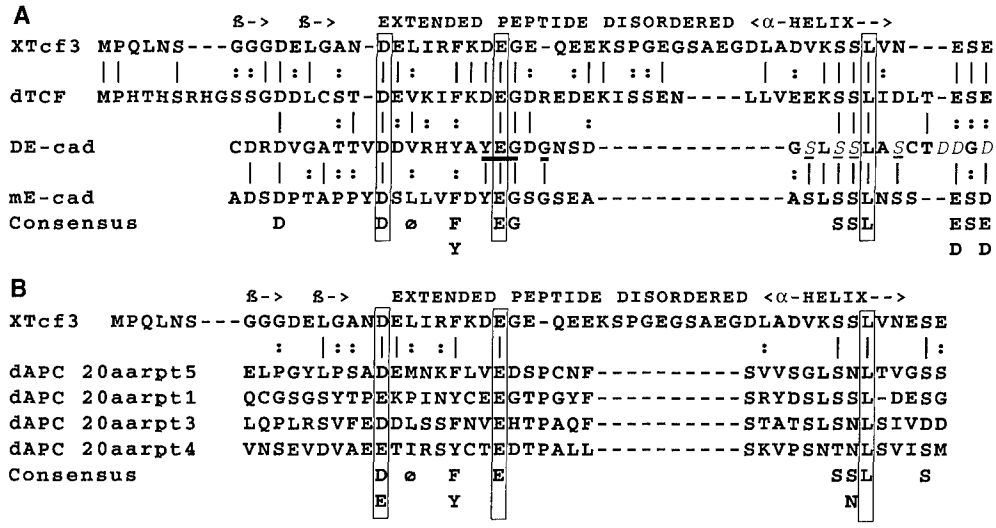

Figure 7. A model for the structure of the β-catenin-binding region of cadherin. (A) The sequence of *Xenopus* Tcf3 (XTcf3) and *Drosophila* TCF (dTCF) are aligned below a diagrammatic representation of the structure of XTcf3 as determined by Graham *et al.* (2000). A β-hairpin motif is indicated by "β ->." Identical residues are indicated by vertical lines and similar residues are indicated by colons. Below is a proposed alignment of *Drosophila* E-cadherin (DE-cad) and mouse E-cadherin (mE-cad) with the extended peptide and α-helical regions of XTcf3. A consensus is displayed at the bottom positions (where at least three fourths of the sequences match). The three residues that are key for XTcf3 binding to β-catenin are boxed, and all are conserved in all sequences. The amino acids altered in mutation DECM2 (YEG G), which have a strong effect on DEC binding to β-catenin/Arm in our assays, are bold and underlined. The amino acids altered in mutation DECM3 (DD D), which had the weakest effect on binding, are shown in italics. The serines altered in mutations DECM1 and DECM9 are in italics and underlined. (B) Alignment of the XTcf3 sequence and structure with four 20-amino acid repeats of *Drosophila* APC (dAPC).

one of the key charge-charge interactions with β-catenin (Figure 7A, bold underline). In contrast, mutation DECM3, which had no effect in yeast and the least severe effect in mammalian cell assays, maps to a region predicted by analogy to be outside the structured portion of the binding site (Figure 7A, italics). The analysis of mutations DECM1 and DECM9 is more complex. Mutation of the four serines targeted in DECM1 to alanine has no effect in yeast but substantially reduces binding in mammalian cells. In contrast, mutation DECM9, which altered these serines to glutamic acid, did not affect binding. Of these four serines, the second and third align with serines in XTcf3. The second serine is predicted to be on the face of the α-helix away from β-catenin, whereas the third serine does not contribute to binding. The first serine is a valine in XTcf3, which participates in hydrophobic contacts, whereas the fourth serine is predicted by analogy to XTcf3 to be beyond the end of the α-helix and to have its side chain pointed away from β-catenin. If, as discussed above, these serines are phosphorylated, then the first and third phosphoserines might make charge-charge interactions with lysine 292 of β-catenin; this would also be the case if they were mutated to glutamic acid.

von Kries *et al.* (2000) also revealed new insights into β-catenin's interaction with its partners. They mutagenized β-catenin to identify amino acids in the Arm repeat region, which are essential for binding to APC, axin/conductin, and TCF/LEF. They found that mutations mapping to distinct Arm repeats blocked binding to individual partners. Thus, LEF-1 binding was inhibited by mutations in Arm repeat 8, whereas conductin binding was inhibited by mutations in Arm repeats 3 and 4. These data suggest that either different partners bind to distinct sites on β-catenin or, if the binding sites coincide, different subsets of the contacts between β-catenin and each its partners provide most of the free energy of binding. In parallel, they also examined whether these β-catenin mutations affected binding to E-cadherin (J.P. von Kries and W. Birchmeier, personal communication). In contrast to their results with the other partners, none of the mutations specifically blocked β-catenin binding to cadherin. Graham *et al.* (2000) also tested mutant forms of β-catenin for binding to XTcf3, C-cadherin, APC, and axin. XTcf3 binding required two key charge-charge interactions with the extended peptide region and a key hydrophobic interaction with the α-helix. For cadherin, mutations predicted from the structure to block the key charge-charge interactions reduced binding, but mutations in the α-helix–binding region had little effect. These data are of interest in relation to the present study in which, contrary to expectations, none of the first series of clustered point mutations (DECM1, DECM2, and DECM3) abolished DEC binding to β-catenin in yeast. One possible explanation for all these results is that the binding of cadherins to β-catenin differs from that of the other partners, with strong contacts made throughout the binding region. Thus, point mutations in either cadherin or β-catenin would have a lesser effect on binding. This might also explain the apparently higher affinity of cadherin for Arm in vivo, as assessed by competition for the limiting pool of Arm present in *arm* mutant embryos (Cox *et al.*, 1996).

We assessed our mutations in the full DE-cadherin cytoplasmic tail. We also assessed DECM2 in a second context, introduced into a 34-amino acid fragment centered on the minimal binding region. In this context, DECM2 had a much more severe effect on β-catenin binding in yeast than it did when present in the full DE-cadherin tail. This result is consistent with the possibility that β-catenin binding is stabilized by interactions with regions of the cadherin tail outside the minimal binding domain or that the entire tail folds into a conformation that facilitates β-catenin binding.

To affect one function of β-catenin without affecting the others, one must design inhibitors that specifically interfere with a particular protein-protein interaction. Our results provide some insight into this issue. Both wild-type and mutant cadherin peptides were more effective in blocking interaction of endogenous β-catenin with TCF/LEF than in blocking interactions between endogenous β-catenin and the axin/APC complex or assembly of adherens junctions. This would be the desired outcome for a specific inhibitor that blocked the oncogenic action of β-catenin. Our data also suggest possible peptide candidates for cocrystallization of cadherin and β-catenin. When combined with the β-catenin–TCF structure, this would set the stage for initiating the design of synthetic inhibitors of different protein-protein interactions, which can be tested in cell culture and animal models for efficacy in blocking Wnt signaling or modulating cell adhesion and cancer progression.

ACKNOWLEDGMENTS

We are grateful to Mary Teachey who made some of the DEC constructs and Daniela Salomon for subcloning them into mammalian expression vectors, to Mary Teachey and Amanda Neisch for assistance with β-galactosidase assays, and to J.P. von Kries, W. Birchmeier, and W. Xu for communicating unpublished data and for valuable discussions. This work was supported by an IDEA Award from the Army Breast Cancer Research Program to M.P (DAMD17-98-1-8223) and by start-up funds from the University of Minnesota to C.K. C.K. was supported by the National Cancer Institute of Canada with funds from the Terry Fox Run. G.P. was supported by NIH 5T32 GM07092 and by a predoctoral fellowship from the Army Breast Cancer Research Program (DAMD17-98-1-8220), and M.P. was supported by a Career Development Award from the U.S. Army Breast Cancer Research Program. A.B.-Z. was supported by grants from the German-Israeli Foundation for Scientific Research and Development, the Cooperation Program in Cancer Research between the German Cancer Research Center and the Israeli Ministry of Science and Arts, CaP CURE, the Crown Endowment Fund for Immunological Research, and Yad Abraham Center for Cancer Diagnosis and Therapy.

REFERENCES

Ben-Ze'ev, A., and Geiger, B. (1998). Differential molecular interactions of β-catenin and plakoglobin in adhesion, signaling and cancer. Curr. Opin. Cell Biol. *10*, 629–639.

Christofori, G., and Semb, H. (1999). The role of the cell-adhesion molecule E-cadherin as a tumor-suppressor gene. Trends Biochem. Sci. *24*, 73–76.

Conti, E., Uy, M., Leighton, L., Blobel, G., and Kuriyan, J. (1998). Crystallographic analysis of the recognition of a nuclear localization signal by the nuclear import factor karyopherin-α. Cell *94*, 193–204.

Cox, R.T., Kirkpatrick, C., and Peifer, M. (1996). Armadillo is required for adherens junction assembly, cell polarity, and morphogenesis during *Drosophila* embryogenesis. J. Cell Biol. *134*, 133–148.

Cox, R.T., Pai, L.-M., Kirkpatrick, C., Stein, J., and Peifer, M. (1999). Roles of the C-terminus of Armadillo in Wingless signaling in *Drosophila*. Genetics *153*, 319–332.

Graham, T.A., Weaver, C., Mao, F., Kimelman, D., and Xu, W. (2000). Crystal structure of a β-catenin/Tcf complex. Cell *103*, 885–896.

Gumbiner, B.M. (1996). Cell adhesion: the molecular basis of tissue architecture and structure. Cell *84*, 345–357.

Hsu, S.C., Galceran, J., and Grosschedl, R. (1998). Modulation of transcriptional regulation by LEF-1 in response to Wnt-1 signaling and association with β-catenin. Mol. Cell. Biol. *18*, 4807–4818.

Huber, A.H., Nelson, W.J., and Weis, W.I. (1997). Three-dimensional structure of the armadillo repeat region of β-catenin. Cell *90*, 871–882.

Jho, E.-H., Lomvardas, S., and Costantini, F. (1999). A GSK3β phosphorylation site in axin modulates interaction with β-catenin and TCF-mediated gene expression. Biochem. Biophys. Res. Commun. *266*, 28–35.

Lickert, H., Bauer, A., Kemler, R., and Stappert, J. (2000). Casein kinase II phosphorylation of E-cadherin increases E-cadherin/β-catenin interaction and strengthens cell adhesion. J. Biol. Chem. *275*, 5090–5095.

Liu, W., Dong, X., Mai, M., Seelan, R.S., Taniguchi, K., Krishnadath, K.K., Halling, K.C., Cunningham, J.M., Qian, C., Christensen, E., Roche, P.C., Smith, D.I., and Thibodeau, S.N. (2000). Mutations in AXIN2 cause colorectal cancer with defective mismatch repair by activating β-catenin/TCF signaling. Nat. Genet. *26*, 146–147.

McCartney, B.M., Dierick, H.A., Kirkpatrick, C., Moline, M.M., Baas, A., Peifer, M., and Bejsovec, A. (1999). *Drosophila* APC2 is a cytoskeletally-associated protein that regulates Wingless signaling in the embryonic epidermis. J. Cell Biol. *146*, 1303–1318.

Nakamura, T., Hamada, F., Ishidate, T., Anai, K., Kawahara, K., Toyoshima, K., and Akiyama, T. (1998). Axin, an inhibitor of the Wnt signaling pathway, interacts with β-catenin, GSK-3β and APC and reduces the β-catenin level. Genes Cells *3*, 395–403.

Omer, C.A., Miller, P.J., Diehl, R.E., and Kral, A.M. (1999). Identification of Tcf4 residues involved in high-affinity β-catenin binding. Biochem. Biophys. Res. Commun. *256*, 584–590.

Pai, L.-M., Kirkpatrick, C., Blanton, J., Oda, H., Takeichi, M., and Peifer, M. (1996). *Drosophila* α-catenin and E-cadherin bind to distinct regions of *Drosophila* Armadillo. J. Biol. Chem. *271*, 32411–32420.

Peifer, M., and Polakis, P. (2000). Wnt signaling in oncogenesis and embryogenesis: a look outside the nucleus. Science *287*, 1606–1609.

Provost, E., and Rimm, D.L. (1999). Controversies at the cytoplasmic face of the cadherin-based adhesion complex. Curr. Opin. Cell Biol. *11*, 567–572.

Rubinfeld, B., Albert, I., Porfiri, E., Fiol, C., Munemitsu, S., and Polakis, P. (1996). Binding of GSK-3β to the APC/β-catenin complex and regulation of complex assembly. Science *272*, 1023–1026.

Rubinfeld, B., Albert, I., Porfiri, E., Munemitsu, S., and Polakis, P. (1997). Loss of β-catenin regulation by the APC tumor suppressor protein correlates with loss of structure due to common somatic mutations of the gene. Cancer Res. *57*, 4624–4630.

Sadot, E., Simcha, I., Shtutman, M., Ben-Ze'ev, A., and Geiger, B. (1998). Inhibition of β-catenin-mediated transactivation by cadherin derivatives. Proc. Natl. Acad. Sci. USA *95*, 15339–15344.

Satoh, S., Daigo, Y., Furukawa, Y., Kato, T., Miwa, N., Nishiwaki, T., Kawasoe, T., Ishiguro, H., Fujita, M., Tokino, T., Sasaki, Y., Imaoka, S., Murata, M., Shimano, T., Yamaoka, Y., and Nakamura, Y. (2000). AXIN1 mutations in hepatocellular carcinomas, and growth suppression in cancer cells by virus-mediated transfer of AXIN1. Nat. Genet. *24*, 245–250.

Shtutman, M., Zhurinsky, J., Simcha, I., Albanese, C., D'Amico, M., Pestell, R., and Ben-Ze'ev, A. (1999). The cyclin D1 gene is a target of the β-catenin/LEF-1 pathway. Proc. Natl. Acad. Sci. USA *96*, 5522–5527.

Simcha, I., Shtutman, M., Salomon, D., Zhurinsky, J., Sadot, E., Geiger, B., and Ben-Ze'ev, A. (1998). Differential nuclear translocation and transactivation potential of β-catenin and plakoglobin. J. Cell Biol. *141*, 1433–1448.

Stappert, J., and Kemler, R. (1994). A short core region of E-cadherin is essential for catenin binding and is highly phosphorylated. Cell Adhes. Commun. *2*, 319–327.

van de Wetering, M., Cavallo, R., Dooijes, D., van Beest, M., van Es, J., Loureiro, J., Ypma, A., Hursh, D., Jones, T., Bejsovec, A., Peifer, M., Mortin, M., and Clevers, H. (1997). Armadillo co-activates transcription driven by the product of the *Drosophila* segment polarity gene *dTCF*. Cell *88*, 789–799.

von Kries, J.P., Winbeck, G., Asbrand, C., Schwarz-Romond, T., Sochnikova, N., Dell'Oro, A., Behrens, J., and Birchmeier, W. (2000). Hot spots in β-catenin for interactions with LEF-1, conductin and APC. Nat. Struct. Biol. *7*, 800–807.

White, P., Aberle, H., and Vincent, J.-P. (1998). Signaling and adhesion activities of mammalian β-catenin and plakoglobin in *Drosophila*. J. Cell Biol. *140*, 183–195.

Willert, K., and Nusse, R. (1998). β-catenin: a key mediator of Wnt signaling. Curr. Opin. Gene Dev. *8*, 95–102.

Wodarz, A., and Nusse, R. (1998). Mechanisms of Wnt signaling in development. Annu. Rev. Cell Dev. Biol. *14*, 59–88.

Zhurinsky, J., Shtutman, M., and Ben-Ze'ev, A. (2000a). Plakoglobin and β-catenin: protein interactions, regulation and biological roles. J. Cell Sci. *113*, 3127–3139.

Zhurinsky, J., Shtutman, M., and Ben-Ze'ev, A. (2000b). Differential mechanisms of LEF/TCF-family dependent transcriptional activation by β-catenin and plakoglobin. Mol. Cell. Biol. *20*, 4238–4252.

CADHERINS IN EMBRYONIC AND NEURAL MORPHOGENESIS

Ulrich Tepass, Kevin Truong‡, Dorothea Godt*, Mitsuhiko Ikura‡ and Mark Peifer§*

Cadherins not only maintain the structural integrity of cells and tissues but also control a wide array of cellular behaviours. They are instrumental for cell and tissue polarization, and they regulate cell movements such as cell sorting, cell migration and cell rearrangements. Cadherins may also contribute to neurite outgrowth and pathfinding, and to synaptic specificity and modulation in the central nervous system.

GROWTH CONE
Exploratory tip of an extending neuronal process such as an axon.

IMMUNOGLOBULIN-TYPE ADHESION MOLECULES
Family of adhesion molecules characterized by the presence of immunoglobulin-like domains, which are also found in antibody molecules.

**Department of Zoology, University of Toronto, 25 Harbord Street, Toronto, Ontario M5S 3G5, Canada.*
‡Division of Molecular and Structural Biology, Ontario Cancer Institute and Department of Medical Biophysics, University of Toronto, Toronto M5G 2M9, Ontario, Canada.
§Department of Biology, University of North Carolina, Chapel Hill, North Carolina 27599, USA.
Correspondence to U.T.
e-mail: utepass@zoo.utoronto.ca

In 1963, two publications appeared that focused attention on the adhesive mechanisms that contribute to embryonic morphogenesis and govern structural differentiation of the nervous system. Malcolm Steinberg laid the groundwork for the 'differential adhesion hypothesis', suggesting that the segregation or 'sorting out' of different embryonic cell types into separate tissues involves qualitative or quantitative differences in cell adhesion[1]. Roger Sperry proposed the 'chemoaffinity hypothesis', which holds that specific synaptic contacts form according to differences in the adhesive properties of individual GROWTH CONES and synapses[2]. Both hypotheses were the result of decades of experimental work, but were formulated before any adhesion molecules had been identified. It is now apparent that a large number of adhesion molecules exist that can be grouped into several superfamilies. The cadherin and IMMUNOGLOBULIN-TYPE ADHESION MOLECULES are the main groups of cell–cell adhesion receptors, whereas the integrins are the predominant contributors to cell–substrate adhesion[3,4]. Adhesive mechanisms that contribute to embryonic or neural morphogenesis share many similarities, revealing that Steinberg's and Sperry's hypotheses are essentially similar proposals applied to different cell populations.

Morphogenesis involves two interrelated themes: structure and movement. For example, the different adhesive properties of two mixed cell populations induce cell movement, leading to the sorting out of the two groups of cells. After the sorting process is completed, adhesive differences maintain the segregation and relative position of the two cell groups, therefore preserving a specific tissue architecture[5–8]. Neuronal morphogenesis follows a similar pattern, in which the neuronal growth cone has to move through a complex environment using differential adhesive cues. On reaching the target, synaptic contacts are formed and maintained by specific adhesive interactions[9].

The first cadherins to draw scientists' attention were vertebrate classic cadherins, which were independently identified for their ability to mediate calcium-dependent adhesion among cultured cells and for their role in the epithelialization of the early mouse embryo[10]. So far, the sequences of over 300 vertebrate cadherins have been reported, and the virtually complete sets of cadherins encoded by the genomes of *Caenorhabditis elegans* and *Drosophila melanogaster* are now known.

Structural diversity of the cadherin superfamily

The recent explosion in genomic sequencing of various animals has shed new light on the diversity of the cadherin superfamily. In humans, more than 80 members of the cadherin superfamily have been sequenced. Current annotation of the *C. elegans* and the *Drosophila* genomes reveals 14 and 16 cadherin genes, respectively. Cadherins are defined by the presence of the cadherin domain (CD), a roughly 110 amino-acid peptide that mediates calcium-dependent homophilic interactions between cadherin molecules (FIG. 1). The CD is typically organized in tandem repeats. Calcium ions associate with the linker region that connects two CDs, and require interaction with amino acids from both CDs (FIG. 1; see below).

Here we present a classification of cadherins into

subfamilies on the basis of the domain layout of individual cadherins, which includes the number and sequence of CDs, and the presence of other conserved domains and sequence motifs (FIG. 2, TABLE 1). This analysis reveals that four cadherin subfamilies are conserved between *C. elegans*, *Drosophila* and humans: classic cadherins, Fat-like cadherins, seven-transmembrane cadherins and a new subfamily of cadherins that is related to *Drosophila* Cad102F. Classic cadherins break up in four subgroups, as listed in TABLE 1. Fat-like cadherins contain a subgroup of highly related molecules that we call Fatoid cadherins. These include all known vertebrate Fat-like cadherins, *Drosophila* Cad76E and *C. elegans* Cdh-4. Cadherins containing protein kinase domains are found in vertebrates (RET cadherins) and in *Drosophila*. Desmosomal cadherins are presumably derived from type I classic cadherins within the CHORDATE lineage, as neither desmosomal cadherins nor DESMOSOMES are found in *Drosophila* or *C. elegans*. Finally, protocadherins also seem to be limited to chordates. The grouping of cadherins into seven subfamilies, which is largely on the basis of the overall protein domain architecture, is corroborated by sequence comparison of CDs only (see online supplementary materials). Note that only about half of the cadherins found in *C. elegans* and *Drosophila* are part of identified subfamilies.

Cadherins are not found in yeast, and only a single, poorly conserved CD has been reported in a secreted protein from *Dictyostelium*[11], indicating that transmembrane proteins of the cadherin superfamily might have evolved to meet the need for the complex cell interactions that are required for the multicellular organization of METAZOANS. The function of classic cadherins during the formation and maintenance of epithelial tissues and cell–cell ADHERENS JUNCTIONS — two other metazoan inventions — is of particular importance. Within the classic cadherin subfamily, an interesting shift in protein organization has taken place during evolution — chordate classic cadherins lack non-chordate classic cadherin domains (NCCDs), laminin G (LG) and epidermal growth factor (EGF) domains and consistently contain five CDs, in contrast to the domain structure of classic cadherins in three other phyla: ECHINODERMS, ARTHROPODS and NEMATODES (FIG. 2, TABLE 1). This finding indicates that, during the early evolution of chordates, the structure of classic cadherins was modified and that a single progenitor might have given rise to the numerous classic cadherins found in vertebrates today, a conclusion supported by the phylogenetic analysis of chordate cadherins[12].

The cadherin families of *C. elegans* and *Drosophila* are small and very similar in size, and these cadherin genes are scattered throughout the genome without any obvious clustering, indicating that gene duplication events might not have occurred recently. So most of these genes were presumably established early during metazoan evolution. In particular, the progenitors of the four conserved subfamilies of cadherins are the result of a GENE RADIATION event that occurred before nematodes, arthropods and chordates diverged. In contrast, classic cadherins and the closely related desmosomal cadherins, as well as the more divergent protocadherins, were all amplified within the chordate lineage, resulting

CHORDATES
Phylum that comprises animals with a notochord and includes all vertebrates.

DESMOSOME
A patch-like adhesive intercellular junction found in vertebrate tissues that is linked to intermediate filaments.

METAZOANS
Refers to the kingdom Animalia (animals) that comprises roughly 35 phyla of multicellular organisms.

ADHERENS JUNCTIONS
Cell–cell or cell–matrix adhesive junctions that are linked to microfilaments.

ECHINODERMS
Animal phylum of marine invertebrates including sea urchins and starfish.

ARTHROPODS
Largest animal phylum composed of invertebrates that have a segmented body, segmented appendages and an external skeleton. This includes insects, spiders and crustaceans.

NEMATODES
Animal phylum of unsegmented roundworms.

GENE RADIATION
Process that leads to the formation of gene families in which gene amplification through gene duplication events is followed by the diversification of gene structure and function.

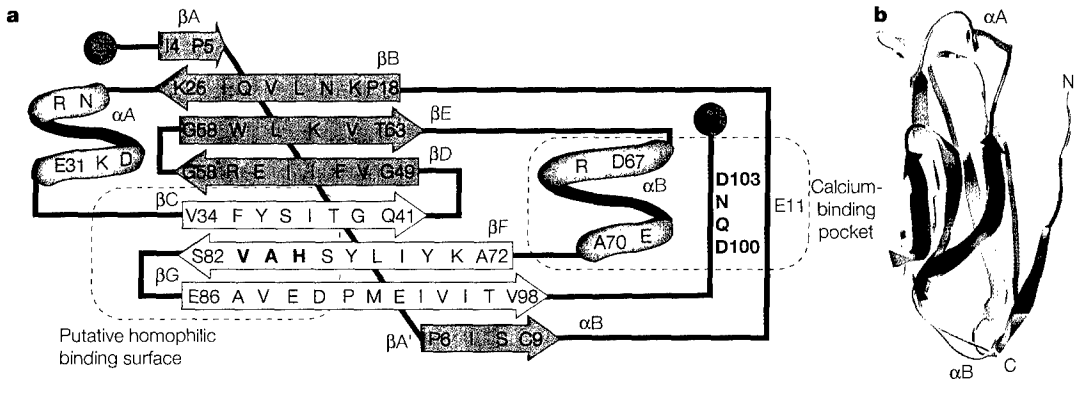

Figure 1 | **Structure of the cadherin domain.** The structure of the first cadherin domain (CD) of mouse E-cadherin is shown in **a** and **b** |. It was solved by NMR spectroscopy[18] and, subsequently, the crystal structure of the first CD of N-cadherin revealed a similar topology[19]. The CD consists of a seven-strand β-sheet with the amino and carboxyl termini located at opposite ends of the molecule. The segment connecting strands B and C adopts an apparently helical structure consisting of a succession of β-turn and β-like hydrogen bonds. This unique quasi-β-helix structure is characteristic of the CD. **a** | Schematic of topology of the amino-terminal CD of mouse E-cadherin. βA, βA′, βB, βE, and βD (green) and βC, βF, and βG (yellow) form β-sheets. The α-helices are shown in magenta. The putative homophilic binding surface including the amino acids HAV (red), and the Ca^{2+}-binding pocket with the amino acids that interact with Ca^{2+} (blue), are indicated by the dotted lines. **b** | Ribbon structure of the CD. The colour coding is the same as in (**a**). **c** | Alignment of the first two N-terminal CDs of mouse E- and N-cadherin. The colour coding is the same as in (a). The CDs are connected by a roughly 10 amino-acid linker region. Note that the amino acids that form a single Ca^{2+} binding pocket (indicated in blue) are found in the first and second CDs and include animo acids in the linker region.

in numerous genes with pronounced clustering[13,14]. In humans, all six desmosomal cadherin genes are found in chromosomal region 18q12.1; three genes that encode more than 50 protocadherins are found in region 5q31–32, and many classic cadherins are organized in gene clusters[13–16]. A similar gene amplification is seen in other unrelated gene clusters, such as in the *C. elegans* collagen genes. It has been proposed that the

Table 1 | **Cadherin subfamilies**

Cadherin subfamily	Type	Cadherin	Species	No. of CDs
(I) Classic cadherins	***Vertebrate Type I classic cadherins***	Examples include:		
• Highly conserved cytoplasmic domain that binds to catenins	• HAV motif in first CD	E-cadherin (CDH1)	Hs	5
		P-cadherin (CDH3)	Hs	5
• Often found at adherens junctions		N-cadherin (CDH2)	Hs	5
		R-cadherin (CDH4)	Hs	5
	Vertebrate Type II classic cadherins	Examples include:		
	• No HAV motif in first CD	VE-cadherin (CDH5)	Hs	5
		Cadherin-7 (CDH7)	Hs	5
		Cadherin-8 (CDH8)	Hs	5
		Br-cadherin (CDH12)	Hs	5
	Ascidian classic cadherins	Cl-cadherin	Ci	5
		BS-cadherin	Bs	5
	Non-chordate classic cadherins	LvG-cadherin	Lv	17
	• Variable number of CDs	DE-cadherin	Dm	8
	• LG and EGF domains	DN-cadherin	Dm	18
	• NCCD domain, only found in these cadherins	Hmr-1 (splice products 1a/1b)	Ce	3/19*
(II) Fat-like cadherins	***Fatoid cadherins***	Examples include:		
• Very large extracellular domain with up to 34 CDs	• More than 30 CDs, closely related in sequence	hFat1	Hs	34
	• Flamingo box in some members	hFat2	Hs	34
• Heterogeneous subfamily	• LG and EGF domains	DCad76E (CG7749)	Dm	34
	• Conserved region in the cytoplasmic domain (between vertebrates and fly)	Cdh4 (F25F2.2)	Ce	32
	Other Fat-like cadherins	Fat	Dm	34
	• Variable number of CDs	Dachsous	Dm	27
	• Flamingo box in Fat	Cdh-3 (ZK112.7)	Ce	19
	• LG and EGF domains in Fat and Cdh-3	Cdh-1 (R10F2.2)	Ce	25
(III) Seven-pass transmembrane cadherins	• Seven-pass transmembrane domain similar to G-protein linked receptors (Secretins)	hFlamingo1	Hs	9
		hFlamingo2	Hs	9
	• Flamingo box	Flamingo/Starry night	Dm	9
	• LG and EGF domains	Cdh-6 (F15B9.7)	Ce	9
(IV) DCad102F-like cadherins	• Sequence conservation throughout much of the protein	KIAA0911	Hs	2
		KIAA0726	Hs	2
	• LG domain	DCad102F (CG11059)	Dm	2
	• Glu/Ser-rich cytoplasmic domain	Cdh-11 (B0034.3)	Ce	2
(V) Protein kinase cadherins	• Tyrosine kinase domain (RET-Cadherins)	RET	Hs	2
		DRet (CG1061+CG14396)	Dm	1‡
	• Putative Ser/Thr kinase	DCad96Ca (CG10244)	Dm	1
(VI) Desmosomal cadherins	***Desmocollins***	Desmocollin-1	Hs	5
• Only found in vertebrates	• Conserved cytoplasmic domain	Desmocollin-2	Hs	5
• Localize at desmosomes		Desmocollin-3	Hs	5
• Interact with plakoglobin, desmoplakin and plakophillins	***Desmogleins***	Desmoglein-1	Hs	5
	• Conserved cytoplasmic domain	Desmoglein-2	Hs	5
		Desmoglein-3	Hs	5
(VII) Protocadherins	***Protocadherins (Pcdh) α, β and γ***	Examples include:		
• Only found in vertebrates	• 52 protocadherins encoded by 3 genes	Pcdh-α3	Hs	6
	• all Pcdh-α/CNR proteins have a constant C-terminal cytoplasmic domain that interacts with Fyn tyrosine kinase	Pcdh-β1	Hs	6
		Pcdh-γA9	Hs	6
	Other protocadherins	Examples include:		
		Pcdh-1	Hs	6
		Pcdh-8 (Arcadlin)	Hs	6

*J. Petite, personal communication; ‡ R. Cagan, personal communication (Species: Hs, *Homo sapiens*; Dm, *Drosophila melanogaster*; Ce, *Caenorhabditis elegans*, Ci, *Ciona intestinalis*; Bs, *Botryllus schlosseri*; Lv, *Lytechinus variegatus*. Domains: CD, cadherin domain; CNR, cadherin-related neuronal receptor; EGF, epidermal growth factor; LG, laminin G; NCCD, non-chordate classic cadherin domain.) Uncharacterized cadherins of *Drosophila* are named according to their cytological map position (for example, DCad 102F).

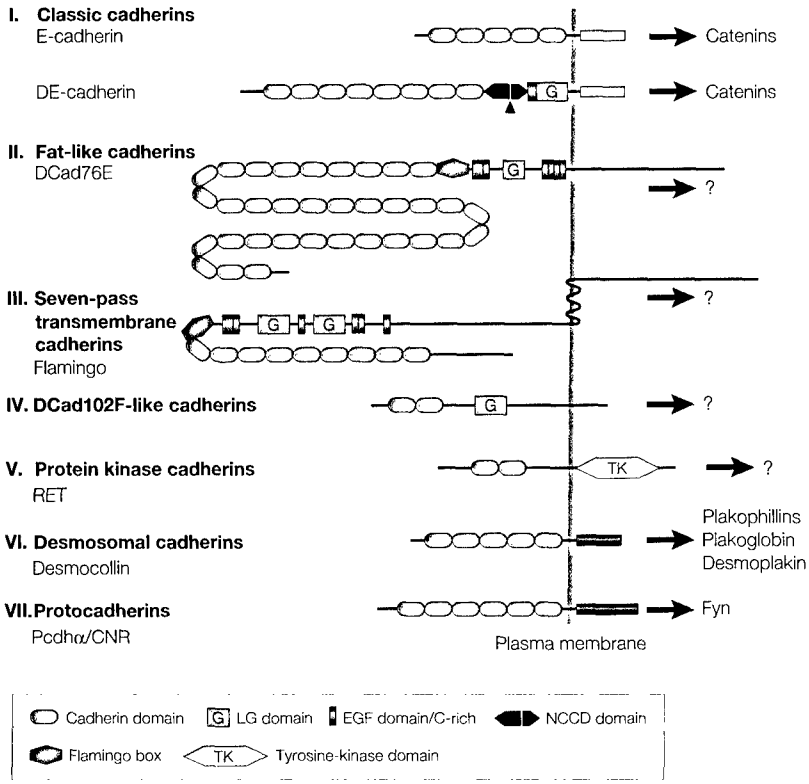

Figure 2 | **Structural diversity of the cadherin superfamily.** Representatives of each of the seven subfamilies of cadherins are shown. Subfamilies I to VII are conserved between nematodes (*Caenorhabditis elegans*), arthropods (*Drosophila melanogaster*) and chordates (humans). Members of subfamily V are found in chordates and *Drosophila*, whereas cadherins of subfamilies VI and VII are at present only known in vertebrates. Binding partners for the cytoplasmic tail of cadherins have been characterized for classic cadherins (subfamily I), for desmosomal cadherins (subfamily VI), and for Pcdhα/CNR protocadherins (subfamily VII). These interacting factors are listed at the right. It was recently shown that DE-cadherin is proteolytically cleaved within the NCCD domain during maturation (arrowhead)[95]. (NCCD, non-chordate classic cadherin domain; EGF, epidermal growth factor; LG, Laminin G)

formation of collagen gene clusters was caused by the evolution of a complex extracellular matrix, the nematode cuticle[17]. The amplification of cadherins in vertebrates might be explained by the more complex tissue interactions found in humans and other vertebrates compared with invertebrates, particularly the large increase in size and complexity in the central nervous system.

Structural basis of cell adhesion

Although it is broadly accepted that the predominant role of cadherins is to mediate adhesive interactions between cells, the mechanism of adhesive contact formation is still a matter of intense research. Structural studies have focused on vertebrate classic cadherins. These molecules are believed to form two types of dimers. Cadherins associate laterally within the same plasma membrane to form parallel *cis* dimers, and cadherins protruding from adjacent plasma membranes associate in an anti-parallel fashion to form *trans* dimers. The structure of the first CD of E-cadherin[18] and of N-cadherin[19] revealed that the cadherin fold consists of a seven-strand β-sheet with its amino and carboxyl termini located at opposite ends of the molecule (FIG. 1b). The crystal structures of peptides containing the first and second CDs (CD1 and CD2) of E-cadherin[20,21], or of N-cadherin[22], indicate that calcium is central in *cis*-dimer formation. Each dimer associates with six calcium ions through residues that are located in the linker region between CD1 and CD2 (FIG. 3a). Single amino-acid substitutions in the calcium binding sites can disrupt cell aggregation *in vivo*[23]. Calcium binding makes CDs arrange in a rigid structure [20,21,24,25] that is resistant to proteolysis[26].

Crystallographic analysis on the first and second CDs of E-cadherin and N-cadherin have provided clues as to how cadherin molecules induce lateral clustering essential for the formation of a stable adhesive interface between adjacent cells. Although different mechanisms underlying *cis* dimerization have been observed in the crystal structures of different cadherin molecules[19,20,22], an emerging theme is that two cadherin molecules form a *cis* dimer that functions as a building block for lateral clustering. These and other studies indicate that *cis* dimerization or more extensive lateral clustering is a prerequisite for stable cell adhesion[27–29]. Although *cis* dimers might primarily form as homodimers, the formation of functional *cis* heterodimers between N- and R-cadherin has been reported[30].

Adhesion between opposing cell membranes requires the formation of *trans* dimers (FIG. 3b). The mechanism of *trans*-dimer formation is, at present, controversial. Several studies indicate that *trans* dimers form by interactions between the amino-terminal CDs of opposing cadherin molecules[19,21,28,31]. These data are corroborated by early findings that located the homophilic binding specificity of classic cadherins within the amino-terminal CD[32,33]. On the basis of the crystal structure of the first CD from N-cadherin, a zipper model for *trans* dimerization was proposed that involved only the tip of the amino-terminal CD[19]. This model provided an early foundation for understanding the mechanics of the cell adhesion interface. However, the subsequent crystal structures of CD1 and CD2 from N-cadherin[22] and E-cadherin[20,21] did not show the adhesion interface seen in the first CD of N-cadherin. In addition, a recent biophysical study indicates a different type of *trans*-dimer association, in which the five CDs show variable degrees of lateral overlap, including the complete anti-parallel overlap of all five CDs (FIG. 3b)[34]. In the presence of calcium, the extracellular part of vertebrate classic cadherins forms a rod-like structure of about 20 nm in length with each individual CD spanning about 4.5 nm (REFS 19,20,25). Full lateral overlap of *trans* dimers would imply a distance between adjacent plasma membranes of 20–25 nm, a value consistent with the distance between plasma membranes at adherens junctions that is found in ultrastructural studies.

Adhesive contacts and adherens junctions

Two types of adhesive contacts are mediated by classic cadherins: diffuse adhesive contacts all along a cell–cell contact surface, and more discrete contacts by ultrastructurally defined adherens junctions, such as the

ZONULA ADHERENS
A cell–cell adherens junction that forms a circumferential belt around the apical pole of epithelial cells.

PDZ DOMAINS
Protein–protein interaction domain, first found in PSD-95, DLG and ZO-1.

SH3 DOMAINS
Src homology region 3 domains. Protein sequences of about 50 amino acids that recognize and bind sequences rich in proline.

FILOPODIUM
Finger-like exploratory cell extension found in crawling cells and growth cones.

LAMELLIPODIUM
Thin sheet-like cell extension found at the leading edge of crawling cells or growth cones

ZONULA ADHERENS. Diffuse adhesive contacts probably involve the oligomerization of cadherin *trans* dimers, as individual *trans* dimers provide little adhesive strength[25,29]. Adherens junctions could simply represent very large arrays of *trans* dimers. However, the situation seems to be more elaborate, as cadherins might not be the principal components of adherens junctions, at least in some cases. Indeed, adherens junctions can form in the absence of Hmr-1 cadherin, the only classic cadherin in *C. elegans*, or in the absence of its associated catenins[35,36]. In mouse and *Drosophila* embryos, where E-cadherin or DE-cadherin, respectively, are essential for adherens junction assembly and epithelial integrity, markedly reduced levels of these cadherins can still support the formation of normally sized adherens junctions[37–39]. These observations are inconsistent with a model in which adherens junctions simply represent a large array of cadherins and associated cytoplasmic proteins. Instead, cadherin *trans* dimers probably form small clusters separated by other proteins, and the density of these clusters in the adherens junctions may vary considerably without affecting the size of the adherens junction. A novel protein complex has recently been characterized that is concentrated at adherens junctions[40–42]. This complex is composed of Nectin, a transmembrane protein of the immunoglobulin superfamily that interacts with the PDZ-DOMAIN protein Afadin, which in turn can bind to Ponsin, a protein containing three SH3 DOMAINS (FIG. 4a). This complex can interact with the actin cytoskeleton. Nectin and cadherin complexes interact with each other and are recruited together to adherens junctions[43]. Initial functional studies indicate that Afadin is important for junctional organization and epithelial integrity[44]. So adherens junctions contain two complexes that interact with each other and with the actin cytoskeleton.

Cell and tissue polarity

Epithelial cells provide a clear example of cell polarity, with various molecules, including proteins, sorting to distinct apical and basolateral membrane domains. The crucial role of classic cadherins and their associated catenins in epithelial differentiation has been well documented, and these protein complexes seem to be broadly important for forming and maintaining epithelial tissues[45,46]. Conversely, downregulation of classic cadherins, such as E-cadherin or DE-cadherin, is often associated with a loss of epithelial morphology during normal development and in many carcinomas. The zinc-finger transcription factor Snail is important for repressing the expression of DE-cadherin and E-cadherin in non-epithelial cells[47–49].

Epithelial cells usually form a continuous tissue structure. However, at certain times during normal development, or in experimental cell-culture models, epithelial cells have free edges that approach each other to establish new lateral contacts[36,50,51]. The initial contact between cells is made by FILOPODIA or LAMELLIPODIA, and such contacts are stabilized by classic cadherins. When these contacts broaden, cadherins concentrate in discrete puncta. The adhesive interactions are further stabilized through linkage of cadherins to the cytoskeleton and, eventually, by the formation of mature adherens junctions. Cadherin-mediated adhesion leads to

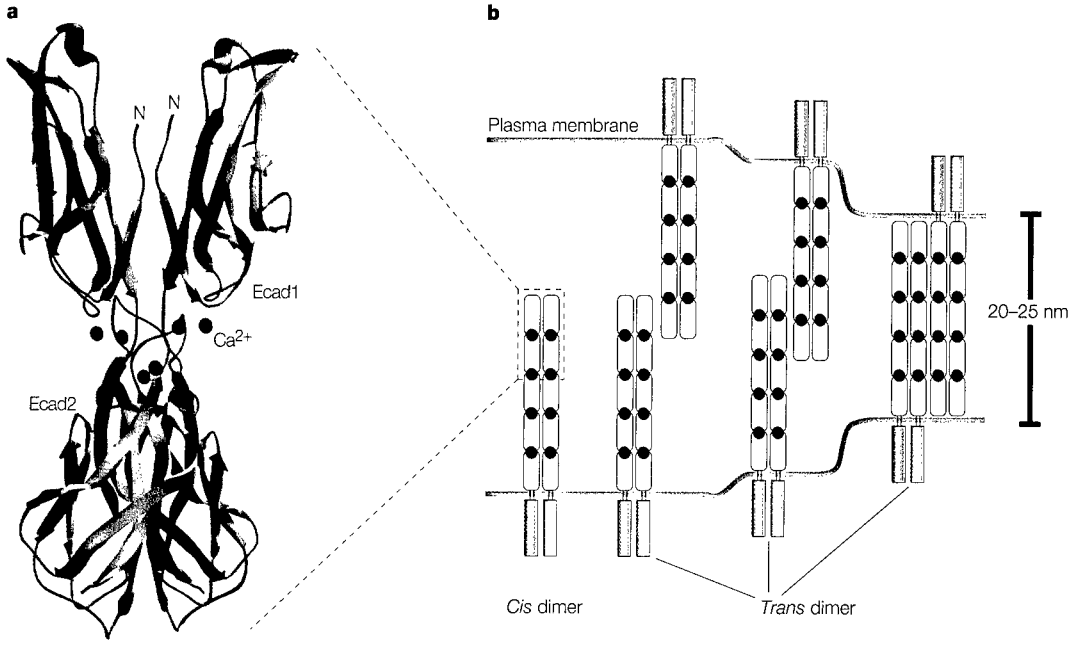

Figure 3 | **Ca^{2+}-mediated *cis*- and *trans*-dimer formation of vertebrate classic cadherins. a** | Dimer interface between two N-terminal repeats of E-cadherin domains 1 (Ecad1) and 2 (Ecad2). Each cadherin molecule binds three calcium ions that are important in the rigidification and *cis*-dimer association of cadherins[20,21]. **b** | A *cis* dimer consists of two cadherin molecules within the same plasma membrane that are associated laterally. The pairs of cadherin molecules from opposing cells that associate with one another are referred to as *trans* dimers. Different models for *trans*-dimer formation have been proposed that suggest different extents of lateral overlap between the extracellular regions. Red dots indicate the location of Ca^{2+} ions between adjacent CDs.

FOLLICLE CELLS
In this review, the term follicle cells refers to cells that surround the developing insect egg and secrete the egg membranes, the chorion and vitelline envelope.

GASTRULATION
Series of morphogenetic movements observed during the early development of most animals that leads to the formation of a multilayered embryo with an outer cell layer (ectoderm), an inner cell layer (endoderm), and an intermediate cell layer (mesoderm).

recruitment of specific cytoskeletal factors, such as the actin-associated factor Mena[51] and other transmembrane proteins, to cell–cell contact sites[46].

Cadherins seem to be directly involved in maintaining cell polarity by directing the localization of the sec6/8 complex, which specifies vesicle targeting to the lateral membrane[52]. This recruitment, and the continuous polarized delivery of specific molecular components to the lateral membrane, establishes and maintains the lateral membrane domain of epithelial cells and contributes to epithelial apical–basal polarity[46,52]. Interestingly, in fully polarized epithelial cells, the sec6/8 complex is not found along the entire lateral membrane but is concentrated in close association with apical adherens junctions, indicating a potentially direct molecular link between the cadherin–catenin complex and the vesicle targeting machinery (FIG. 4a)[52].

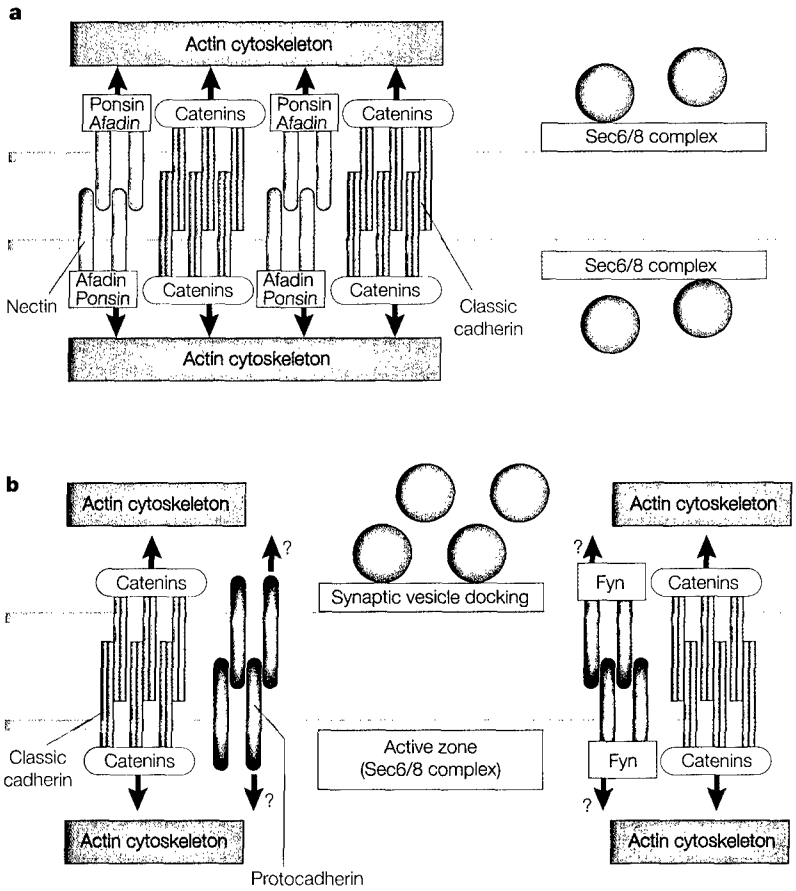

Figure 4 | **Comparison between cadherin-mediated adhesive interactions at epithelial and synaptic adherens junctions. a** | Schematic of the zonula adherens, a circumferential adherens junction found in epithelial cells. This junction contains the classic cadherin–catenin complex and the recently identified nectin/afadin/ponsin complex[40–42]. Both complexes interact with the actin cytoskeleton and with each other[10,43]. The zonula adherens is closely associated with a vesicle docking site that contains the Sec6/8 complex[52]. **b** | At the interneuronal synapse, we also find a close association between adherens junctions and vesicle docking zones. The sec6/8 complex was found to associate with the postsynaptic membrane only during synaptogenesis[96]. The classic cadherin–catenin complex is a principal component of synaptic adherens junctions similar to the zonula adherens. Protocadherins that localize to synapses include Arcadlin[84] and the Pcdhα/CNR protocadherins[75]. Whether protocadherins contribute to synaptic adhesion remains to be established. The Pcdhα/CNR protocadherins interact with the cytoplasmic protein kinase Fyn, and seem to reside within the active zone, indicating that they might have a primary role in signalling rather than adhesion[13,75].

In addition to their role in apical–basal polarity, cadherin superfamily members were recently implicated in a second form of cell polarity called planar epithelial polarity (FIG. 5). This property is found in many epithelia. One example is the fly wing epithelium, where each cell polarizes its actin cytoskeleton along the proximal–distal axis, such that a bundle of actin filaments polymerizes and projects from the surface at the distal-most vertex of each cell, ultimately forming a wing hair (FIG. 5a). Genes involved in establishing the planar polarity of the wing epithelium include components of the Wnt/Frizzled signalling pathway, Frizzled and Dishevelled[53], and three different cadherins, Fat, Dachsous[54] and Flamingo/Starry Night[55,56]. Although the mechanism by which cadherins affect planar polarity is unknown, it was found that Flamingo/Starry Night adopts an asymmetric distribution during polarity establishment, becoming enriched at the proximal and distal cell surfaces (FIG. 5b)[55]. Planar polarity also influences polymerization of the microtubule cytoskeleton, manifesting itself through orientation of the mitotic spindle and thereby the axis of cell division along the body axes. Studies in both *C. elegans* and *Drosophila* implicate the Wnt/Frizzled pathway in this process[53]. Many planar polarity genes have not been examined in this context, but it is at least clear that Flamingo/Starry Night is essential for spindle orientation[57].

Two other examples that highlight important roles of cadherins in generating asymmetric tissue organization are the contribution of DE-cadherin to the formation of the anterior–posterior axis in *Drosophila*, and the function of N-cadherin in setting up left–right asymmetry in the chick. A cell sorting process that is driven by different levels of DE-cadherin directs the oocyte to the posterior pole of the egg chamber during *Drosophila* oogenesis[8,58]. This highly reproducible positioning event allows the oocyte to interact with a specific group of FOLLICLE CELLS, thereby initiating a cascade of cell interactions that are crucial for the formation of the embryonic anterior–posterior axis. Disruption of the function of N-cadherin during chick GASTRULATION leads to a random orientation of the heart along the left–right axis[59]. Asymmetric N-cadherin expression and cell movements that prefigure the position of the heart and other organs along the left–right axis are seen during gastrulation. How N-cadherin contributes to these asymmetric cell movements remains a mystery.

Cell movement

Many of the changes in cell shape or movement observed during development occur while cells are in direct contact and require, therefore, dynamic changes in adhesive interactions. These changes may play a permissive role, as the release of adhesion is important for the relative movement of cells that are in contact. However, adhesive interactions also directly promote movement, as traction must be generated between cells for cell rearrangements to occur in solid tissues. To determine whether changes in cadherin activity play a permissive or a more active role can be difficult, as illustrated by the analysis of C-cadherin function during

NEUROEPITHELIUM
Epithelial layer of cells that gives rise to the nervous system.

NEURULATION
Morphogenetic process during which the progenitors of the nervous system segregate from the ectoderm.

convergent extension movements in *Xenopus* gastrulation. In this process, cells move towards the dorsal midline of the embryo, thereby rearranging by cell intercalation, leading to an extension of the embryo along the anterior–posterior axis (FIG. 6a)[60]. Adhesion mediated by the classic cadherin C-cadherin must be reduced to permit these movements to occur[61]. However, the disruption of C-cadherin activity causes defects not only during gastrulation movements, but also in tissue structure[62], raising the possibility that the disruptions in cell movement might be a secondary consequence of a compromised cell architecture. Similar difficulties have emerged from the analysis of DE-cadherin in embryonic morphogenesis where its role in epithelial maintenance might mask a function in promoting cell rearrangements[37,38].

Paraxial protocadherin (PAPC) seems to be directly involved in convergent extension in *Xenopus* and zebrafish embryos, where it is expressed in the mesoderm during gastrulation[63,64]. PAPC, which can promote homotypic cell adhesion, is required for convergent extension of the mesoderm. Notably, overexpression of PAPC can promote convergent extension under certain experimental conditions[63]. These findings argue that PAPC acts as an adhesion receptor that directly promotes cell movement, perhaps providing traction needed for cell motility. Alternative and non-exclusive possibilities are that PAPC is primarily a signalling receptor, as was suggested for other protocadherins[13]. PAPC activity might also generate the tissue polarization that is observed during convergent extension (FIG. 6a)[60,63], functioning similarly to the activity of other cadherins in planar epithelial polarization, outlined above. Intriguingly, cell polarization during convergent extension resembles planar polarity in that it also requires Wnt/Frizzled signalling[65–67].

The requirement for DE-cadherin in cell migration during *Drosophila* oogenesis is a convincing example for a direct role of classic cadherins in cell migration on a cellular substrate. DE-cadherin is involved in the migration of a small group of somatic cells, the 'border' cells, on the surface of the much larger germline cells[68] (FIG. 6b). It is required in both the somatic and germline cells for this movement to occur. DE-cadherin is not required for the formation of the border cell cluster and, more importantly, is not required for maintaining integrity of the border cell cluster during migration. In the case of integrin-based cell migration, it was shown that intermediate levels of adhesion to the substrate promotes maximal migration speed, with both positive and negative deviations slowing or halting motility[69]. Similarly, reduction in the level of DE-cadherin reduces the speed of border cell migration[68], indicating that DE-cadherin might not have just a permissive role, but might be the key adhesion molecule that provides traction for border cells to travel over germline cells.

Organization of the nervous system

Various cadherins are expressed in the nervous system in complex patterns. The first example was N-cadherin, which is broadly expressed in the NEUROEPITHELIUM, beginning at NEURULATION. This expression pattern led to the speculation that N-cadherin might be critical for the segregation of neural and epidermal tissues during neural tube formation. However, an essential role in neurulation was disproved by the knockout of mouse *N-cadherin*[70]. After neurulation, but before neuronal differentiation, many classic cadherins, including N-cadherin, are expressed in the developing central nervous system (CNS) in a region-specific manner that often coincides with morphological boundaries[71]. The most direct evidence that these cadherins contribute to the subdivision of the neuroepithelium has come from analysis of the *Xenopus* type II classic cadherin F-cadherin[72]. The expression of F-cadherin confines neuroepithelial cells to the sulcus limitans, a region separating the dorsal and ventral halves of the caudal neural tube. One apparent consequence of F-cadherin expression in

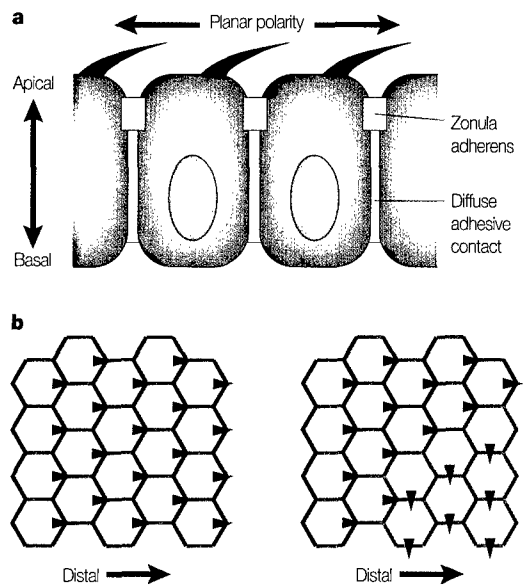

Figure 5 | **Cadherins in apicobasal and planar epithelial polarity. a** | The example depicted here is the wing epithelium of *Drosophila melanogaster*, shown in cross section. Classic cadherins mediate lateral cell contacts (yellow) between epithelial cells that can take the form of either a diffuse adhesive contact, or an adherens junction, such as the zonula adherens, that can be seen in electron micrographs as an electron-dense specialization of the plasma membrane. Epithelial sheets are obviously different across their apical–basal axis, but many epithelial cells can also discern directions in the plane of the epithelium with respect to the organ or body axis of which they are a part. They use this information to polarize their actin and microtubule cytoskeletons along this axis. The most obvious indication of planar polarity in the wing epithelium is the hair that is formed by each cell. Hairs emerge from a distal region of the apical cell surface and all point distally. **b** | The array of cells in a *Drosophila* wing epithelium, viewed from above. A wild-type array is shown on the left, illustrating the uniform planar polarity (wing hair orientation) and the distribution of Flamingo/Starry Night (green), which accumulates at the proximal and distal surfaces of every cell. The right array shows a group of cells that contain Flamingo/Starry Night mutant cells (absence of green), in which the orientation of wing hairs and therefore the axis of planar polarity has shifted[55,56].

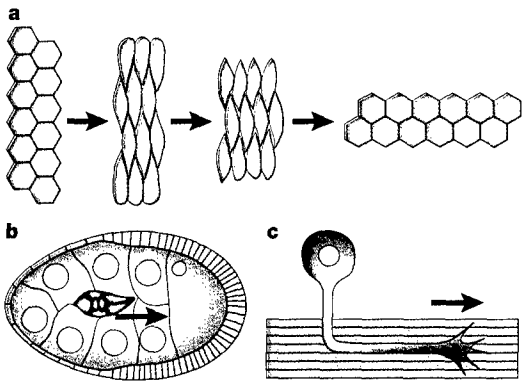

Figure 6 | **Cell movements that involve cadherins. a** | Convergent extension is a cell rearrangement that involves the transient polarization of cells, which then move, converging towards the centre of the tissue. Cell intercalation leads to an extension of the tissue perpendicular to the axis of convergence. This movement is seen, for example, during frog gastrulation, where it may involve C-cadherin and paraxial protocadherin[61,63]. **b** | The border cell cluster (green) is a small group of *Drosophila* follicle cells that migrate on the surface of much larger germline cells (green/yellow). This movement is driven by DE-cadherin, which is required in both border cells and germline cells[68]. **c** | N-cadherin and DN-cadherin mediate the movement of neuronal growth cones (red) on cellular substrates such as axon bundles (green)[76–78].

the sulcus limitans is that these cells remain a coherent group and do not participate in the extensive cell rearrangments that take place during neurulation.

Protocadherins also contribute to CNS regionalization by controlling the migration of neurons that will organize into different cortical layers during brain morphogenesis. Although cadherins, including protocadherins, are generally viewed as homophilic adhesion molecules, recent work indicates that the Pcdhα/CNR protocadherins might also function as receptors or co-receptors for extracellular ligands in the brain[13,73]. This work began with studies of the secreted molecule Reelin, identified because mutant mice have a marked behavioural disorder. Two protein families have been shown to function as reelin receptors, perhaps as a heteromeric complex: members of the LDL-receptor-related protein family, which couple to the cytoplasmic adaptor protein mDab1; and members of the Pcdhα/CNR family, which bind the non-receptor tyrosine kinase Fyn[73,74]. As Pcdhα/CNR protocadherins show considerable molecular diversity and differential expression patterns within local brain areas, it is possible that Reelin receptor complexes that contain different Pcdhα/CNR protocadherins are instructive in positioning and differentiating neuronal sub-populations within the cortex[73,75].

Classic cadherins are also important during the outgrowth of NEURITES and during axonal patterning and FASCICULATION (FIG. 6c). Early studies that indicated that N-cadherin can function as a substrate for neurite extension in cultured cells were reinforced by the finding that N-cadherin is required for the normal outgrowth and guidance of retinal axons[76,77]. In *Drosophila*, DN-cadherin is the only classic cadherin expressed in the developing embryonic CNS[78]. Null mutations in *DN-cadherin* and the *Drosophila* catenin gene *armadillo* affect axon outgrowth, although in a mild fashion, with many axons finding their targets appropriately[78,79]. In this respect, cadherins resemble various other axon guidance cues that direct axon outgrowth in a combinatorial fashion, with individual cues having subtle functions[9]. In addition, it was recently found that the patterning of dendrites that extend from *Drosophila* sensory neurons requires Flamingo/Starry Night[80].

Both classic and protocadherins localize to synapses, indicating that they may contribute to the generation of adhesive specificity needed to build complex neural networks[75,81–84]. The synapse is an adhesive contact between two neurons, with the transmitter release zone framed by adherens junctions that are ultrastructurally similar to epithelial adherens junctions, and that share with them the cadherin–catenin complex as a principal molecular component (FIG. 4b)[82,83]. In synapses, as in epithelial cells, adherens junctions are closely associated with vesicle-release zones (FIG. 4). It is believed that classic cadherins are important during synaptic adhesion, whereas the adhesive role of protocadherins at synapses remains to be clarified. Recent intriguing evidence indicates that synaptic activity can change the distribution and adhesive state of N-cadherin[85]. Cadherins, in turn, can influence synaptic activity[84,86,87]. These findings indicate an intimate relationship between synaptic adhesion and activity, raising the possibility that cadherins are important regulators of synaptic plasticity and activity modulation[13,89].

Some classic cadherins, such as cadherin-6, are expressed in groups of neurons that form neural circuits, indicating that cadherins might functionally integrate such neural circuits[71,90]. Protocadherins are also expressed in divergent and restricted patterns in the CNS, indicating that they might have a function in integrating neural circuits[91,92]. Moreover, the protocadherin genes *Pcdhα*, *Pcdhβ* and *Pcdhγ* can give rise to over 50 protocadherins[18] and the Pcdhα/CNR proteins have a differential expression pattern within individual brain areas[75]. These findings raise the possibility that a 'cadherin code' exists, which could identify individual neurons and their synaptic contacts[75,89], although neurexins and immunoglobulin-type adhesion receptors have also been proposed to contribute to synaptic specificity[93,94]. The structures of the *Pcdhα*, *Pcdhβ* and *Pcdhγ* genes show provocative similarities to the gene organization of immunoglobulins or T-cell receptors, which has led to the proposal that gene rearrangement might function in determining protocadherin expression patterns[13,15,16], a speculation that remains to be proved.

The future

The analysis of cadherins emphasizes the similarities between embryonic and neural morphogenesis. Cadherins have emerged as the predominant group of cell–cell adhesion molecules involved in embryonic morphogenesis, determining cell and tissue architecture, and controlling dynamic changes in cell shape and position. The role of individual cadherins in several specific morphogenetic processes has been determined, which

NEURITE
Process extended by a nerve cell that can give rise to an axon or a dendrite.

FASCICULATION
Bundling of axonal processes of neurons.

will now allow the study of how the adhesive activity of cadherins is modulated by cell signalling to facilitate coordinated cell behaviour. Cadherins are also important during neural morphogenesis, although the functional significance of cadherins in neural development remains less well understood. One important challenge will be to determine the exact mechanism underlying the specificity and stability of cadherin-mediated cell–cell adhesion, and to explore the variation in adhesive mechanisms and cellular responses of different types of cadherins. A second important challenge will be to substantiate the conjecture that cadherins provide an adhesive code that controls synaptic specificity. Elucidating whether and how different families of adhesion receptors cooperate in this process will represent an enormous advance in our understanding of complex neural network formation.

Links

DATABASE INFORMATION | Cadherin domain | Cadherins | RET | Protocadherins | EGF-like domain | LG domain | E-cadherin | N-cadherin | R-cadherin | Catenins | DE-cadherin | Nectin | Afadin | Ponsin | Snail | Mena | Frizzled | Disheveled | Fat | Dachsous | Flamingo/ Starry night | Reelin | LDL-receptor | mDab1 | Fyn | DN-Cadherin | Armadillo | Cadherin-6 | Pcdhα | Pcdhβ | Pcdhγ | Neurexin

FURTHER INFORMATION The cadherin resource | Godt and Tepass labs *Drosophila* cadherin resource | Cadherin web site at the LMB, Cambridge | Pfeifer lab page | Ikura lab page | Godt lab page | Tepass lab page

ENCYCLOPEDIA OF LIFE SCIENCES Adhesive specificity and the evolution of multicellularity

1. Steinberg, M. S. Reconstruction of tissue by dissociated cells. *Science* **141**, 401–408. (1963).
2. Sperry, R. W. Chemoaffinity in the orderly growth of nerve fiber patterns and connections. *Proc. Natl Acad. Sci. USA* **50**, 703–710 (1963).
3. Gumbiner, B. M. Cell adhesion: The molecular basis of tissue architecture and morphogenesis. *Cell* **84**, 345–579 (1996).
4. Hynes, R. O. Cell adhesion: Old and new questions. *Trends Cell Biol.* **9**, M33–M37 (1999).
5. Townes, P. L. & Holtfreter, J. Directed movements and selective adhesion of embryonic amphibian cells. *J. Exp. Zool.* **128**, 53–120 (1955).
6. Nose, A., Nagafuchi, A, & Takeichi, M. Expressed recombinant cadherins mediate cell sorting in model systems. *Cell* **54**, 993–1001 (1988).
   This paper shows for the first time cadherin-mediated cell sorting in cell-culture cells.
7. Steinberg, M. S. & Takeichi, M. Experimental specification of cell sorting, tissue spreading, and specific spatial patterning by quantitative differences in cadherin expression. *Proc. Natl Acad. Sci. USA* **91**, 206–209 (1994).
8. Godt, D. & Tepass, U. *Drosophila* oocyte localization is mediated by differential cadherin-based adhesion. *Nature* **395**, 387–391 (1998).
   This paper documents for the first time an *in vivo* cell sorting process that is driven by differential expression of a cadherin.
9. Tessier-Lavigne, M. & Goodman, C. S. The molecular biology of axon guidance. *Science* **274**, 1123–1133 (1996).
10. Takeichi, M. Cadherin cell adhesion receptors as a morphogenetic regulator. *Science* **251**, 1451–1455 (1991).
11. Wong, E. F. S., Brar, S. K., Sesaki, H., Yang, C. & Siu, C. H. Molecular cloning and characterization of DdCAD-1, a Ca^{2+}-dependent cell–cell adhesion molecule, in *Dictyostelium discoideum*. *J. Biol. Chem.* **271**, 16399–16408 (1996).
12. Gallin, W. J. Evolution of the 'classical' cadherin family of cell adhesion molecules in vertebrates. *Mol. Biol. Evol.* **15**, 1099–1107 (1998).
13. Yagi, T. & Takeichi, M. Cadherin superfamily genes: Functions, genomic organization, and neurologic diversity. *Genes Dev.* **14**, 1169–1180 (2000).
14. Nollet, F., Kools, P. & van Roy, F. Phylogenetic analysis of the cadherin superfamily allows identification of six major subfamilies besides several solitary members. *J. Mol. Biol.* **299**, 551–72 (2000).
15. Wu, Q. & Maniatis, T. A. striking organization of a large family of human neural cadherin-like cell adhesion genes. *Cell* **97**, 779–790 (1999).
16. Sugino, H. *et al.* Genomic organization of the family of CNR cadherin genes in mice and humans. *Genomics* **63**, 75–87 (2000).
17. Hutter, H. *et al.* Conservation and novelty in the evolution of cell adhesion and extracellular matrix genes. *Science* **287**, 989–994 (2000).
18. Overduin, M. *et al.* Solution structure of the epithelial cadherin domain responsible for selective cell adhesion. *Science* **267**, 386–389 (1995).
19. Shapiro, L. *et al.* Structural basis of cell–cell adhesion by cadherins. *Nature* **374**, 327–337 (1995).
20. Nagar, B., Overduin, M., Ikura, M. & Rini, J. M. Structural basis of calcium-induced E–cadherin rigidification and dimerization. *Nature* **380**, 360–364 (1996).
    This is one of several papers (see also refs 18–26,31) that describe the three-dimensional structure of the cadherin domain, and analyse the role of calcium ions in the formation of cadherin dimers.
21. Pertz, O. *et al.* A new crystal structure, Ca^{2+} dependence and mutational analysis reveal molecular details of E–cadherin homoassociation. *EMBO J.* **18**, 1738–1747 (1999).
22. Tamura, K., Shan, W. S., Hendrickson, W. A., Colman, D. R. & Shapiro, L. Structure–function analysis of cell adhesion by neural (N-) cadherin. *Neuron* **20**, 1153–1163 (1998).
23. Ozawa, M., Engel, J. & Kemler, R. Single amino acid substitutions in one Ca^{2+} binding site of uvomorulin abolish the adhesive function. *Cell* **63**,1033–1038 (1990).
24. Pokutta, S., Herrenknecht, K., Kemler, R. & Engel, J. Conformational changes of the recombinant extracellular domain of E–cadherin upon calcium binding. *Eur. J. Biochem.* **223**, 1019–1026 (1994).
25. Baumgartner, W. *et al.* Cadherin interaction probed by atomic force microscopy. *Proc. Natl Acad. Sci. USA* **97**, 4005–4010 (2000).
26. Hyafil, F., Babinet, C. & Jacob, F. Cell–cell interactions in early embryogenesis: a molecular approach to the role of calcium. *Cell* **26**, 447–454 (1981)
27. Brieher, W. M., Yap, A. S., & Gumbiner, B. M. Lateral dimerization is required for the homophilic binding activity of C-cadherin. *J. Cell Biol.* **135**, 487–496 (1996).
28. Alattia, J. R. *et al.* Lateral self-assembly of E-cadherin directed by cooperative calcium binding. *FEBS Lett.* **417**, 405–408 (1997).
29. Yap, A. S., Brieher, W. M., Pruschy, M. & Gumbiner, B. M. Lateral clustering of the adhesive ectodomain: a fundamental determinant of cadherin function. *Curr. Biol.* **7**, 308–315 (1997).
30. Shan, W. S. *et al.* Functional *cis*-heterodimers of N- and R-cadherins. *J. Cell Biol.* **148**, 579–590 (2000).
31. Tomschy, A., Fauser, C., Landwehr, R. & Engel, J. Homophilic adhesion of E-cadherin occurs by a co-operative two-step interaction of N–terminal domains. *EMBO J.* **15**, 3507–3514 (1996).
32. Nose, A., Tsuji, K. & Takeichi, M. Localization of specificity determining sites in cadherin cell adhesion molecules. *Cell* **61**,147–155 (1990).
33. Blaschuk, O. W., Sullivan, R., David, S. & Pouliot, Y. Identification of a cadherin cell adhesion recognition sequence. *Dev. Biol.* **139**, 227–229 (1990).
34. Sivasankar, S., Brieher, W., Lavrik, N., Gumbiner, B. & Leckband, D. Direct molecular force measurements of multiple adhesive interactions between cadherin ectodomains. *Proc. Natl Acad. Sci. USA* **96**, 11820–11824 (1999).
    A recent paper that suggests a new model of cadherin *trans*-dimer formation.
35. Costa, M. *et al.* A putative catenin–cadherin system mediates morphogenesis of the *Caenorhabditis elegans* embryo. *J. Cell Biol.* **141**, 297–308 (1998).
36. Raich, W. B., Agbunag, C. & Hardin, J. Rapid epithelial-sheet sealing in the *Caenorhabditis elegans* embryo requires cadherin-dependent filopodial priming. *Curr. Biol.* **9**, 1139–1146 (1999).
    This paper analyses the dynamics of cadherin-dependent contact formation between epithelial cells during *C. elegans* embryogenesis.
37. Uemura, T. *et al.* Zygotic *Drosophila* E-cadherin expression is required for processes of dynamic epithelial cell rearrangement in the *Drosophila* embryo. *Genes Dev.* **10**, 659–671 (1996).
38. Tepass, U. *et al. shotgun* encodes *Drosophila* E–cadherin and is preferentially required during cell rearrangement in the neuroectoderm and other morphogenetically active epithelia. *Genes Dev.* **10**, 672–685 (1996).
39. Ohsugi, M., Larue, L., Schwarz, H. & Kemler, R. Cell-junctional and cytoskeletal organization in mouse blastocysts lacking E-cadherin. *Dev. Biol.* **185**, 261–271 (1997).
40. Mandai, K. *et al.* Afadin: A novel actin filament-binding protein with one PDZ domain localized at cadherin-based cell-to-cell adherens junction. *J. Cell Biol.* **139**, 517–528 (1997).
41. Mandai, K. *et al.* Ponsin/SH3P12: An l-afadin- and vinculin-binding protein localized at cell-cell and cell-matrix adherens junctions. *J. Cell Biol.* **144**, 1001–1017 (1999).
42. Takahashi, K. *et al.* Nectin/PRR: An immunoglobulin-like cell adhesion molecule recruited to cadherin-based adherens junctions through interaction with Afadin, a PDZ domain-containing protein. *J. Cell Biol.* **145**, 539–549 (1999).
    One of a series of papers (refs 40–44) that describe a new protein complex that localizes to adherens junctions, and that might interact with the cadherin–catenin complex functionally.
43. Tachibana, K. *et al.* Two cell adhesion molecules, nectin and cadherin, interact through their cytoplasmic domain-associated proteins. *J. Cell Biol.* **150,** 1161–1175 (2000).
44. Ikeda, W. *et al.* Afadin: A key molecule essential for structural organization of cell–cell junctions of polarized epithelia during embryogenesis. *J. Cell Biol.* **146**, 1117–1132 (1999).
45. Tepass, U. Genetic analysis of cadherin function in animal morphogenesis. *Curr. Opin. Cell Biol.* **11**, 540–548 (1999).
46. Yeaman, C., Grindstaff, K. K. & Nelson, W. J. New perspectives on mechanisms involved in generating epithelial cell. *Phys. Rev.* **79**, 73–98 (1999).
47. Oda, H., Tsukita, S. & Takeichi, M. Dynamic behavior of the cadherin-based cell–cell adhesion system during *Drosophila* gastrulation. *Dev. Biol.* **203**, 435–450 (1998).
48. Cano, A. *et al.* The transcription factor *snail* controls epithelial–mesenchymal transitions by repressing E-cadherin expression. *Nature Cell Biol.* **2**, 76–83 (2000).
49. Batlle, E. *et al.* The transcription factor snail is a repressor of E–cadherin gene expression in epithelial tumour cells. *Nature Cell Biol.* **2**, 84–89 (2000).
50. Adams, C. L. *et al.* Mechanisms of epithelial cell–cell adhesion and cell compaction revealed by high-resolution tracking of E-cadherin–green fluorescent protein. *J. Cell Biol.* **142**, 1105–1119 (1998).
51. Vasioukhin, V., Bauer, C., Yin, M. & Fuchs, E. Directed actin polymerization is the driving force for epithelial cell–cell adhesion. *Cell* **100**, 209–219 (2000).
52. Grindstaff, K. K. *et al.* Sec6/8 complex is recruited to cell–cell contacts and specifies transport vesicle delivery to the basal–lateral membrane in epithelial cells. *Cell* **93**, 731–740 (1998).
    This paper shows a close association between the sec6/8 complex, which is involved in lateral vesicle targeting, and cadherin-based adherens junctions.
53. Peifer, M. & Polakis, P. Wnt signaling in oncogenesis and embryogenesis — a look outside the nucleus. *Science* **287**, 1606–1609 (2000).
54. Adler, P. N., Charlton, J. & Liu, J. Mutations in the cadherin superfamily member gene *dachsous* cause a tissue

polarity phenotype by altering Frizzled signaling. *Development* **125**, 959–968 (1998).
55. Usui, T. *et al.* Flamingo, a seven-pass transmembrane cadherin, regulates planar cell polarity under the control of Frizzled. *Cell* **98**, 585–595 (1999).
56. Chae, J. *et al.* The *Drosophila* tissue polarity gene starry night encodes a member of the protocadherin family. *Development* **126**, 5421–5429 (1999).
References 55 and 56 show a role for the Flamingo/Starry Night cadherin in planar epithelial polarity. Reference 55 also shows that the subcellular distribution of Flamingo/Starry Night depends on the direction of Wnt/Frizzled signalling.
57. Lu, B., Usui, T., Uemura, T., Jan, L. & Jan, Y. N. Flamingo controls the planar polarity of sensory bristles and asymmetric division of sensory organ precursors in *Drosophila*. *Curr. Biol.* **9**, 1247–1250 (1999).
58. Gonzalez-Reyes, A. & St Johnston, D. The *Drosophila* AP axis is polarised by the cadherin-mediated positioning of the oocyte. *Development* **125**, 3635–3644 (1998).
59. Garcia-Castro, M. I., Vielmetter, E. & Bronner-Fraser, M. N-Cadherin, a cell adhesion molecule involved in establishment of embryonic left–right asymmetry. *Science* **288**, 1047–1051 (2000).
60. Shih, J. & Keller, R. Cell motility driving mediolateral intercalation in explants of *Xenopus laevis*. *Development* **116**, 901–914 (1992).
61. Zhong, Y., Brieher, W. M. & Gumbiner, B. M. Analysis of C-cadherin regulation during tissue morphogenesis with an activating antibody. *J. Cell Biol.* **144**, 351–359 (1999).
62. Lee, C. H. & Gumbiner, B. M. Disruption of gastrulation movements in *Xenopus* by a dominant-negative mutant for C-cadherin. *Dev. Biol.* **171**, 363–373 (1995).
63. Kim, S. H., Yamamoto, A., Bouwmeester, T., Agius, E. & Robertis, E. M. The role of paraxial protocadherin in selective adhesion and cell movements of the mesoderm during *Xenopus* gastrulation. *Development* **125**, 4681–4690 (1998).
Experiments in this paper indicate an important role for a protocadherin in the convergent extension movements during frog gastrulation.
64. Yamamoto, A. *et al.* Zebrafish paraxial protocadherin is a downstream target of *spadetail* involved in morphogenesis of gastrula mesoderm. *Development* **125**, 3389–3397 (1998).
65. Heisenberg, C. P. *et al.* Silberblick/Wnt11 mediates convergent extension movements during zebrafish gastrulation. *Nature* **405**, 76–81 (2000).
66. Wallingford, J. B. *et al.* Dishevelled controls cell polarity during *Xenopus* gastrulation. *Nature* **405**, 81–85 (2000).
67. Tada, M. & Smith, J. C. Xwnt11 is a target of *Xenopus brachyury*: regulation of gastrulation movements via *dishevelled*, but not through the canonical *wnt* pathway. *Development* **127**, 2227–2238 (2000).
68. Niewiadomska, P., Godt, D. & Tepass, U. DE-cadherin is required for intercellular motility during *Drosophila* oogenesis. *J. Cell Biol.* **144**, 533–547 (1999).
This paper documents a cadherin-dependent cell migration process.
69. Palecek, S. P., Loftus, J. C., Ginsberg, M. H., Lauffenburger, D. A. & Horwitz, A. F. Integrin-ligand binding properties govern cell migration speed through cell-substratum adhesiveness. *Nature* **385**, 537–540 (1997).
70. Radice, G. L. *et al.* Developmental defects in mouse embryos lacking N-cadherin. *Dev. Biol.* **181**, 64–78 (1997).
71. Redies, C. Cadherins in the central nervous system. *Prog. Neurobiol.* **61**, 611–648 (2000).
72. Espeseth, A., Marnellos, G. & Kintner, C. The role of F-cadherin in localizing cells during neural tube formation in *Xenopus* embryos. *Development* **125**, 301–312 (1998).
73. Senzaki, K., Ogawa, M. & Yagi, T. Proteins of the CNR family are multiple receptors for Reelin. *Cell* **99**, 635–647 (1999).
Protocadherins of the CNR family are identified as receptors of the extracellular matrix protein Reelin, an interaction that might contribute to the migration and differentiation of neurons within the brain cortex.
74. Gilmore, E. C. & Herrup, K. Cortical development: receiving *reelin*. *Curr. Biol.* **10**, R162–R166 (2000).
75. Kohmura, N. *et al.* Diversity revealed by a novel family of cadherins expressed in neurons at a synaptic complex. *Neuron* **20**, 1137–1151 (1998).
This paper identifies a closely related group of protocadherins that are differentially expressed in the brain and localize to synapses.
76. Riehl, R. *et al.* Cadherin function is required for axon outgrowth in retinal ganglion cells *in vivo*. *Neuron* **17**, 837–848 (1996).
77. Inoue, A. & Sanes, J. R. Lamina-specific connectivity in the brain: Regulation by N-cadherin, neurotrophins, and glycoconjugates. *Science* **276**, 1428–1431 (1997).
78. Iwai, Y. *et al.* Axon patterning requires DN-cadherin, a novel neuronal adhesion receptor, in the *Drosophila* embryonic CNS. *Neuron* **19**, 77–89 (1997).
79. Loureiro, M. *et al.* Anomalous origin of the left pulmonary artery (Sling): A case report and review of the literature. *Rev. Port. Cardiol.* **17**, 811–815 (1998).
80. Gao, F. B., Brenman, J. E., Jan, L. Y. & Jan, Y. N. Genes regulating dendritic outgrowth, branching, and routing in *Drosophila*. *Genes Dev.* **13**, 2549–2561 (1999).
81. Yamagata, M., Herman, J. P. & Sanes, J. R. Lamina-specific expression of adhesion molecules in developing chick optic tectum. *J. Neurosci.* **15**, 4556–4571 (1995).
82. Fannon, A. M. & Colman, D. R. A model for central synaptic junctional complex formation based on the differential adhesive specificities of the cadherins. *Neuron* **17**, 423–434 (1996).
83. Uchida, N., Honjo, Y., Johnson, K. R., Wheelock, M. J. & Takeichi, M. The catenin/cadherin adhesion system is localized in synaptic junctions bordering transmitter release zones. *J. Cell Biol.* **135**, 767–779 (1996).
References 82 and 83 show that classic cadherins are components of synaptic adherens junctions.
84. Yamagata, K. *et al.* Arcadlin is a neural activity-regulated cadherin involved in long term potentiation. *J. Biol. Chem.* **274**, 19473–19479 (1999).
85. Tanaka, H. *et al.* Molecular modification of N-cadherin in response to synaptic activity. *Neuron* **25**, 93–107 (2000).
86. Tang, L., Hung, C. P. & Schuman, E. M. A role for the cadherin family of cell adhesion molecules in hippocampal long-term potentiation. *Neuron* **20**, 1165–1175 (1998).
87. Manabe, T. *et al.* Loss of Cadherin-11 adhesion receptor enhances plastic changes in hippocampal synapses and modifies behavioral responses. *Mol. Cell. Neurosci.* **15**, 534–546 (2000).
88. Uemura, T. The cadherin superfamily at the synapse: More members, more missions. *Cell* **93**, 1095–1098 (1998).
89. Shapiro, L. & Colman, D. R. The diversity of cadherins and implications for a synaptic adhesive code in the CNS. *Neuron* **23**, 427–430 (1999).
90. Suzuki, S. C., Inoue, T., Kimura, Y., Tanaka, T. & Takeichi, M. Neuronal circuits are subdivided by differential expression of type-II classic cadherins in postnatal mouse brains. *Mol. Cell. Neurosci.* **9**, 433–447 (1997).
91. Obata, S. *et al.* A common protocadherin tail: Multiple protocadherins share the same sequence in their cytoplasmic domains and are expressed in different regions of brain. *Cell. Adhes. Commun.* **6**, 323–333 (1998).
92. Hirano, S., Yan, Q. & Suzuki, S. T. Expression of a novel protocadherin, OL-protocadherin, in a subset of functional systems of the developing mouse brain. *J. Neurosci.* **19**, 995–1005 (1999).
93. Missler, M. & Südhof, T. C. Neurexins: Three genes and 1001 products. *Trends Genet.* **14**, 20–26 (1998).
94. Schmücker, D. *et al. Drosophila* Dscam is an axon guidance receptor exhibiting extraordinary molecular diversity. *Cell* **101**, 671–684 (2000).
95. Oda, H., & Tsukita, S. Nonchordate classic cadherins have a structurally and functionally unique domain that is absent from chordate classic cadherins. *Dev. Biol.* **216**, 406–422 (1999).
96. Hazuka, C. D. *et al.* The sec6/8 complex is located at neurite outgrowth and axonal synapse-assembly domains. *J. Neurosci.* **19**, 1324–1334 (1999).

Acknowledgements
We would like to thank Y. Takai, J. Petite, R. Cagan and T. Uemura for communicating unpublished results. The work on cadherins in the authors' laboratories is funded by grants from the National Cancer Institute of Canada with funds from the Canadian Cancer Society (to U.T. and M.I.), the Canadian Institute for Health Research (to U.T. and D.G.), University of Toronto Connaught Committee (to D.G.), the National Institutes of Health (to M.P.), the Human Frontier Science Program (to M.P.) and the US Army Breast Cancer Research Program (to M.P.).

Development 127, 3607-3617 (2000)
Printed in Great Britain © The Company of Biologists Limited 2000
DEV8744

The canonical Wg and JNK signaling cascades collaborate to promote both dorsal closure and ventral patterning

Donald G. McEwen[1,*], Rachel T. Cox[2,*] and Mark Peifer[1,2,3,‡]

[1]Lineberger Comprehensive Cancer Center, [2]Curriculum in Genetics and Molecular Biology, [3]Department of Biology, The University of North Carolina, Chapel Hill, NC 27599-3280, USA
*These authors contributed equally
‡Author for correspondence (e-mail: peifer@unc.edu)

Accepted 31 May; published on WWW 20 July 2000

SUMMARY

Elaboration of the *Drosophila* body plan depends on a series of cell-identity decisions and morphogenetic movements regulated by intercellular signals. For example, Jun N-terminal kinase signaling regulates cell fate decisions and morphogenesis during dorsal closure, while Wingless signaling regulates segmental patterning of the larval cuticle via Armadillo. *wingless* or *armadillo* mutant embryos secrete a lawn of ventral denticles; *armadillo* mutants also exhibit dorsal closure defects. We found that mutations in *puckered*, a phosphatase that antagonizes Jun N-terminal kinase, suppress in a dose-sensitive manner both the dorsal and ventral *armadillo* cuticle defects. Furthermore, we found that activation of the Jun N-terminal kinase signaling pathway suppresses *armadillo*-associated defects. Jun N-terminal kinase signaling promotes dorsal closure, in part, by regulating *decapentaplegic* expression in the dorsal epidermis. We demonstrate that Wingless signaling is also required to activate *decapentaplegic* expression and to coordinate cell shape changes during dorsal closure. Together, these results demonstrate that MAP-Kinase and Wingless signaling cooperate in both the dorsal and ventral epidermis, and suggest that Wingless may activate both the Wingless and the Jun N-terminal kinase signaling cascades.

Key words: Armadillo, Dorsal closure, Segment polarity, Puckered, Wingless, JNK, Wnt, β-catenin, *Drosophila*

INTRODUCTION

Proper patterning of multicellular organisms depends on stringent regulation of cell-cell signaling. Members of the Wnt/Wingless (Wg) family of secreted glycoproteins direct cell fates in both insects and vertebrates (reviewed in Wodarz and Nusse, 1998). Genetic studies revealed many of the genes required for Wg signaling in *Drosophila*. Mutations in several of these, including *armadillo* (*arm*), were first identified in a screen for genes whose zygotic expression is required for embryonic viability and proper patterning of the larval cuticle (Nusslein-Volhard and Wieschaus, 1980). *arm* mutant embryos exhibit segment polarity defects characterized by secretion of a ventral lawn of denticles and a concomitant loss of naked cuticle. This phenotype resembles that of *wg* mutants, because Arm functions in the transduction of Wg signal.

Arm is the *Drosophila* ortholog of human β-catenin (β-cat). Both are found associated with cell-cell adherens junctions, in the cytoplasm and in nuclei. Wg/Wnt signaling elicits a cellular response by regulating the free pool of Arm/β-cat. In the absence of Wg/Wnt signal, cytoplasmic Arm/β-cat is rapidly degraded via a proteasome-mediated pathway (reviewed in Polakis, 1999). Cells of the *Drosophila* epidermis that receive Wg signal accumulate Arm in the cytoplasm and nucleus (reviewed in Wodarz and Nusse, 1998). This depends upon Wg binding cell surface receptors of the Frizzled (Fz) family, the activation of Dishevelled (Dsh) and subsequent inactivation of Zeste white-3 (Zw3, the *Drosophila* ortholog of glycogen synthase kinase-3β). From studies of mammals, two additional proteins, APC and Axin, were implicated in regulating β-cat stability (reviewed in Polakis, 1999). Members of the TCF/LEF family of transcription factors are also required for Wnt/Wg signal transduction (reviewed in Wodarz and Nusse, 1998). TCF/LEF transcription factors bind DNA, and recruit Arm/β-cat as a co-activator, thus activating Wg/Wnt-responsive genes. Therefore, Wg/Wnt signaling regulates cell fate choices directly by altering the patterns of gene expression.

In *Drosophila*, upstream components of the Wg pathway are also required during the establishment of planar polarity, the process whereby epithelial cells acquire positional information relative to the body axes of the animal. For example, both Fz and Dsh are required to coordinate the proximal-to-distal orientation of actin-based wing hairs (reviewed in Shulman et al., 1998). Most tests have suggested that planar polarity is independent of Arm function, while genetic and biochemical studies suggest that the Jun N-terminal kinase (JNK) signaling pathway functions downstream of Fz and Dsh to establish planar polarity (reviewed in Boutros and Mlodzik, 1999). It remains unclear whether Fz is activated by Wg, or any Wnt, during the establishment of planar polarity. It has been

suggested that JNK signaling and the canonical Wg pathway function as alternate signal transduction pathways downstream of Fz, with Dsh functioning as a branch point from which different cellular processes are elicited in a tissue-specific manner.

In *Drosophila*, the JNK pathway is best known for its role in dorsal closure (reviewed in Noselli and Agnes, 1999). During stage 13 of embryogenesis, two lateral epidermal sheets migrate toward the dorsal midline where they fuse. Mutations in the *Drosophila* orthologs of JNK kinase (JNKK; Hemipterous; Hep; Glise et al., 1995), JNK (Basket; Bsk; Riesgo-Escovar et al., 1996; Sluss et al., 1996), as well as the transcription factors Fos (Kayak; Kay; Riesgo-Escovar and Hafen, 1997; Zeitlinger et al., 1997) and Djun (Hou et al., 1997; Kockel et al., 1997; Riesgo-Escovar and Hafen, 1997), block dorsal closure. Other regulators of dorsal closure include Misshapen, a Ste20 relative (Paricio et al., 1999; Su et al., 1998), Puckered (Puc), a VH1-like phosphatase (Martin-Blanco et al., 1998), and Decapentaplegic (Dpp), a TGFβ relative (reviewed in Noselli and Agnes, 1999). Both Puc and Dpp are activated in the dorsalmost epidermal cells by JNK signaling (reviewed in Noselli and Agnes, 1999). Dpp then acts over several cell diameters to coordinate cell shape changes throughout the epidermis. Puc, in contrast, antagonizes JNK signaling in cells adjacent to the leading edge. The ligand that initiates JNK signaling in this context remains to be identified.

Mutations in APC and β-cat play roles in both colorectal cancer and melanoma (reviewed in Polakis, 1999), but these mutations fail to account for all cases, suggesting that other Wnt signaling antagonists might be involved in oncogenesis. To identify antagonists that function in embryogenesis and/or oncogenesis, a modifier screen for suppressors of the *arm* zygotic phenotype was performed (Cox et al., 2000). In the course of this screen, an unexpected connection between JNK and Wg signaling was discovered. Previous models suggested that distinct signaling pathways operate in the ventral and dorsal epidermis, with JNK signaling coordinating dorsal closure and Wg signaling acting through Arm to establish segment polarity in the ventral epidermis. Here, we demonstrate that mutations in *puc*, a known negative regulator of JNK signaling, suppress both the dorsal closure and ventral segment polarity defects associated with a decrease in Wg signaling. Furthermore, we present evidence that downstream components of the Wg signaling pathway, like Arm and dTCF, act together with JNK signaling pathways in both ventral patterning and dorsal closure. Our data are consistent with a model whereby Wg activates separate, yet parallel, signaling cascades that are required to promote dorsal closure and establish ventral pattern.

MATERIALS AND METHODS

Fly stocks and phenotypic analysis

The wild-type stock was Canton S. Mutants used are described at http://flybase.bio.indiana.edu. Unless otherwise noted, $arm=arm^{XP33}/Y$, $puc=puc^{A251.1}$, $wg^{weak}=wg^{PE4}/Df(2)DE$ and $wg^{null}=wg^{IG22}$. $zw3^{M1-1}$ and dsh^{75} germline clones were generated as in Peifer et al. (1994). Stocks were obtained as follows: $puc^{A251.1}$, $Djun^{2}$ and kay^{1}, the Bloomington *Drosophila* stock center; puc^{R10} and puc^{E69}, A. Martinez Arias; *UAS-dpp*, *UAS-tkvA*, *UAS-tkv*^{Q253D}, *UAS-DTak*^{WT3}, *UAS-DTak1* and *UAS-DTak*$^{KN(1-1)}$, M. B. O'Connor; *UAS-Bsk* and *UAS-Hep*, M. Mlodzik; *LE-Gal4*, S. Noselli; *UAS-Wg*, A. Bejsovec; *arm-Gal4>>VP16* and β-*tubulin-flp*, J. P. Vincent and D. St. Johnston. To express Gal4::VP16, *arm-Gal4>>VP16/TM3* females were mated to β-*tubulin-flp* males. Non-*TM3* F_1 males were collected and mated en masse to UAS females.

In situ hybridization and immunofluorescence

Dechorionated embryos were fixed for 5 minutes with 1:1 37% formaldehyde/heptane, devitellinized with 1:1 heptane/methanol, postfixed for 15 minutes in 1.85% formaldehyde/PBT (1× PBS + 0.1% Triton X-100), washed extensively with PBT, and transferred to 1× HYB buffer (50% formamide, 5× SSC, 100 μg/ml salmon sperm DNA, 100 μg/ml *E. coli* tRNA, 50 μg/ml heparin, 0.1% Tween-20, pH 4.5) for 1 hour at 70°C. Embryos were incubated overnight at 70°C with heat-denatured digoxigenin-labeled antisense RNA, washed at 70°C once each with 1× HYB, 2:1 HYB/PBT and 1:2 HYB/PBT, four times with PBT, incubated for 1 hour at 25°C with alkaline phosphatase-conjugated anti-digoxigenin (1:2000; Boehringer Mannheim), washed with PBT, and equilibrated with 1× AP buffer (100 mM Tris (pH 9.5), 100 mM NaCl, 50 mM $MgCl_2$, 0.1% Tween-20). Transcripts were visualized with NBT and BCIP. Immunofluorescence was as in Cox et al. (1996).

RESULTS

puc mutations suppress loss of Arm function

Wg signaling is required to establish posterior cell fates in each larval epidermal segment. In wild-type embryos, anterior cells of each segment secrete cuticle covered with denticles, while posterior cells secrete naked cuticle (Fig. 1A). *arm* mutants, like other mutations disrupting Wg signaling (Nusslein-Volhard and Wieschaus, 1980), exhibit a lawn of ventral denticles and thus loss of naked cuticle (Fig. 1B). In addition, strong hypomorphic or null *arm* alleles, like arm^{XP33} and arm^{YD35}, have a dorsal hole, suggesting problems during dorsal closure. Thus, Arm is required during establishment of segment polarity and during dorsal closure.

During a screen for suppressors of *arm*'s embryonic phenotype (Cox et al., 2000), we found that one suppressor was a P-element-induced allele of *puckered (puc)*. *puc* encodes a VH-1-like phosphatase that acts as a negative/feedback regulator of the JNK signaling pathway during dorsal closure (Martin-Blanco et al., 1998). $puc^{A251.1}$ is a strong *puc* allele, exhibiting the characteristic 'puckering' of the dorsal epidermis (Fig. 1E; unless noted, *puc* henceforth refers to $puc^{A251.1}$), and results from the insertion of a P-element enhancer trap in intron 2 (Martin-Blanco et al., 1998).

Heterozygosity for *puc* ($arm;puc^{A251.1}/+$) strongly suppresses *arm*'s dorsal closure defects, while ventral patterning defects are moderately suppressed (Fig. 1C). $arm;puc^{A251.1}$ double mutants have a more pronounced suppression of the segment polarity phenotype, with naked cuticle reappearing (arrowheads in Fig. 1D). In addition, $arm;puc^{A251.1}$ double mutants have a novel dorsal phenotype, characterized by loss of dorsal cuticle (* in Fig. 1D). Another strong *puc* allele, puc^{R10} (Martin-Blanco et al., 1998), suppresses *arm* to a similar extent, while weak alleles like puc^{E69} fail to suppress either the dorsal or ventral defects (data not shown). Thus, a reduction in Puc activity suppresses, in a dose-sensitive manner, both the dorsal and ventral cuticle phenotypes of *arm*.

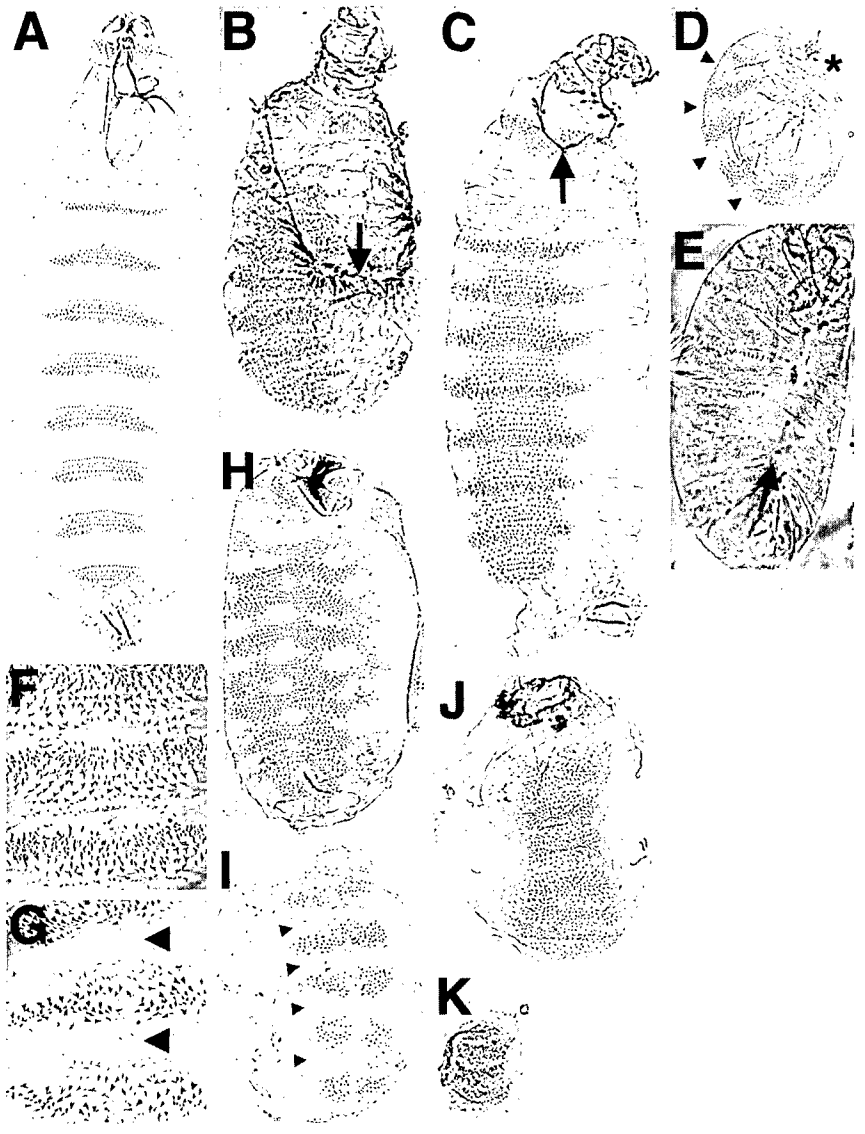

Fig. 1. Inactivation of Puc suppresses defects in Wg signaling. Ventral views (except E) of cuticles, with anterior up. (A) Wild type; (B) arm^{XP33}/Y. Note the hole in the dorsal cuticle (arrow). (C) $arm^{XP33}/Y;puc^{A251.1}/+$. Note increase in cuticle length and lack of a dorsal hole – an anterior hole remains (arrow). (D) $arm^{XP33}/Y;puc^{A251.1}$, * denotes loss of dorsal cuticle. Arrowheads (D,G,I) denote patches of naked cuticle. (E) $puc^{A251.1}$. Note displacement of anterior and posterior ends towards the dorsal surface and loss of patterning at the dorsal midline (arrow). (F) $dTCF^2$. (G) $puc^{A251.1};dTCF^2$. (H) $Df(2)DE/wg^{PE4}$ (wg^{weak}). (I) $wg^{weak};puc^{A251.1}$. (J) wg^{IG22}. (K) $wg^{IG22};puc^{A251.1}$. No suppression is seen.

puc mutations suppress mutations in Wg signaling

To assess whether this suppression was specific to *arm*, the cuticle phenotypes of $puc;dTCF^2$, $wg^{weak};puc$ and $wg^{null};puc$ double mutants were examined. Loss of Puc function suppressed the ventral segment polarity defects of both $dTCF^2$ (Fig. 1F versus G) and a weak *wg* mutant (wg^{weak}; Fig. 1H versus I). In contrast, loss of Puc function did not suppress the segment polarity defects of wg^{null} alleles (Fig. 1J versus K). $puc;dTCF^2$, $wg^{weak};puc$ and $wg^{null};puc$ double mutants all also have a reduction in dorsal epidermis (data not shown) similar to that of *arm;puc* double mutants (Fig. 1D). These data suggest that Puc normally antagonizes Wg signaling and suggest that Puc functions either downstream of or in parallel to the Wg pathway.

Puc antagonizes Wg signaling in ventral patterning, perhaps via the JNK pathway

Puc was previously reported to specifically affect dorsal closure (Martin-Blanco et al., 1998; Ring and Martinez Arias, 1993). To assess whether loss of Puc function also affects cell fate choices in the ventral epidermis, the cuticle pattern of *puc* mutants was examined. In *puc* mutants, the denticle belts are narrowed in the anteroposterior (AP) axis with the strongest narrowing at the ventral midline (compare Fig. 2A to B). This phenotype is similar to that caused by weak activation of the Wg signaling pathway (Pai et al., 1997), further suggesting that Puc normally antagonizes Wg signaling in the ventral epidermis.

The only known biochemical role for Puc is as an antagonist of JNK activity (Martin-Blanco et al., 1998). While the JNK pathway has only been shown to act during dorsal closure, *hemipterous* mRNA is expressed uniformly throughout the epidermis (Glise et al., 1995) and *basket* mRNA is expressed throughout the epidermis but enriched at the leading edge (Riego Escovar et al., 1996; Sluss et al., 1996). To test whether Puc may affect ventral patterning by regulating JNK signaling ventrally, we first examined the expression of the $puc^{A251.1}$ enhancer trap, a JNK target gene, in the ventral epidermis of *puc* mutants. In phenotypically wild-type embryos, expression of β-gal, driven by *puc* enhancer traps, is completely restricted to the dorsalmost epidermal cells (Fig. 2C), where *puc* mRNA is also normally enriched – no expression is seen in the ventral epidermis (Fig. 2C; Glise and Noselli, 1997; Martin-Blanco et al., 1998; Ring and Martinez Arias, 1993).

In contrast in *puc* homozygotes, we found significant activation of this JNK target gene in the ventral epidermis, in addition to its previously reported activation in cells adjacent to the leading edge (Fig. 2D; Glise and Noselli, 1997; Martin-Blanco et al., 1998; Ring and Martinez Arias, 1993). The $puc^{A251.1}$ enhancer trap was activated in intermittent stripes of cells extending from the dorsal epidermis to the ventral midline (Fig. 2E). These stripes are at the anterior margin of the presumptive denticle belts (brackets in Fig. 2F) and co-localize, in part, with Engrailed in the posterior compartment of each segment (data not shown). In the ventral epidermis, substantial activation of the enhancer trap was also observed near the ventral midline with the strongest expression just posterior to and overlapping the prospective denticle belts (Fig. 2F). Ectopic expression of the enhancer trap correlates well with the narrowing of denticle belts in *puc* mutants; the

puc enhancer trap is activated in the cells that are converted from a denticle-bearing cell fate to a naked cuticle cell fate (compare Fig. 2B and F). These data are consistent with the idea that Puc normally represses JNK activity in the ventral epidermis.

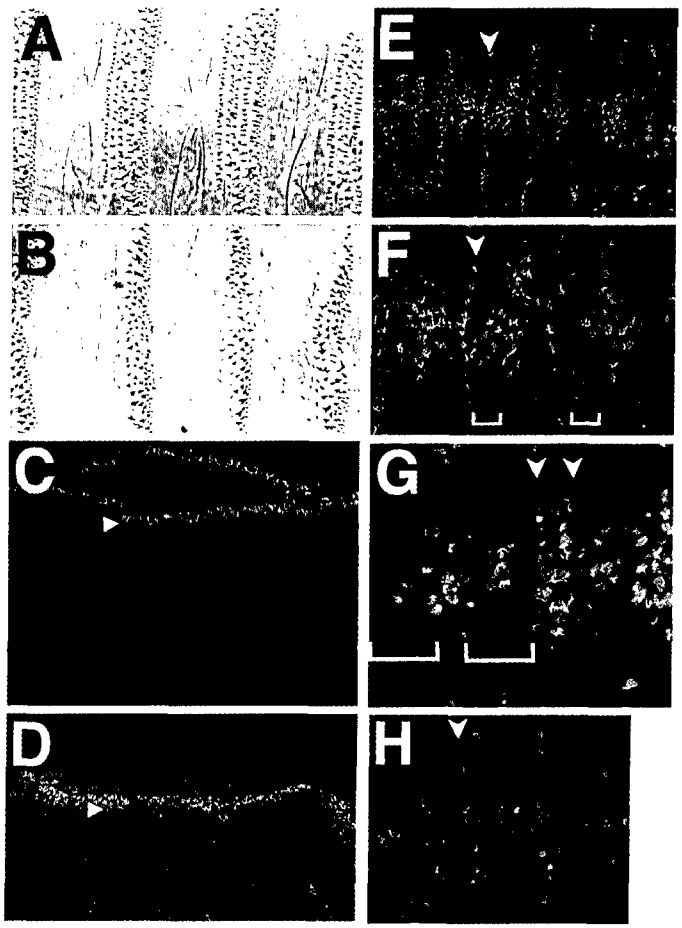

Fig. 2. Puc antagonizes Wg and negatively regulates a JNK reporter during ventral patterning. (A) Ventral view of wild-type cuticle; (B) ventral view of $puc^{A251.1}$. Note narrowing of denticle belts and occasional gaps in denticles at the midline. (C-H) Embryos double-labeled with anti-β-gal (green; indicates expression of the *puc* enhancer trap), and anti-PTyr (red; labels adherens junctions). (C) Lateral view of stage 12 wild-type ($puc^{A251.1}$/+) embryo. The enhancer trap is expressed exclusively in cells of the leading edge of the dorsal epidermis (arrowhead) and not expressed at all in the ventral epidermis. (D) Lateral view of stage 12 *puc* mutant ($puc^{A251.1}/puc^{A251.1}$) embryo. Note expansion of enhancer trap expression into several rows of cells adjacent to the leading edge (arrowhead). (E,F) (close-up) Ventral views of stage 14 $puc^{A251.1}$ embryo. β-gal expression is found in the ventral epidermis where it is never observed in a wild-type embryo. Brackets (F) denote prospective denticle belts. Note β-gal expression both near the ventral midline and in a row of cells at the anterior edge of the developing denticle belts (arrowhead); these cells will be converted from denticle to naked cuticle fates. (G) Ventral view of stage 14 $arm^{XP33}/Y;puc^{A251.1}$ embryo. Expanded stripes of enhancer trap expression (arrowheads) correlate with reappearance of naked cuticle (Fig. 1D). Brackets denote prospective denticle belts. (H) Ventral view of stage 14 $wg^{IG22};puc^{A251.1}$ embryo. Segmental expression of the enhancer trap is diminished (arrowhead). Anterior is to the left in all panels.

A correlation between expression of the *puc* enhancer trap and conversion to naked cuticle fate was also observed in *arm;puc* double mutants. Domains of β-gal expression up to three cells wide appear in the ventral epidermis (arrowheads in Fig. 2G). Double labeling for anti-phosphotyrosine (PTyr), to visualize developing denticles, and β-gal demonstrated that cells expressing $puc^{A251.1}$ enhancer trap differentiate into naked cuticle (Fig. 2G). In $wg^{null};puc$ embryos, in contrast, while cells along the midline continue to express β-gal, the segmental stripes of β-gal are diminished (Fig. 2H). This reduction in enhancer trap expression correlates with the failure of $wg^{null};puc$ double mutants to secrete naked cuticle (Fig. 1K). One possible explanation of this observation is that Wg signaling promotes *puc* expression; however, the loss of *puc*-expressing cells might also result from the ectopic apoptosis that occurs in *wg* mutants.

To further test whether *puc* mutations affect ventral patterning via activation of JNK signaling, we directly tested whether activation of the pathway by elevated expression of the kinases mimics the effects of *puc* mutations. We mis-expressed Hep or Bsk, the *Drosophila* JNKK and JNK orthologs (reviewed in Noselli and Agnes, 1999), in an *arm* mutant background using the GAL4-UAS system (Brand and Perrimon, 1993). Ubiquitous expression of either Bsk and Hep (Fig. 3C,D) results in a partial suppression of the *arm* phenotype, to a degree similar to the suppression by *puc* heterozygosity (Fig. 1C). The size of the embryo is expanded and dorsal closure defects are often alleviated, but naked cuticle is not restored. Expression of the *Drosophila* TAK1 ortholog DTak, a putative JNKK kinase (Takatsu et al., 2000), had a more dramatic effect. Mis-expression of DTak in even numbered segments of the developing *arm* epidermis using the *paired-GAL4* driver resulted in the reappearance of naked cuticle in those segments (Fig. 3F). Furthermore, mis-expression of DTak in a wild-type background using the same *paired-GAL4* driver resulted in narrowing of the denticle belts (Fig. 3G), similar to that caused by weak activation of the Wg pathway (Pai et al., 1997) or by loss of Puc function (Fig. 2B). These data are consistent with the idea that Puc's effects on the ventral pattern occur via regulation of the JNK signaling pathway, though other mechanisms, such as a direct role for Puc in the canonical Wg pathway, remain possible.

In both *puc* and *arm;puc* mutants, cells that activate the JNK pathway acquire naked cuticle cell fates. This is consistent with the hypothesis that Puc normally antagonizes production of naked cuticle in the ventral epidermis by suppressing JNK signaling. It should be noted, however, that loss-of-function mutations in JNK pathway components, including *bsk*, *Djun* and *kayak (Dfos)*, do not substantially alter the ventral denticle pattern (data not shown). This suggests that, if the JNK pathway plays a role in ventral patterning, it may function semiredundantly with other MAPK signaling pathways, as it does in planar polarity in the eye (Boutros et al., 1998). This could also explain why DTak has a stronger effect, as it may be upstream of more than one MAPK module.

We also tested a second means by which Puc could influence ventral patterning. The EGF-receptor (EGFR), acting via the ras-ERK pathway, promotes development of denticle cell fates and thus antagonizes Wg signaling, which promotes naked cuticle (O'Keefe et al., 1997; Szuts et al., 1997). If Puc upregulated this pathway, perhaps via effects on ERK, this

might explain Puc's effects on ventral patterning. Therefore, we tested whether heterozygosity or homozygosity for loss-of-function mutations in the EGFR pathway suppressed *arm*. Mutations in the ligand *vein*$^{147-2}$, the receptor *EGFR*^{C18} (heterozygotes only), *rolled* (MAPK/ERK) and *ras85B*^{e1B} did not significantly suppress either the dorsal or ventral *arm* phenotypes (Cox et al., 2000; data not shown). As heterozygosity for these mutations suppresses other phenotypes resulting from activation of MAPK signaling (e.g., Simon et al., 1991), these results suggest that Puc is unlikely to influence ventral pattern via the EGFR pathway, a result consistent with Puc's inability to regulate ERK activity (Martin-Blanco et al., 1998).

Wg signaling regulates *dpp* expression at the leading edge

Previous studies identified a role for JNK signaling during dorsal closure. The unexpected interaction between Puc and Wg signaling in ventral patterning, as well as *puc's* suppression of *arm*'s dorsal closure defect (Fig. 1C), led us to examine the potential role of Wg signaling during dorsal closure. Cells of the leading edge, which initiate dorsal closure, activate a specific transcriptional program. Thus, we assessed whether Wg signaling plays a role in dorsal closure by regulating expression of *dpp*, a TGF-β family member. Dpp is expressed in cells of the presumptive leading edge before germband retraction and by leading edge cells after germband retraction (Fig. 4A). It is thought to promote dorsal closure by initiating cell elongation in the dorsoventral (DV) axis (reviewed in Noselli and Agnes, 1999). JNK signaling is essential for continued *dpp* expression at the leading edge (reviewed in Noselli and Agnes, 1999); in embryos mutant for the JNK pathway, *dpp* expression in these cells is lost (Fig. 4B,C), resulting in a failure to complete dorsal closure (Fig. 4J).

We thus examined *dpp* expression in embryos where Wg signaling was compromised. In embryos mutant for strong alleles of *wg* (*wg*^{IG22} or *wg*^{CX4}), *dpp* expression was initiated at the leading edge but then decayed; by the onset of dorsal closure, *dpp* expression was strongly reduced or absent (Fig. 4D). Similar results were seen in embryos zygotically mutant for strong (*arm*^{XP33}; Fig. 4F) or null *arm* alleles (*arm*^{YD35}; data not shown). To further reduce Arm function, we made embryos maternally and zygotically mutant for *arm*^{XM19}, an allele that preferentially eliminates Arm function in Wg signaling. In these embryos, leading edge expression of *dpp* was reduced substantially, with no detectable expression observed during dorsal closure (Fig. 4G). *dpp* expression was also lost from lateral epidermal cells as well as from the foregut and hindgut, both ectodermal derivatives. In contrast, *dpp* expression remained in several other tissues, including the midgut (white arrows) and clypeolabrum. Similar loss of *dpp* expression both at the leading edge and in the lateral epidermis was seen in embryos maternally and zygotically mutant for a strong *dsh* allele, *dsh*^{75} (Fig. 4E). Together, these results suggest that Wg signaling promotes *dpp* expression in leading edge cells after germband retraction. Furthermore, Dsh and Arm are required for *dpp* expression in other ectodermal tissues.

dTCF encodes a transcription factor that co-operates with Arm to activate Wg target genes. *dTCF* is maternally contributed to the embryo; to overcome this maternal pool, a N-terminally truncated form of dTCF, dTCFΔN, which functions as a constitutive repressor of Wg target genes (Cavallo et al., 1998), was overexpressed in the developing epidermis. In such embryos, *dpp* expression in the dorsalmost epidermal cells was attenuated but not eliminated (Fig. 4H); expression of *dpp* in the lateral epidermis was also strongly reduced. This suggests that dTCF may also be required for Wg's activation of *dpp*.

The *puc* enhancer trap is a second JNK target gene activated in leading edge cells (Fig. 5A; reviewed in Noselli and Agnes, 1999). Therefore, we examined its expression in several *wg*-class mutants – zygotic *arm* (Fig. 5B,C), *wg*^{null} (Fig. 5D) and embryos maternally and zygotically mutant for *arm*^{XM19} (Fig. 5E) or *dsh*^{75} (Fig. 5F). In all, enhancer trap expression was reduced or lost in a subset of leading edge cells, although detectable expression of the enhancer trap always remained. To further examine the role Wg signaling plays in regulating the *puc* enhancer trap, we examined *arm;puc* and *wg*^{null}*;puc* double mutant embryos. In *puc* single mutant embryos, *puc* enhancer trap expression expands during dorsal closure into additional lateral cells (Glise and Noselli, 1997; Ring and Martinez Arias,

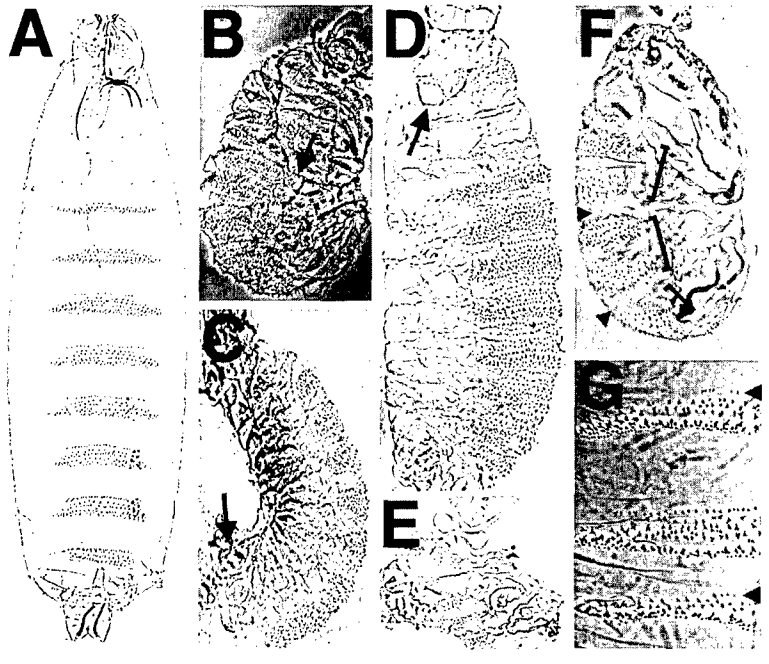

Fig. 3. Elevated JNK signaling suppresses *arm*. Cuticle preparations with anterior up. (A) Wild type; (B) *arm*^{XP33}*/Y*. Note defects in segment polarity and dorsal closure (arrow). (C) *arm*^{XP33}*/Y;UAS-Bsk/arm-Gal4::VP16*. Note suppression of ventral defects without rescue of dorsal closure (arrow). (D) *arm*^{XP33}*/Y;UAS-Hep/arm-Gal4::VP16*. Note suppression of both dorsal closure (arrow) and ventral defects. (E) *arm*^{XP33}*/Y;UAS-Hep/arm-Gal4::VP16*. A subset of embryos where JNK signaling was elevated, such as this one, secrete cuticles that are fragmented (The frequencies were: *UAS-Hep*=11%, *UAS-Bsk*=20%, *UAS-DTak*^{WT}=20%). (F) *arm*^{XP33}*/Y;UAS-DTak*^{WT}*;prd-Gal4*. Note suppression of *arm*'s segment polarity defect, leading to reappearance of naked cuticle (arrowheads) between fused denticle belts (brackets). (G) *UAS-DTak1;prd-Gal4*. Anterior rows of denticles are lost in even-numbered segments (arrowheads).

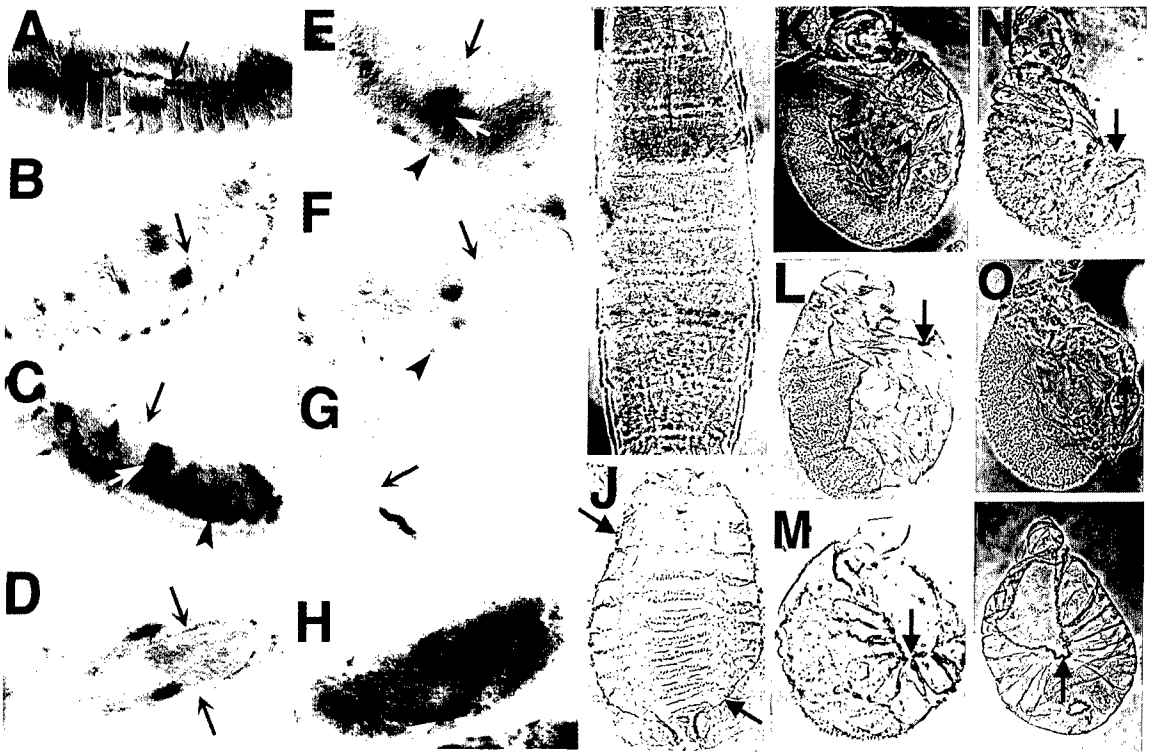

Fig. 4. Wg signaling is required for *dpp* expression and dorsal closure. (A-H) Lateral views of stage 13 embryos labeled for *dpp* mRNA, with anterior at left. Note *dpp* at the leading edge (black arrows), in the midgut (white arrows) and in the lateral epidermis (black arrowheads). (A) Wild type; (B) *Djun*^{1}; (C) *UAS-puc/arm-GAL4::VP16*; (D) *wg*^{CX4}; (E) maternal and zygotic *dsh*^{75}; (F) *arm*^{XP33}*/Y*; (G) maternal and zygotic *arm*^{XM19}; (H) *UAS-dTCFΔN;arm-GAL4::VP16*. Note loss of *dpp* mRNA at the leading edge (black arrows) while midgut expression (white arrows) remains. (I-P) Cuticles. (I) Dorsal view of wild type. (J) *UAS-puc/arm-GAL4::VP16*. The dorsal surface is completely open, with edges of the large dorsal hole indicated by arrows. (K,L) *wg*^{IG22}. Many *wg* embryos (K) are dorsally closed but exhibit severe defects in dorsal patterning; note abnormal cuticular structures (arrowhead). (L) 18% are mildly dorsally open. In K-P, the arrow indicates the posterior extent of the dorsal hole. (M) Maternal and zygotic *dsh*^{75} mutant; (N) *arm*^{XP33}*/Y* mutant; (O) maternal and zygotic *arm*^{XM19} mutant; (P) *UAS-dTCFΔN; arm-GAL4::VP16* mutant. Note dorsal closure defects.

1993; Fig. 5G), due to hyperactivation of the JNK pathway. In *arm;puc* and *wg*^{null}*;puc* double mutants, this expansion was attenuated (Fig. 5H,I), consistent with a role for Wg in regulating *puc* expression in dorsal epidermal cells.

Constitutive activation of Wg signaling drives ectopic *dpp* expression

These data suggest that both the JNK and canonical Wg pathways regulate *dpp* in leading edge cells. When the JNK pathway is ectopically activated, as occurs in *puc* mutants, *dpp* expression expands into a subset of the more lateral epidermal cells (Fig. 6A versus B; reviewed in Noselli and Agnes, 1999). We thus examined whether ectopic activation of the Wg pathway also expands the domain of *dpp* expression. We activated the Wg pathway by removing maternal and zygotic Zw3 (Fig. 6C,D) or by mis-expressing Wg (data not shown) or a constitutively active form of Arm (data not shown) throughout the dorsal epidermis. In all cases, *dpp* expression expanded from the leading edge into more lateral cells.

Ectopic activation of Wg signaling also mimics the effects of *puc* on the dorsal cuticle. *puc* mutants exhibit a characteristic 'puckering' of the anterior and posterior epidermis towards the dorsal surface, as well as defects in dorsal hair diversity and patterning (Fig. 6E versus F; Martin-Blanco et al., 1998; Ring and Martinez Arias, 1993). Activation of Wg signaling throughout the dorsal epidermis, by ubiquitously expressing Wg (Fig. 6G) or Arm^{S10} (Fig. 6I), or in *zw3* mutants (Fig. 6H), results in a very similar disruption of the dorsal cuticle, including 'puckering', dorsal hair patterning and identity defects (4°only), and 'bald' scars along the dorsal midline. Thus, overactivation of either JNK or Wg signaling pathways has a similar effect upon patterning of the dorsal epidermis.

Activation of JNK or Dpp signaling in the leading edge rescues dorsal closure of *arm* mutants

Misexpression of Hep throughout the epidermis suppresses the phenotype of *arm* (Fig. 3D). To address whether decreases in Puc activity rescue *arm* dorsal closure by upregulating JNK signaling and/or *dpp* expression in leading edge cells, a leading-edge-specific GAL4 driver (*LE-Gal4*) was used to activate either JNK or Dpp signaling in an *arm* mutant. Over-expression of DTak specifically in leading edge cells ameliorated the *arm* dorsal phenotype (Fig. 7B) while ectopic expression of a dominant-negative DTak transgene (*UAS-DTak*$^{KN(1-1)}$) throughout the epidermis augmented *arm*'s dorsal closure defects (Fig. 7C). Furthermore, expression of either *dpp* (Fig. 7D) or activated *thick veins* (*tkv*; Fig. 7E,F), a Dpp receptor, in leading edge cells of *arm* mutants partially suppressed the dorsal closure defects associated with loss of Arm function. Together, these results suggest that elevation in

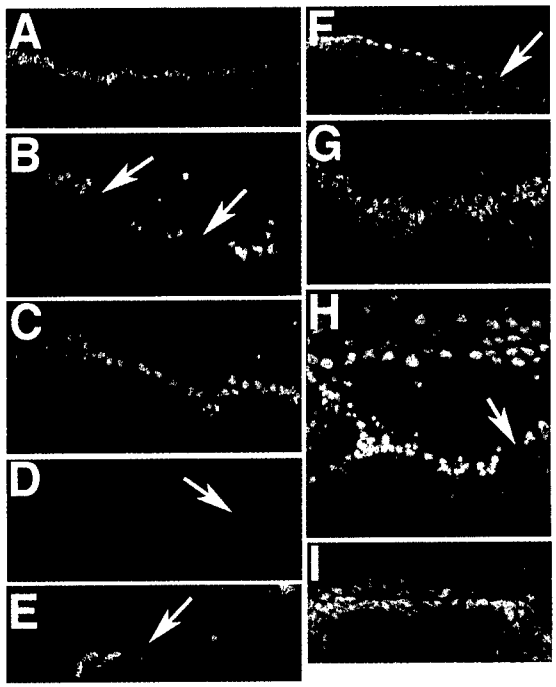

Fig. 5. *puc* enhancer trap expression in *wg*-class mutants. Lateral views of stage 14 embryos double-labeled as in Fig. 2. (A) $puc^{A251.1}$/+. Only leading edge cells express the enhancer trap. (B,C) arm^{XP33}/Y;$puc^{A251.1}$/+; (D) wg^{IG22};$puc^{A251.1}$/+; (E) Maternal and zygotic arm^{XM19};$puc^{A251.1}$/+; (F) maternal and zygotic dsh^{75};$puc^{A251.1}$/+; (G) $puc^{A251.1}$. Enhancer trap expression expands into 2-4 rows of leading edge cells. (H) arm^{XP33}/Y;$puc^{A251.1}$. (I) wg^{IG22};$puc^{A251.1}$. *wg*-class mutants lose enhancer trap expression in a subset of leading edge cells (arrows).

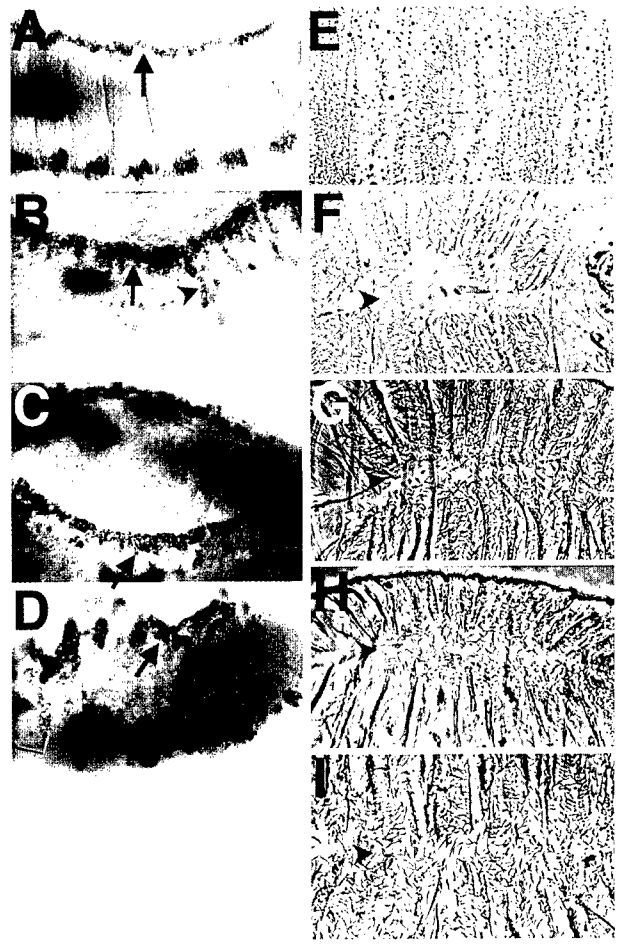

Fig. 6. Ectopic activation of Wg signaling mimics loss of Puc function. (A-D) Lateral views, stage 14 embryos labeled for *dpp* mRNA. Anterior is at left. (A) Wild type. *dpp* mRNA accumulates at the leading edge (arrow) and in lateral patches. (B) $puc^{A251.1}$; (C,D) Maternally $zw3^{M1-1}$ mutant embryos; (C) presumptive zygotically wild-type embryo; (D) a presumptive maternal and zygotic mutant. Expression of *dpp* expands at the leading edge (arrows) and into the lateral epidermis (arrowheads). (E-I) Dorsal views of cuticles. (E) Wild type. Note the patterning and diversity of dorsal hairs. (F) $puc^{A251.1}$; (G) *UAS-wg/arm-GAL4::VP16*; (H) maternal and zygotic $zw3^{M1-1}$; (I) $UAS\text{-}arm^{S10}$;*arm-GAL4::VP16*. Activation of Wg signaling mimics $puc^{A251.1}$, with loss in dorsal hair diversity, a naked scar at the dorsal midline (arrowheads) and 'puckering' of the cuticle.

JNK signaling, either via inactivation of Puc or over-expression of JNK pathway kinases, can suppress *arm*'s dorsal defects while reductions in JNK signaling in leading edge cells augment *arm*'s dorsal closure defects.

Constitutive activation of the Wg pathway results in the upregulation of *dpp* expression (Fig. 6). To assess whether activation of the Wg pathway is sufficient to suppress defects associated with a loss of JNK signaling, Wg (data not shown) or Arm^{S10} (Fig. 7H) were misexpressed in the kay^2 mutant background. Although it was previously demonstrated that activation of Dpp signaling in the dorsalmost epidermal cells rescues JNK pathway mutants (e.g., Hou et al., 1997), constitutive activation of the Wg cascade fails to promote *dpp* expression in leading edge cells (data not shown) or to rescue the dorsal closure defect of *kay* (Fig. 7G versus H). Arm's role during dorsal closure can be bypassed by activating Dpp signaling whereas the requirement for Kayak remains even if the Wg pathway is activated. Therefore, Arm may amplify JNK-dependent expression of *dpp*, JNK may be required for *dpp*-independent events during dorsal closure, or both. Finally, Arm likely contributes to dorsal closure in a Wg-independent way, through its maintenance of cadherin/catenin-based adherens junctions.

Wg signaling is required to coordinate dorsal closure

The dorsal closure defects of *arm* mutants were previously ascribed to Arm's role in adherens junctions, as wg^{null} mutants (Nusslein-Volhard and Wieschaus, 1980) and *arm* mutants specifically affecting Wg signal transduction are not completely open dorsally. However, given the similar alterations in the transcriptional program of leading edge cells caused by defects in either JNK or Wg signaling, we re-examined dorsal closure in Wg pathway mutants. wg^{null} cuticles have significant defects in dorsal pattern, characterized by loss of dorsal hairs and the presence of abnormal cuticular structures (Fig. 4K,L). While most wg^{null} mutants are closed dorsally, 18% remain open at the dorsal anterior end (Fig. 4L); similar defects are seen in embryos maternally and zygotically mutant for *dsh* (Fig. 4M) or arm^{XM19} (Fig. 4O), or in embryos

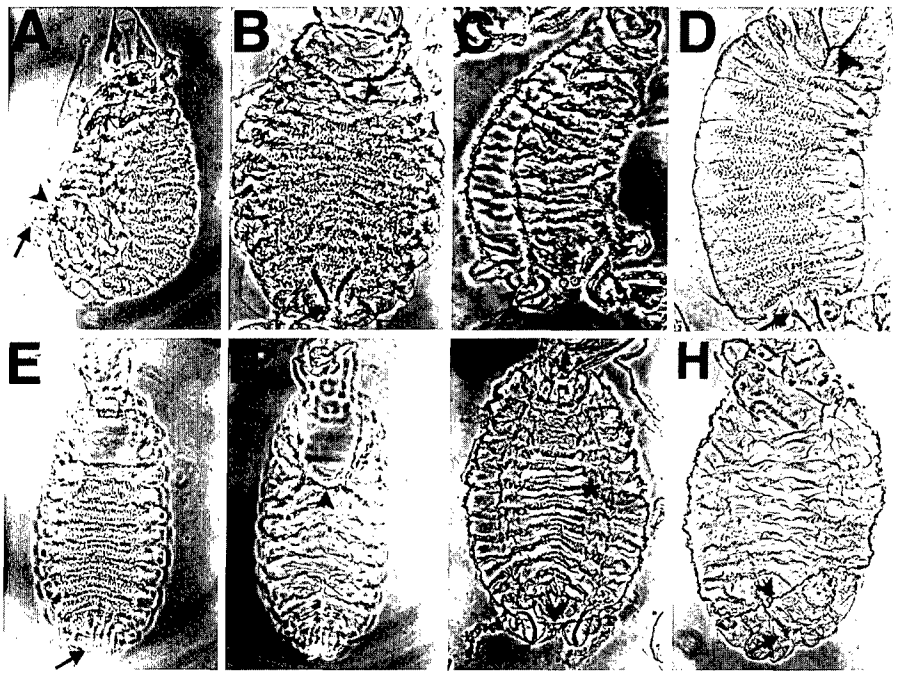

Fig. 7. Ectopic Dpp signaling rescues *arm*'s dorsal closure defects while activation of Wg signaling fails to rescue JNK signaling mutants. Arrowheads denote the posteriormost extent of the dorsal hole; arrows denote filzkörper, the posteriormost structure. (A) Lateral view of arm^{XP33}/Y; (B) ventral view of arm^{XP33}/Y;*LE-Gal4;UAS-DTak*^{WT3}. Note rescue of dorsal closure. (C) Lateral view of arm^{XP33}/Y;*LE-Gal4/+;UAS-DTak*$^{KN(1-1)}$/+. The dorsal defect is enhanced. (D) Ventral view of arm^{XP33}/Y;*LE-Gal4;UAS-dpp*. Note rescue of dorsal closure. (E,F) Ventral and dorsal views of arm^{XP33}/Y;*UAS-tkv*^{Q253D}/*LE-Gal4*. Note rescue of dorsal closure. (G) Dorsal view of kay^2 *arm-Gal4::VP16/kay*^{2}. * denotes ventral denticle belts. (H) Dorsal view of *UAS-arm*^{S10}/+;kay^2 *arm-Gal4::VP16/kay*^{2}. Note the loss of denticles.

expressing dTCFΔN throughout the epidermis (Fig. 4P). Thus, the endpoint of dorsal closure, the dorsal cuticle pattern, is altered in *wg*-class mutants.

These analyses of cuticle pattern and *dpp* expression suggest that Wg signaling regulates dorsal closure. To examine this directly, the cell shape changes that accompany dorsal closure were monitored by confocal microscopy, utilizing fluorescent-phalloidin to label filamentous actin and anti-PTyr antibody to label adherens junctions (Fig. 8). In wild-type embryos, cells begin to change shape during germband retraction (Fig. 8A,J). Cells of the leading edge are organized into a single well-defined row, and elongated in the DV axis by the end of germband retraction (Fig. 8B,K). As dorsal closure initiates, an additional 3-4 lateral cell rows also begin to stretch ventrally. Leading edge cells meet first at the posterior (Fig. 8C,L). Next, anterior leading edge cells meet and the embryo completes dorsal closure.

Loss of *wg* completely blocks the well-ordered cell shape changes that normally accompany dorsal closure. Leading edge cells never elongate along the DV axis (Fig. 8D,M); instead they stretch along the AP axis (Fig. 8E,N). This AP stretching may correlate with the 'purse string' tightening of actin filaments thought to help drive dorsal closure (Young et al., 1993). Presumptive leading edge cells of *wg* mutants accumulate actin and PTyr where they contact the amnioserosa, though they do so in an uneven fashion compared to wild type (Fig. 8E,N; data not shown). In addition to these defects, certain lateral cells contract like leading edge cells, stretching along the AP axis (Fig. 8N). Thus lateral cells in *wg* mutants may not acquire proper DV identities.

It has been hypothesized that the concerted cell shape changes characteristic of wild-type embryos are essential for dorsal closure. Thus, we were quite surprised to observe that, despite the severe abnormality in cell shape changes in a *wg* mutant, dorsal closure proceeds, though in a very abnormal fashion (Fig. 8F,O). Due to incomplete germband retraction, cells still cover the dorsal side at the posterior end; this may help bring posterior cells together. Gradually most leading edge cells meet at the midline and resume a cuboidal appearance.

We also examined wg^{null};*puc* double mutants (Fig. 9A-D), to determine what happens to cells that normally secrete dorsal and lateral cuticle. *wg;puc* double mutants resemble *wg* single mutants until germband retraction. Several differences then become apparent in *wg;puc* double mutants. First, dorsal closure is never initiated. Second, lateral epidermal cells, which elongate along the AP axis, activate the *puc* enhancer trap, thus further resembling leading edge cells (Fig. 9A). Finally, massive cell degeneration is seen in the lateral and dorsal epidermis of late embryos (Fig. 9B,C), likely explaining the complete absence of dorsal cuticle. The *puc* enhancer trap comes on strongly in the cells destined to degenerate. A small group of ventral epidermal cells survives (Fig. 9D); presumably these are the cells that secrete cuticle.

In *arm* mutants, certain aspects of dorsal closure are more severely affected than in *wg* while others proceed more normally. This may reflect the fact that *arm* zygotic mutants retain some Wg signaling, albeit greatly reduced, but also have reductions in cadherin-catenin function. *arm* mutants are quite normal through germband retraction. At this point, leading edge cells initiate cell shape changes (Fig. 8G,P), but do not do so in a coordinated fashion, producing a variety of cell shapes (Fig. 8P). A subset of more lateral cells fail to elongate (Fig. 8H,Q). Most *arm* embryos fail to initiate dorsal closure and leading edge cells often curl under their more lateral neighbors. At a stage when dorsal closure would finish in wild-type embryos, the amnioserosa rips away from the leading edge cells (Fig. 8I,R), with detached cells resuming a cuboidal shape. *arm;puc* double mutants resemble *arm* single mutants until the point at which dorsal closure should be complete. At this point, ectopic enhancer trap expression appears in the amnioserosa and at the anterior and posterior ends of the embryos (Fig. 9F,G), as in *puc* single mutants. Enhancer trap expression expands to nearly fill the dorsal and lateral epidermis of the double mutant (Fig. 9I), perhaps leading to eventual cell

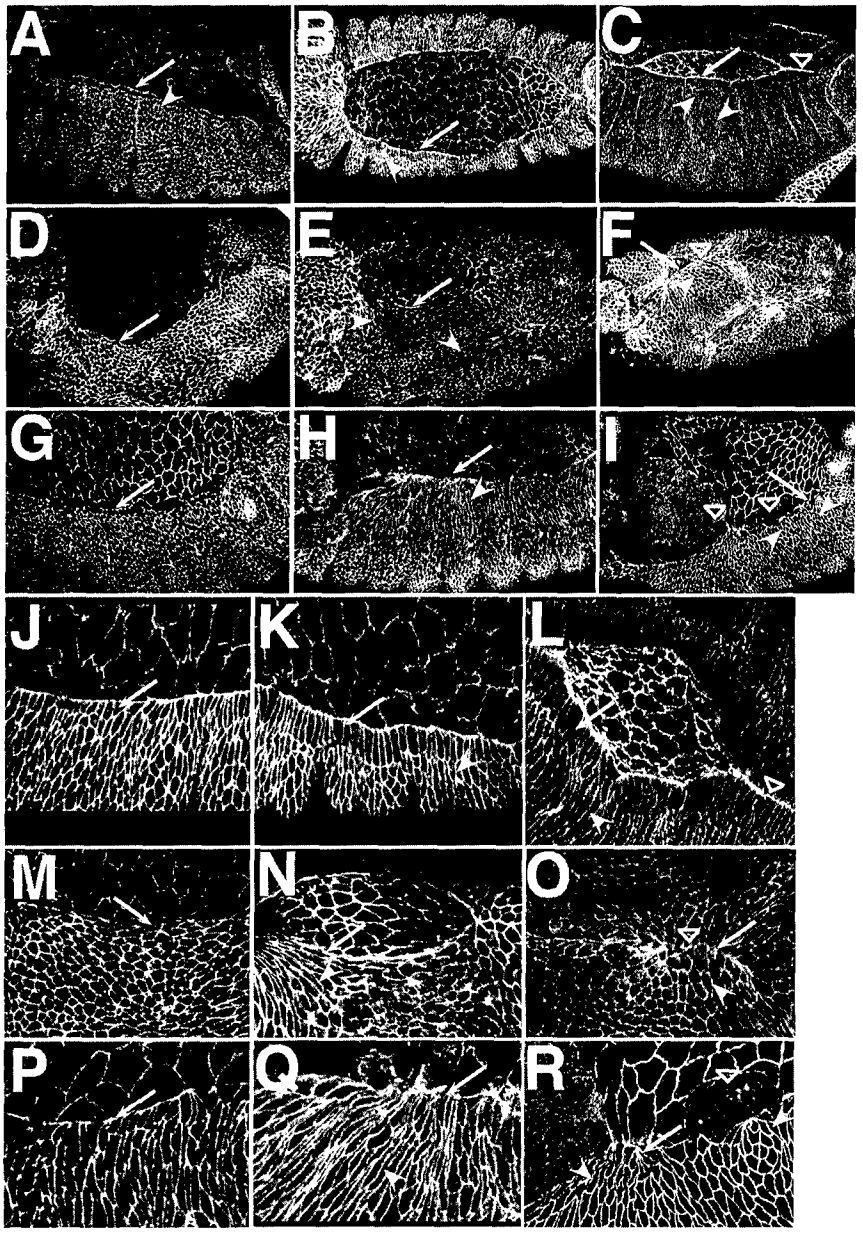

Fig. 8. Dorsal closure is aberrant in both *wg* and *arm*. Embryos labeled for PTyr to view cell boundaries. Dorsal closure in successively later wild-type (A-C, J-L), wg^{IG22} (D-F, M-O) and arm^{XP33} (G-I, P-R) embryos. Anterior is to the left. (A,J) Lateral views, late stage 12 wild type. Leading edge cells (arrows) begin change shape and align in a row; lateral neighbors remain cuboidal (arrowhead). (B,K) Dorsal and lateral views of stage 14 wild type. Leading edge cells are elongated (arrows); lateral neighbors are beginning to change shape (arrowheads). (C,L) Late stage 14 wild type. Both leading edge (arrows) and lateral cells (arrowheads) are highly elongated. At the leading edge and where cells join they accumulate PTyr (open arrowheads). (D,M) Lateral views of stage 12-13 wg^{IG22} mutants. Segmentation is not apparent. Germband retraction is not completed. Leading edge cells (arrows) never initiate proper cell shape changes, nor do they form a single row. During stage 13, they elongate in the AP axis, as do certain lateral cells. (E,N) Lateral views of stage 14 wg^{IG22} mutants. Leading edge cells (arrows) and certain lateral neighbors (arrowheads) are highly elongated. Dorsal closure proceeds. (F,O) Lateral/dorsal views of stage 15 wg^{IG22} mutants. Dorsal closure has gone to (O) or nearly to (F) completion. Upon completion of closure, leading edge cells (arrows) resume a cuboidal shape, and their more lateral neighbors remain cuboidal (arrowhead). Cells at the midline are not well-aligned nor do they accumulate high levels of PTyr (open arrowheads). (G,P) Lateral views of stage 13 arm^{XP33} mutants. Leading edge cells initiate elongation, but are much less uniform in shape (arrows). (H,Q) Lateral views of stage 14 arm^{XP33} mutants. Leading edge (arrows) and lateral cells (arrowheads) elongate in the DV axis but do so irregularly. (I,R) Lateral views of stage 14/15 arm^{XP33} mutants. The amnioserosa rips from the leading edge (open arrowheads). Leading edge cells attached to the amnioserosa remain elongated (arrows), but those that detach resume a cuboidal shape (arrowheads).

death of the dorsal and lateral epidermis as in *wg;puc* embryos.

DISCUSSION

Wg and JNK signaling co-operate during embryogenesis

The JNK and Wg signaling pathways were thought to function in distinct domains, with JNK regulating dorsal closure and Wg regulating segment polarity. Here we demonstrate that Wg signaling is critical for normal dorsal closure and that a negative regulator of the JNK pathway, Puc, plays an unexpected role in ventral patterning. This connection emerged from the observation that reduction in Puc function suppresses both the dorsal closure and ventral segment polarity phenotypes of non-null mutations in the Wg pathway.

Puc encodes a MAPK phosphatase that antagonizes JNK signaling (Martin-Blanco et al., 1998). Thus the simplest hypothesis to explain our results is that *puc* suppresses *arm* by hyperactivating the JNK pathway. Consistent with this, the *puc* enhancer trap, a JNK target gene, is ectopically activated in certain ventral epidermal cells in *puc* mutants. In addition, activation of JNK signaling suppresses *arm* in a fashion very similar to that resulting from reduction in Puc function, and activation of a JNKKK in a wild-type embryo mimics weak activation of the Wg pathway (Pai et al., 1997).

Zygotic loss-of-function mutations in the JNK pathway fail to appreciably affect ventral segment polarity (data not shown), however. This is reminiscent of the role of JNK signaling in planar polarity (Boutros et al., 1998). Loss-of-function mutations in the JNK pathway suppress dominant activation of Fz or Dsh, but these mutations fail to exhibit planar polarity defects themselves. This may result from functional redundancy and/or cross-talk between different MAPKKs and/or MAPKs (Paricio et al., 1999). Such crosstalk occurs:

both DMKK4 and Hep can activate Bsk, while *Drosophila* p38 orthologs can phosphorylate Djun and ATF2, both known targets of Bsk (Han et al., 1998). Thus, the JNK signaling pathway may function redundantly with other MAPK pathways, both in planar polarity and in segment polarity. As JNK-independent expression of *puc* has also reported (Zecchini et al., 1999), additional studies will be required to assess the ability of Puc to antagonize other MAPK signaling pathways. While these circumstantial arguments are consistent with a role for the JNK pathway in ventral patterning, the caveats raised by the lack of effects of loss-of-function JNK mutations leave open the possibility that Puc has a role in ventral patterning that is independent of its role in regulating JNK activity – for example, it could directly regulate the canonical Wg pathway.

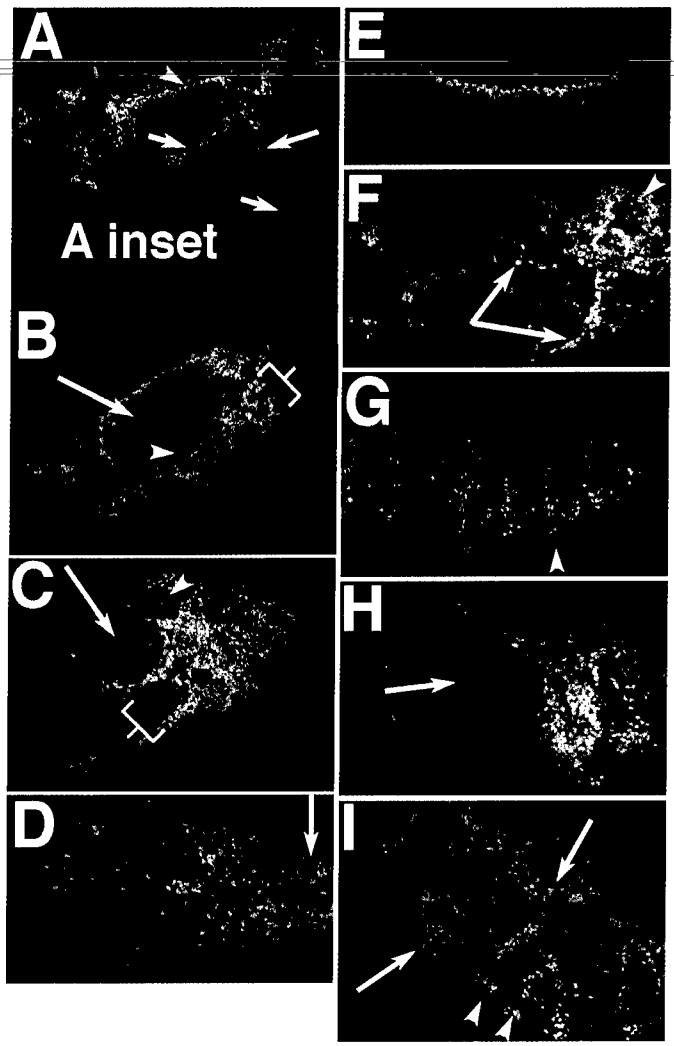

Fig. 9. Dorsal closure in *wg;puc* and *arm;puc*. Embryos double-labeled for PTyr revealing cell boundaries (red) and anti-β-gal revealing *puc* enhancer trap expression (green). (A-D) wg^{IG22};$puc^{A251.1}$. (A, A inset) Stage 14; inset shows only PTyr. Enhancer trap expression is seen at the leading edge (arrowhead). Stripes of dorsal and lateral cells also activate the enhancer trap and become highly elongated along the AP axis (arrows), while other cells remain hexagonal. (B,C) Lateral views of successively later embryos. Enhancer trap expression in the lateral epidermis expands (brackets). Dorsal, anterior and posterior cells begin to degenerate (arrowheads). (D) Terminal stage. Only a small ball of ventral epidermal cells remain (arrow). (E-I) arm^{XP33};$puc^{A251.1}$. (E) Stage 14; (F,G) dorsal and ventral views of a slightly later embryo. The amnioserosa has ripped from the epidermis (arrows), and the *puc* enhancer trap is coming on in ventral (arrowhead, G) and posterior (arrowhead, F) cells. (H) Dorsal view of a later embryo. The gut has protruded (arrow). (I) Terminal stage. The epidermis has slipped ventrally. The enhancer trap is on strongly in posterior and lateral epidermal cells (arrows) and in ventral stripes (arrowheads).

Wg and JNK – one pathway or two?

Our data, combined with previous studies of JNK signaling (reviewed in Noselli and Agnes, 1999), further suggest that Wg and JNK signaling act in parallel during dorsal closure. Both pathways regulate *dpp* expression in dorsal epidermal cells and are required for the proper coordinated cell shape changes to occur. These data are compatible with several different models. It may be that the two pathways both impinge on the same process and the same target gene, but that they do so in response to independent upstream inputs. However, when our data is combined with other recent studies, a potential direct connection between the Wg and JNK pathways is suggested. Using both genetics and in vitro studies, others demonstrated that JNK pathway kinases act downstream of Frizzled and Dsh in planar polarity and that Dsh can activate the JNK signaling cascade directly (Boutros et al., 1998; Li et al., 1999). This suggested that Dsh may function as a binary switch, deciding between the canonical Wg pathway and the JNK pathway during the establishment of segment polarity and planar polarity, respectively. Here, we demonstrate that both the canonical Wg and the JNK pathways are required for proper dorsal closure, and that both pathways affect expression of the same target gene, *dpp*. One plausible model accommodating these data is that Wg, acting via Frizzled receptors and Dsh, activates both the JNK pathway and the canonical Wg pathway simultaneously and in parallel during both dorsal closure and ventral patterning. The possibility that Wg activates both pathways, while exciting in principle, remains quite speculative, and must now be tested by more direct biochemical and cell biological means.

Wg as a permissive signal

It also is possible that Wg functions as a permissive signal required to allow other effectors to promote *dpp* expression. For example, *dTCF* could repress *dpp* expression in the absence of Wg signaling by recruiting Groucho (Cavallo et al., 1998), a transcriptional repressor, to the *dpp* promotor. Wg signaling might relieve this repression by displacing Groucho with stabilized Arm. Consistent with this hypothesis, constitutive activation of Arm fails to rescue the dorsal closure defects of *kay* mutants. Thus activation of the canonical Wg signaling pathway is necessary but not sufficient to promote *dpp* expression. Wg signaling may thus only amplify JNK-dependent expression of *dpp* in the dorsal epidermis.

One possible intersection between MAPK signaling cascades and TCF-mediated repression has been reported (reviewed in Bowerman and Shelton, 1999). Transcriptional repression of Wnt target genes in *C. elegans* depends upon POP-1, a TCF family member. POP-1 repressor activity is regulated by Mom-4, a Tak1-like kinase, and Lit-1, a Nemo-like MAP kinase relative (Nlk). In mammalian cells, the

transcriptional activity and DNA-binding properties of TCF can be repressed by Tak1/Nlk activation. Therefore, the canonical Wg and MAPK/JNK pathways might converge at dTCF, with MAPK kinase signaling affecting dTCF activity. Additional studies will be required to assess the mechanism by which these pathways interact.

Cell shape changes and Dpp appear dispensable for dorsal closure

The current model suggests that a sequential series of cellular events drive dorsal closure. Leading edge cells are thought to initiate closure by elongating in the DV axis and upregulating Dpp, thus signaling lateral cells to initiate similar cell shape changes (reviewed in Noselli and Agnes, 1999). We found that the events of dorsal closure apparently do not proceed in lockstep, with each event requiring the successful completion of the previous event. The stereotypical cell shape changes are lost in *wg* mutants; however, the lateral epidermal sheets usually meet at the dorsal midline. In contrast, while cell shape changes are initiated in *arm* mutants, though not in a coordinated fashion, the epidermis does not close. Further, as *dpp* expression in leading edge cells is lost in *wg* mutants, Dpp may not be essential for dorsal closure (a similar model was suggested by Zecchini et al., 1999). Finally, because dorsal closure is more normal in *wg* than in JNK pathway mutants, the JNK pathway likely depends upon activation by signals other than Wg and must affect other processes in addition to Dpp signaling. Further work is required to clarify the semi-redundant mechanisms regulating dorsal closure.

We are grateful to the Bloomington *Drosophila* Stock Center, A. Bejsovec, A. Martinez-Arias, M. Mlodzik, S. Noselli, M. O'Connor, D. St. Johnston, and J. P. Vincent for fly stocks, and M. O'Connor and A. Martinez-Arias for sharing unpublished data. This work was supported by NIH RO1GM47857 (M. P.), by NIH 5T3CA09156 and 1F32GM19824 (D. G. M.), and in part by a US Army Breast Cancer Research Program Career Development Award (M. P.).

REFERENCES

Boutros, M., Paricio, N., Strutt, D. I. and Mlodzik, M. (1998). Dishevelled activates JNK and discriminates between JNK pathways in planar polarity and wingless signaling. *Cell* **94**, 109-118.

Boutros, M. and Mlodzik, M. (1999). Dishevelled: at the crossroads of divergent intracellular signaling pathways. *Mech. Dev.* **83**, 27-37.

Bowerman, B. and Shelton, C. A. (1999). Cell polarity in the early Caenorhabditis elegans embryo. *Curr. Opin. Genet. Dev.* **9**, 390-395.

Brand, A. H. and Perrimon, N. (1993). Targeted gene expression as a means of altering cell fates and generating dominant phenotypes. *Development* **118**, 401-415.

Cavallo, R. A., Cox, R. T., Moline, M. M., Roose, J., Polevoy, G. A., Clevers, H., Peifer, M. and Bejsovec, A. (1998). Drosophila Tcf and Groucho interact to repress Wingless signalling activity. *Nature* **395**, 604-608.

Cox, R. T., Kirkpatrick, C. and Peifer, M. (1996). Armadillo is required for adherens junction assembly, cell polarity, and morphogenesis during Drosophila embryogenesis. *J. Cell Biol.* **134**, 133-148.

Cox, R. T., McEwen, D.G., Myster, D.L., Duronio, R.J., Loureiro, J. and Peifer, M. (2000). A screen for mutations that suppress the phenotype of *Drosophila armadillo*, the β-catenin homolog. *Genetics*, in press.

Glise, B., Bourbon, H. and Noselli, S. (1995). hemipterous encodes a novel Drosophila MAP kinase kinase, required for epithelial cell sheet movement. *Cell* **83**, 451-461.

Glise, B. and Noselli, S. (1997). Coupling of Jun amino-terminal kinase and Decapentaplegic signaling pathways in Drosophila morphogenesis. *Genes Dev.* **11**, 1738-1747.

Han, Z. S., Enslen, H., Hu, X., Meng, X., Wu, I. H., Barrett, T., Davis, R. J. and Ip, Y. T. (1998). A conserved p38 mitogen-activated protein kinase pathway regulates Drosophila immunity gene expression. *Mol. Cell. Biol.* **18**, 3527-3539.

Hou, X. S., Goldstein, E. S. and Perrimon, N. (1997). Drosophila Jun relays the Jun amino-terminal kinase signal transduction pathway to the Decapentaplegic signal transduction pathway in regulating epithelial cell sheet movement. *Genes Dev.* **11**, 1728-1737.

Kockel, L., Zeitlinger, J., Staszewski, L. M., Mlodzik, M. and Bohmann, D. (1997). Jun in Drosophila development: redundant and nonredundant functions and regulation by two MAPK signal transduction pathway. *Genes Dev.* **11**, 1748-1758.

Li, L., Yuan, H., Xie, W., Mao, J., Caruso, A. M., McMahon, A., Sussman, D. J. and Wu, D. (1999). Dishevelled proteins lead to two signaling pathways. Regulation of LEF- 1 and c-Jun N-terminal kinase in mammalian cells. *J. Biol. Chem.* **274**, 129-134.

Martin-Blanco, E., Gampel, A., Ring, J., Virdee, K., Kirov, N., Tolkovsky, A. M. and Martinez-Arias, A. (1998). puckered encodes a phosphatase that mediates a feedback loop regulating JNK activity during dorsal closure in Drosophila. *Genes Dev.* **12**, 557-570.

Noselli, S. and Agnes, F. (1999). Roles of the JNK signaling pathway in Drosophila morphogenesis. *Curr. Opin. Genet. Dev.* **9**, 466-472.

Nusslein-Volhard, C. and Wieschaus, E. (1980). Mutations affecting segment number and polarity in Drosophila. *Nature* **287**, 795-801.

O'Keefe, L., Dougan, S. T., Gabay, L., Raz, E., Shilo, B. Z. and DiNardo, S. (1997). Spitz and Wingless, emanating from distinct borders, cooperate to establish cell fate across the Engrailed domain in the Drosophila epidermis. *Development* **124**, 4837-4845.

Pai, L. M., Orsulic, S., Bejsovec, A. and Peifer, M. (1997). Negative regulation of Armadillo, a Wingless effector in Drosophila. *Development* **124**, 2255-2266.

Paricio, N., Feiguin, F., Boutros, M., Eaton, S. and Mlodzik, M. (1999). The Drosophila STE20-like kinase misshapen is required downstream of the Frizzled receptor in planar polarity signaling. *EMBO J.* **18**, 4669-4678.

Peifer, M., Sweeton, D., Casey, M. and Wieschaus, E. (1994). wingless signal and Zeste-white 3 kinase trigger opposing changes in the intracellular distribution of Armadillo. *Development* **120**, 369-380.

Polakis, P. (1999). The oncogenic activation of beta-catenin. *Curr. Opin. Genet. Dev.* **9**, 15-21.

Riesgo-Escovar, J. R., Jenni, M., Fritz, A. and Hafen, E. (1996). The Drosophila Jun-N-terminal kinase is required for cell morphogenesis but not for DJun-dependent cell fate specification in the eye. *Genes Dev.* **10**, 2759-2768.

Riesgo-Escovar, J. R. and Hafen, E. (1997). Common and distinct roles of DFos and DJun during Drosophila development. *Science* **278**, 669-672.

Ring, J. M. and Martinez Arias, A. (1993). puckered, a gene involved in position-specific cell differentiation in the dorsal epidermis of the Drosophila larva. *Dev. Suppl.*, 251-259.

Shulman, J. M., Perrimon, N. and Axelrod, J. D. (1998). Frizzled signaling and the developmental control of cell polarity. *Trends Genet.* **14**, 452-458.

Simon, M. A., Bowtell, D. D., Dodson, G. S., Laverty, T. R. and Rubin, G. M. (1991). Ras1 and a putative guanine nucleotide exchange factor perform crucial steps in signaling by the sevenless protein tyrosine kinase. *Cell* **67**, 701-716.

Sluss, H. K., Han, Z., Barrett, T., Davis, R. J. and Ip, Y. T. (1996). A JNK signal transduction pathway that mediates morphogenesis and an immune response in Drosophila. *Genes Dev.* **10**, 2745-2758.

Su, Y. C., Treisman, J. E. and Skolnik, E. Y. (1998). The Drosophila Ste20-related kinase misshapen is required for embryonic dorsal closure and acts through a JNK MAPK module on an evolutionarily conserved signaling pathway. *Genes Dev.* **12**, 2371-2380.

Szuts, D., Freeman, M. and Bienz, M. (1997). Antagonism between EGFR and Wingless signalling in the larval cuticle of Drosophila. *Development* **124**, 3209-3219.

Takatsu, Y., Nakamura, M., Stapleton, M., Danos, M. C., Matsumoto, K., O'Connor, M. B., Shibuya, H. and Ueno, N. (2000). TAK1 participates in JNK signaling during Drosophila development. *Mol. Cell. Biol.* **In press.**

Wodarz, A. and Nusse, R. (1998). Mechanisms of Wnt signaling in development. *Annu Rev. Cell Dev. Biol.* **14**, 59-88.

Young, P. E., Richman, A. M., Ketchum, A. S. and Kiehart, D. P. (1993). Morphogenesis in Drosophila requires nonmuscle myosin heavy chain function. *Genes Dev.* **7**, 29-41.

Zecchini, V., Brennan, K. and Martinez-Arias, A. (1999). An activity of Notch regulates JNK signalling and affects dorsal closure in Drosophila. *Curr. Biol.* **9**, 460-469.

Zeitlinger, J., Kockel, L., Peverali, F. A., Jackson, D. B., Mlodzik, M. and Bohmann, D. (1997). Defective dorsal closure and loss of epidermal decapentaplegic expression in Drosophila fos mutants. *EMBO J.* **16**, 7393-7401.

A Screen for Mutations That Suppress the Phenotype of *Drosophila armadillo*, the β-Catenin Homolog

Rachel T. Cox,* Donald G. McEwen,† Denise L. Myster,† Robert J. Duronio,*,†,‡,§ Joseph Loureiro‡ and Mark Peifer*,†,‡

‡*Department of Biology,* **Curriculum in Genetics and Molecular Biology,* †*Lineberger Comprehensive Cancer Center and* §*Program in Molecular Biology and Biotechnology, University of North Carolina, Chapel Hill, North Carolina 27599-3280*

Manuscript received February 24, 2000
Accepted for publication April 13, 2000

ABSTRACT

During development signaling pathways coordinate cell fates and regulate the choice between cell survival or programmed cell death. The well-conserved Wingless/Wnt pathway is required for many developmental decisions in all animals. One transducer of the Wingless/Wnt signal is Armadillo/β-catenin. Drosophila Armadillo not only transduces Wingless signal, but also acts in cell-cell adhesion via its role in the epithelial adherens junction. While many components of both the Wingless/Wnt signaling pathway and adherens junctions are known, both processes are complex, suggesting that unknown components influence signaling and junctions. We carried out a genetic modifier screen to identify some of these components by screening for mutations that can suppress the *armadillo* mutant phenotype. We identified 12 regions of the genome that have this property. From these regions and from additional candidate genes tested we identified four genes that suppress *arm*: *dTCF*, *puckered*, *head involution defective* (*hid*), and *Dpresenilin*. We further investigated the interaction with *hid*, a known regulator of programmed cell death. Our data suggest that Wg signaling modulates Hid activity and that Hid regulates programmed cell death in a dose-sensitive fashion.

THE development of a fertilized egg into a multicellular organism requires coordination of many processes. Each cell must choose the proper cell fate and must also assume its place as part of an organized tissue. In addition, apoptosis (programmed cell death; PCD) plays an important role in shaping an organism by eliminating unneeded cells. One conserved pathway that directs cell fate decisions in many animals is the Wingless (Wg)/Wnt signal transduction pathway (proteins listed as X/Y represent nomenclature in Drosophila/mammals). Loss-of-function mutations in this pathway are lethal, while inappropriate activation can be oncogenic. Wg/Wnt signals are transduced by homologous components in Drosophila, Xenopus, and mammals (reviewed in Polakis 1999). During normal development, most cells do not receive Wg/Wnt signals. In these cells the pathway is kept off through the actions of several proteins, including Zestewhite3/GSK3β, the tumor-suppressor adenomatous polyposis coli, and axin, which work in conjunction to target Armadillo (Arm)/β-catenin (βcat) for degradation via the proteasome. Arm/βcat is thus the pivotal component in the pathway. When Wg/Wnt is absent, cytoplasmic levels of Arm/βcat are very low. However, Wg/Wnt signal relieves the destruction of Arm/βcat. Arm/βcat accumulates, translocates into the nucleus, and binds dTCF/TCF, forming a bipartite transcription factor that turns on Wg/Wnt-responsive genes.

The components of the Wg pathway are encoded by a subset of the segment polarity genes, mutations that affect cell fate in the embryonic epidermis. In normal fly embryos, anterior cells of each segment secrete denticles, while posterior cells secrete naked cuticle. Wg signal directs cells to choose posterior fates and thus secrete naked cuticle. In an embryo mutant for *wg* or other positively acting components of the Wg pathway, cell fates are altered such that all surviving cells secrete denticles. It is important to note, however, that in a *wg* mutant many epidermal cells fail to survive to secrete cuticle, instead undergoing PCD. Embryos mutant for genes in either the Wg or the Hedgehog pathways have elevated levels of epidermal PCD (Martinez Arias 1985; Klingensmith *et al.* 1989; Pazdera *et al.* 1998).

Arm's role in Wg signaling is not its only function. The earliest requirement for Arm is in cell adhesion (Cox *et al.* 1996). Arm/βcat is an essential component of epithelial cell-cell adherens junctions (reviewed in Provost and Rimm 1999). The core components of this junction are classic cadherins, transmembrane proteins that mediate homotypic adhesion between neighboring cells. Arm/βcat binds to the cadherin cytoplasmic tail. α-Catenin then binds to Arm/βcat, linking the actin cytoskeleton to adherens junctions. In Drosophila, Arm helps assemble adherens junctions very early during embryogenesis. This is initiated by maternal Arm, which is supplemented by zygotic Arm once transcription begins. If the embryo lacks maternal and zygotic Arm, it

Corresponding author: Mark Peifer, Biology, CB#3280, University of North Carolina, Chapel Hill, NC 27599-3280.
E-mail: peifer@unc.edu

does not form proper adherens junctions, and cells of the cellularized blastoderm cannot form epithelia (Cox *et al.* 1996). In addition to the essential role that Arm/βcat and adherens junctions play in embryogenesis, loss-of-function mutations in the cadherin-catenin system contribute to tumorigenicity, as tumor cells must alter their adhesive properties to metastasize.

While the roles of Arm/βcat in Wg/Wnt signaling and adherens junctions have become clearer, many questions remain concerning both processes. In addition, biochemical approaches identified many other proteins that bind βcat, perhaps implicating it in other functions: for example, Arm/βcat binds the epidermal growth factor (EGF) receptor at the cell surface (Hoschuetzky *et al.* 1994), the actin-binding protein fascin in the cortex (Tao *et al.* 1996), Presenilin proteins, presumably in the endoplasmic reticulum (ER) (Zhou *et al.* 1997; Yu *et al.* 1998), and the transcription factor Teashirt (Gallet *et al.* 1998). One strategy to identify novel proteins involved in cell adhesion and Wg signaling and simultaneously to search for biological functions of the interaction of Arm with other partners is to look for mutations that interact genetically with *arm*.

In designing such a genetic screen, we took advantage of Arm's dual roles in signaling and adhesion. It has been suggested that cells may use this coupling, allowing one process to regulate the other via competition for a limited pool of Arm. Although in wild-type Drosophila embryos more than enough Arm is synthesized to fulfill its roles in both signaling and adhesion, one can manipulate the pool of Arm to make signaling and adhesion competitive. For example, if one expresses excess cadherin, it titrates out all the Arm, leaving none available for Wg signaling and resulting in a segment polarity phenotype (Sanson *et al.* 1996). We utilized this balance between Arm assembled into adherens junctions and that remaining for Wg signaling to create a sensitized genetic background. We reduced the amount of available Arm until adhesion and Wg signaling became competitive by using a zygotic *arm* mutant that retains wild-type maternal Arm, sufficing for Arm's role in adherens junctions (Cox *et al.* 1996). With most wild-type maternal Arm assembled in adherens junctions, the embryo drops below the critical threshold of Arm necessary for Wg signaling, resulting in segment polarity defects. Such an embryo is very sensitive to slight changes in *arm* dose; for example, doubling the maternal Arm substantially suppresses the segment polarity phenotype (Wieschaus and Noell 1986). Thus this represents a sensitized background well suited for a modifier screen. Mutations in genes that affect adherens junction assembly, which negatively regulate Wg signaling or encode other proteins that bind the limited supply of maternal Arm, could all potentially suppress the segment polarity phenotype of *arm*. We previously demonstrated the feasibility of this idea, showing that reduction in DE-cadherin suppressed *arm*'s segment polarity phenotype (Cox, *et al.* 1996).

We used the sensitized background of a zygotic *arm* mutant to carry out a modifier screen, looking for changes in the segment polarity phenotype. We screened through deficiencies covering >80% of the second, third, and fourth chromosomes, searching for regions of the genome containing a gene or genes that, when heterozygous deficient, suppress the cuticle phenotype of *arm*. We found 12 such regions and identified four genes with this property. One interactor is the PCD-promoting gene *head involution defective* (*hid*). Our data suggest that Hid acts as a dose-sensitive regulator of PCD in the ventral epidermis of segment polarity mutants.

MATERIALS AND METHODS

Fly stocks: References for mutants used were the following: arm^{XP55}, arm^{XM19}, and $zw3^{m1\text{-}1}arm^{XM19}$ (Cox *et al.* 1996; Peifer *et al.* 1994); hid^{05014} (Grether *et al.* 1995); hid^{Wh+X1} (Abbott and Lengyel 1991); *Df(3)H99* (White *et al.* 1994); wg^{IG22} (Nüsslein-Volhard and Wieschaus 1980); UAS-p35 (Hay *et al.* 1994); other mutations, http://flybase.bio.indiana.edu/. The deficiency kits were from the Bloomington Drosophila Stock Center, the *P*-lethals from Bloomington or the Berkeley Drosophila Genome Project (BDGP), and the *Dpresenilin* alleles from D. Curtis.

Cuticle preparations and counting: Cuticle preparations were as in Wieschaus and Nüsslein-Volhard (1986). Care was taken to be consistent in cuticle preparations, as differences in baking and pressing alter cuticle appearance. If the first cross suggested an interaction, the cross was repeated. Each candidate interacting region was tested in two or more separate crosses, with ≥200 cuticles scored per cross. Percentage of suppression equaled the number of cuticles in the least severe classes divided by the total number of cuticles scored.

Terminal transferase dUTP nick end labeling (TUNEL), phalloidin and antibody staining: TUNEL was done using reagents from Boehringer Mannheim (Indianapolis). Embryos were dechorionated in 50% bleach, fixed in 1:1 4% formaldehyde:heptane for 30 min, hand devitellinized, rinsed once in TdT reaction buffer (2.5 mM $CoCl_2$, 1× transferase buffer), and reacted in TdT reaction mix (50 units terminal transferase, 2:1 10 μM final concentration of dUTP:dUTP-biotin in reaction buffer) for 3 hr at 37°. After washing three times for 10 min in PBS + 0.1% Triton X-100 (PBT), the end-labeling was first amplified using the Vectastain kit (Vector Labs, Burlingame, CA) as recommended by the manufacturer, amplified with Cy3tyramide (New England Nuclear, Boston), and washed three times for 10 min in PBT. BODIPY, phalloidin (Molecular Probes, Eugene, OR) was added during the avidin-biotin reaction of the first amplification. Antiphosphotyrosine labeling was as in Cox *et al.* (1996).

Phosphohistone H3 staining: The 2- to 7-hr-old embryos were dechorionated in 50% bleach, fixed in 1:1 5% formaldehyde:heptane for 20 min, blocked (50 mM Tris pH 7.4, 150 mM NaCl, 0.5% NP-40, 5 mg/ml BSA) at 4° for 2 hr and stained overnight at 4° with 1:1000 antiphosphohistone H3 (Upstate Biotechnology, Lake Placid, NY) and 1:500 anti-β-gal (Bochringer Mannheim, Indianapolis). Secondary antibodies were from Molecular Probes. Pictures of the ventral epidermis and dorsal germband were taken, mitotic figures (stained for phosphohistone H3) counted, and means and standard deviations calculated.

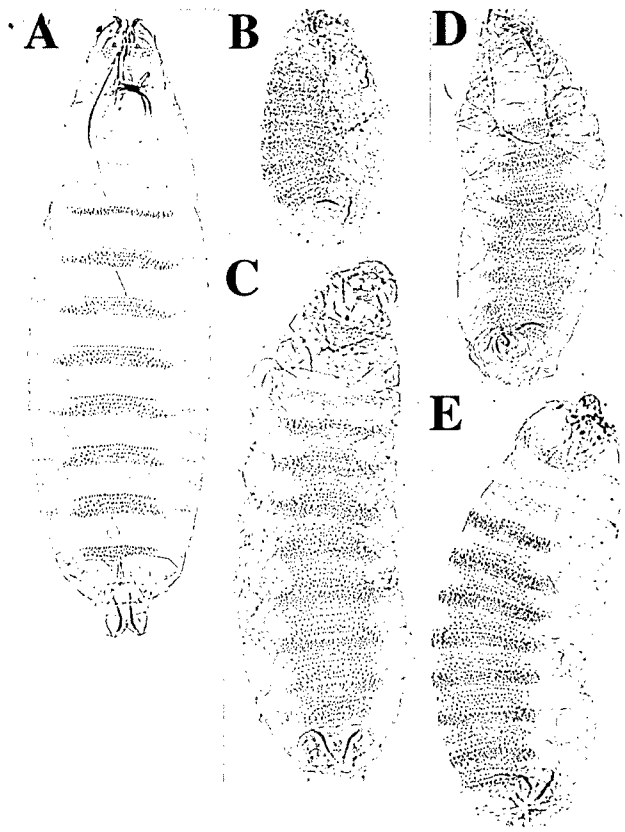

FIGURE 1.—Reducing dosage of DE-cadherin or Zw3 suppresses *arm*'s embryonic phenotype. (A) Wild-type cuticle. The cuticle is closed dorsally and the ventral surface has alternating belts of denticles and naked cuticle. (B) arm^{XP33}/Y. arm^{XP33} mutant cuticles are shorter than wild type, with a lawn of ventral denticles, no naked cuticle, and incomplete dorsal closure. (C) arm^{XP33}/Y; *Df(3) E2*/+. When the dose of DE-cadherin is reduced by half, the *arm* phenotype is suppressed. The cuticle is longer, the lawn of denticles is less dense, and the dorsal closure defect is rescued. (D) arm^{XM19}/Y, a somewhat weaker allele. (E) arm^{XM19} $zw3^{M1-1}$/Y. When zygotic *zw3* is removed (leaving only maternal *zw3*), the phenotype of arm^{XM19} is suppressed.

RESULTS

Strategy for the screen for modifiers: arm^{XP33} encodes a carboxy-terminally truncated Arm protein that cannot function in Wg signaling and has almost no function in adherens junctions (Cox *et al.* 1996). In an arm^{XP33} zygotic mutant, maternal wild-type Arm provides sufficient function for adherens junctions. However, as nearly all maternal Arm is recruited into junctions (Cox *et al.* 1996), little Arm remains to transduce Wg signal, resulting in a strong segment polarity phenotype (Figure 1, A *vs.* B). We reasoned that if one elevated the level or function of the limiting pool of maternal Arm, this should suppress the defect in Wg signaling. We hypothesized that this could occur by freeing maternal Arm from junctions, reducing the effectiveness of negative regulation of Arm's role in Wg signaling or by reducing the level of a distinct Arm-binding protein. Of course in genetic screens modifiers are also found that operate by unexpected mechanisms.

The feasibility of this hypothesis was supported by two observations. We previously found that heterozygosity for a chromosomal deficiency removing *DE-cadherin*, *Df(3R)E2*, suppresses the embryonic phenotype of arm^{XP33}—the cuticle is longer, the dorsal closure defect is substantially reduced, and denticle diversity is partially restored (Figure 1, B *vs.* C; Cox *et al.* 1996). We presume that reducing the gene dose of DE-cadherin by half creates an embryo with fewer Arm/Cadherin complexes. Although this has no apparent effect on cell-cell adhesion, wild-type maternal Arm is freed up to function in Wg signaling, leading to a suppressed phenotype. A similar suppression of *arm* was seen by removing the zygotic contribution of one of Arm's negative regulators, Zw3 (Figure 1, D *vs.* E; we tested this on arm^{XM19}, a less severe allele).

A modifier screen for Arm interactors: These examples demonstrated that a 50% reduction in the dose of certain genes suppresses *arm*. We thus screened for dose-sensitive modifiers. Rather than examining single genes one by one by mutagenesis, we evaluated large regions of the genome simultaneously by making animals heterozygous for chromosomal deficiencies that remove many genes. We obtained the "deficiency kits" for three of the four chromosomes from the Bloomington Drosophila Stock Center. These kits are designed to delete as much of the chromosome as possible using the fewest stocks; 70–80% of the euchromatin was covered by this collection of Deficiencies when we obtained them. We extended our analysis by obtaining additional Deficiencies that either covered regions not covered in the kit or overlapped interacting Deficiencies. We estimate we covered >80% of the autosomes. We have not examined the X chromosome thus far, as *arm* is on the X and the screen would require recombination of *arm* onto each deficiency. To carry out the screen, we crossed virgin arm^{XP33} females to males heterozygous for each Deficiency and prepared cuticles from the dead embryonic progeny (Figure 2A). One-quarter of the progeny are arm^{XP33}/Y (since *arm* is X-linked), and these die due to loss of *arm* function. Half of these embryos will be hemizygous for genes deleted by the deficiency and could potentially have a modified segment polarity phenotype.

To determine if there was an interaction, we grouped cuticles into phenotypic classes. arm^{XP33} mutants exhibit a segment polarity phenotype, with all surviving cells adopting anterior fates and secreting denticles. However, arm^{XP33} mutants show a range of severities; the phenotypes vary about a mean (Figure 2B). In embryos with the most severe phenotype (like that of the zygotic null), the cuticle is much shorter than the wild type and is open dorsally. In less severe embryos, dorsal closure is partially complete, and the embryonic cuticle is longer. Most mutant embryos fall into these classes. At a very

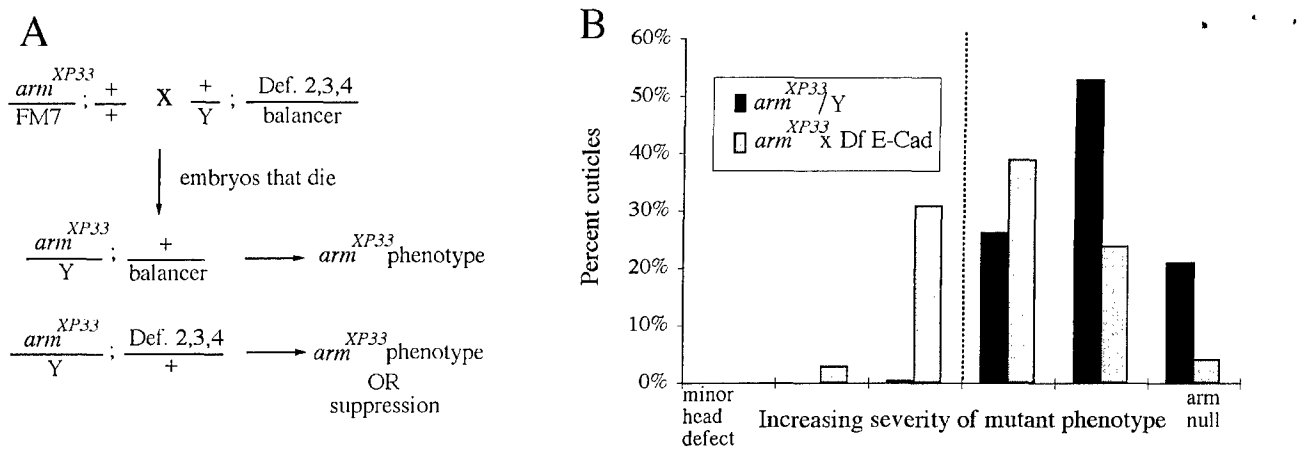

FIGURE 2.—Modifier screen strategy. (A) Cross scheme. arm^{XP33}/FM7 virgin females were crossed to males carrying a single deficiency on chromosome 2, 3, or 4. One-quarter of the progeny are arm^{XP33}/Y and die with a segment polarity phenotype. Half of these are heterozygous for the deficiency. Cuticles were prepared from dead embryonic progeny of each cross. If there is an interaction, these cuticles show suppression of *arm*. (B) The arm^{XP33} cuticle phenotype varies about a mean (black bars). Removing one copy of DE-cadherin shifts the distribution, greatly increasing the fraction with the least severe phenotypes (light bars). Our scoring scheme for phenotypic severity was based on cuticle size, strength of the segment polarity phenotype, and degree of dorsal closure. We counted ≥200 embryos per cross. Percentage of suppression = the number of progeny in the least severe classes (left of the dashed line) divided by the total number of progeny scored.

low frequency (0.5%), arm^{XP33}/Y cuticles have the least severe phenotype: these are nearly wild type in length, have greater denticle diversity, and are dorsally closed (they retain an anterior hole). If one does a similar analysis of arm^{XP33}/Y; *Df-DE-cadherin*/+ embryos, as an example of suppression, one finds that the phenotypic distribution is strongly shifted toward the less severe end (Figure 2B)—in this example, 33% of the cuticles fall in the least severe classes (embryos to the left of the dotted line in Figure 2B). On the basis of this, we focused on the frequency of embryos in the least severe classes. To score whether a Deficiency suppressed the arm^{XP33} phenotype, we prepared cuticles from the dead embryos, scored their phenotypes, and calculated the percentage of cuticles in the least severe classes; if this was at least six times the frequency in the control (*i.e.*, ≥3%), we scored this as an interaction.

By these criteria, 32 deficiencies interacted with arm^{XP33} (Table 1); a representative suppressed cuticle is shown in Figure 3B. Tables 1 and 2, Figure 4, and APPENDIXES A and B summarize the screen, showing which regions were covered by deficiencies and which regions interacted. In all cases the suppression was qualitatively similar; embryos in the least severe class showed an increase in cuticle length, improvement in dorsal closure, and an increase in denticle diversity. The fraction of cuticles in the least severe phenotypic class ranged from 3 to 40% (each number is an average of two to three independent crosses; Tables 1 and 2). We retested each interacting stock—all reliably interacted although in some cases the percentage of suppression varied. Of the 32 stocks that interacted, we arbitrarily made a cutoff between "weak" and "strong" interactions at the level of 6% of the embryos in the least severe phenotypic classes. Eighteen Deficiencies were thus classified as weak interactors, with 3–5.9% of the cuticles in the least severe category (Table 1; APPENDIXES A and B). Although this degree of suppression was reproducible, there were enough regions that suppressed arm^{XP33} more robustly that weakly interacting regions were not investigated further. We noted in passing that six stocks had hemizygous dominant cuticle phenotypes other than effects on segment polarity (Table 2B); one was also one of the strong interactors.

TABLE 1

Summary of the Deficiency screen by chromosome

Chromosome	No. of stocks/chrom.	(0–2.9%) No interaction	(3–5.9%) Weak interaction	(>6%) Strong interaction
2	67	47	12	8
3	64	53	6	5
4	3	2	0	1
Total	134	102	18	14

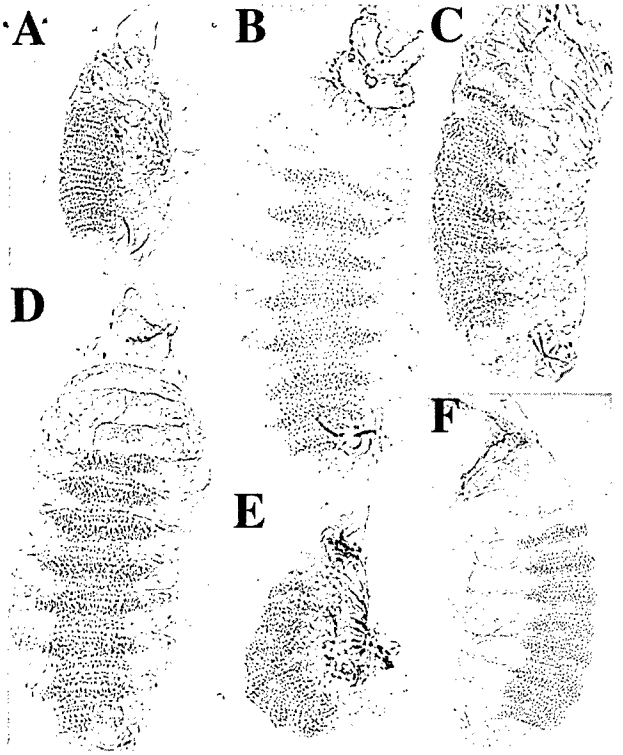

FIGURE 3.—Suppression by Deficiencies from the screen and *Dpresenilin*. (A) arm^{XP33}/Y. (B) arm^{XP33}/Y; *Df(2R)PC4*/+. Example of the suppression observed in the screen. (C) arm^{XP33}/Y; $Dpresenilin^{10}$/+. Heterozygosity for *Dpresenilin* significantly suppressed the arm^{XP33} phenotype. (D) Putative arm^{XP33}/Y; $Dpresenilin^{10}$/*Df(3L)ri-79c* embryo. A slightly more robust suppression was seen in progeny of flies heterozygous for $Dpresenilin^{10}$ crossed to flies heterozygous for *Df(3L)ri-79c*. (E) arm^{YD35}/Y. The zygotic null allele. (F) arm^{YD35}/Y; $Dpresenilin^{10}$/+. Heterozygosity for *Dpresenilin* also suppressed arm^{YD35}.

Fourteen deficiency stocks were "strong" interactors; with 6–40% of the cuticles in the least severe classes (Tables 1 and 2; Figure 4). Two of these deficiencies, *Df(3L)W10* and *Df(3L)Cat*, overlap, suggesting that the gene responsible for that interaction lay in the overlapping region (75B8;C1-2) and reducing the number of interacting genomic regions to 13. While two other interacting deficiencies, *Df(2L)spd* and *Df(2L)TE29*, should not quite overlap based on their reported cytology, they fail to complement one another, strongly suggesting that they do in fact overlap, reducing the number of interacting regions to 12. We analyzed other deficiencies in the regions of the strongly interacting Deficiencies, allowing us in most cases to further pinpoint the interacting region (see APPENDIXES A and B for details). In four cases, smaller interacting Deficiencies were identified. In nine cases, overlap of the original deficiency with other Deficiencies that either interacted or did not interact allowed us to further define the interacting region.

None of the deficiencies tested resulted in any obvious enhancement of the arm^{XP33} phenotype, either producing defects in epithelial integrity or enhancing the segment polarity defects. The wild-type maternal contribution of Arm appears to completely provide adherens junction function, so reducing levels of components required for adherens junction function by 50% apparently does not affect epithelial integrity in arm^{XP33} mutants. In fact, when Müller and Wieschaus examined embryos homozygous for large deficiencies, they found no regions that were zygotically essential for adherens junction assembly and few that had a strong effect on junction function (MÜLLER and WIESCHAUS 1996). We realized in retrospect that the severity of the arm^{XP33} segment polarity phenotype made it unlikely one could reliably recognize an enhancer of this defect.

One possible confounding factor was that mutations on the Balancer chromosomes with which the Deficiency chromosomes were heterozygous could have been the true cause of the phenotypic suppression. We think this is quite unlikely, as only a small number of Balancer chromosomes were used and none showed a consistent effect on the *arm* phenotype. A second potential problem is that second site mutations on the Deficiency chromosomes could in principle be responsible for certain observed interactions. This is highly unlikely for the seven strongly interacting regions that are defined by either two or more interacting Deficiencies or by a Deficiency and an identified gene (Figure 4). For the other five strongly interacting regions, some may be due to linked mutations outside the Deficiency interval, although given the overall frequency at which interactions were detected, we think this is unlikely to be the case for all.

Finding interactors by testing candidate genes: Our first approach to identify the gene(s) within each Deficiency responsible for the interaction was to test candidate genes in each region. We considered as candidate genes those with a mutant phenotype indicating an effect on cell fate choice in the ventral epidermis, genes known to act in Wg signaling, and genes known to affect cell-cell junctions or the actin cytoskeleton. We identified one interactor by this candidate gene approach and ruled out many other candidates by two methods: testing complementation between a candidate and the interacting deficiency and checking directly whether the candidate could suppress *arm*.

We tested four candidate genes that are part of the Wg signal transduction pathway or that affect segment polarity: *dTCF*, *cubitis interruptis*, *naked*, and *wg*. Removing one copy of the fourth chromosome gave a very strong interaction. In examining candidates on the fourth chromosome, we found that mutations in the gene encoding the DNA-binding protein dTCF, which is required for Wg signaling, suppress arm^{XP33}. This was a surprise and revealed a previously unexpected role for dTCF as a repressor as well as an activator of Wg-responsive genes (CAVALLO *et al.* 1998). However, while null alleles of *dTCF* interact strongly, they do not suppress arm^{XP33} to the same degree as removing the entire

TABLE 2

Deficiencies that had a strong interaction with *arm*^{XP33}

A. Original interacting deficiency	Smallest region	% Supp.	Gene
Df(2L)sc19-5/SM6b, Cy[1] Roi[1]; Dp(2;1)B19, Df(1)y-ac, sc[1] pn[1], ed[1] dp[o2] cl[1]	25C8-9;25D2-4	7.9	
Df(2L)spd, al[1] dp[ov1]/CyO	28B3-4;28C	6.0	
In(1)w[m4h], y[1]; Df(2L) TE29Aa-11/CyO	28E4-7;29B2-C1	7.0	
Df(2L)TW137, cn[1] bw[1]/CyO, Dp(2;2) M(2) m[+]	36CD1-E1; 36E1-E2	6.6	
Df(2R)ST1, pr[1] cn[*]/CyO	42B3-5;42E	6.0	
Df(2R)PC4/CyO	55C;55F	9.5	
Df(2R)017/SM1	56F5;56F15	11.0	
Df(3L)W10, ru[1] h[1] Sb[sbd-2]/TM6b	75A6-7;75C1-2	14.0	*hid*
Df(3L)Cat, ri[*] e[*]/TM6	75B8;75F1	9.8	*hid*
Df(3L)Pc-MK/TM3, Sb[1] Ser[1]	78A2-78C9	7.0	
Df(3R)Scr, p[p] e[s]/TM3	84A1-2;84B1-2	9.3	
Df(3R)p712, red[1] e[1]/TM3	84D3-5;84F1-2	10.0	*puc*
Df(3R)D1-BX12, ss[1] e[4] ro[1]/TM6B	91F5;92D3-6	6.0	
C(4)RM, ci[1] ey[R]	101F1;102B	37.0	*dTCF*
B. Hemizygous dominant phenotype			
Df(3L)31A/Dp(3;3)C126, st[1] cp[1] in[1] ri[1] p[1]	78A;78E, 78D;79B		
Dp(3;1)2-2, w[1118]/?;Df(3R)2-2/TM3	81F;82F10-11;3D		
Df(3R)p712, red[1] e[1]/TM3	84D4-6;85B6, 25D;085B6		*puc*
Df(3R)P14, sr[1]/T(2;3)ap[Xa]	90C2-D1;91A1-2		
Df(3R)23D1, ry[506]/TM3 Sb[1]/mus309[Horka] e[1]	93F-94F1-6		
Df(3R)awd-KRB, ca[1]/TM3, y[+] Sb[1] e[1] Ser[1]	100C;100D		

A: Column 1, the original interacting Deficiencies from the Deficiency kits; column 2, the smallest interacting region, derived from comparing interacting and noninteracting Deficiencies (see APPENDIXES A and B for details); column 3, the percent of individuals in the weakest phenotypic classes; column 4, identified interacting genes. B: Six Deficiencies were associated with partially penetrant dominant phenotypes. One also was a suppressor.

fourth chromosome. Thus, there may be a second suppressor on the fourth chromosome. *cubitis interruptis*, a gene involved in *hedgehog* signaling, was ruled out as this suppressor by testing a null allele for interaction (CAVALLO *et al.* 1998). *naked* is a known negative regulator of Wg signaling and maps near *Df(3L)Cat*. However,

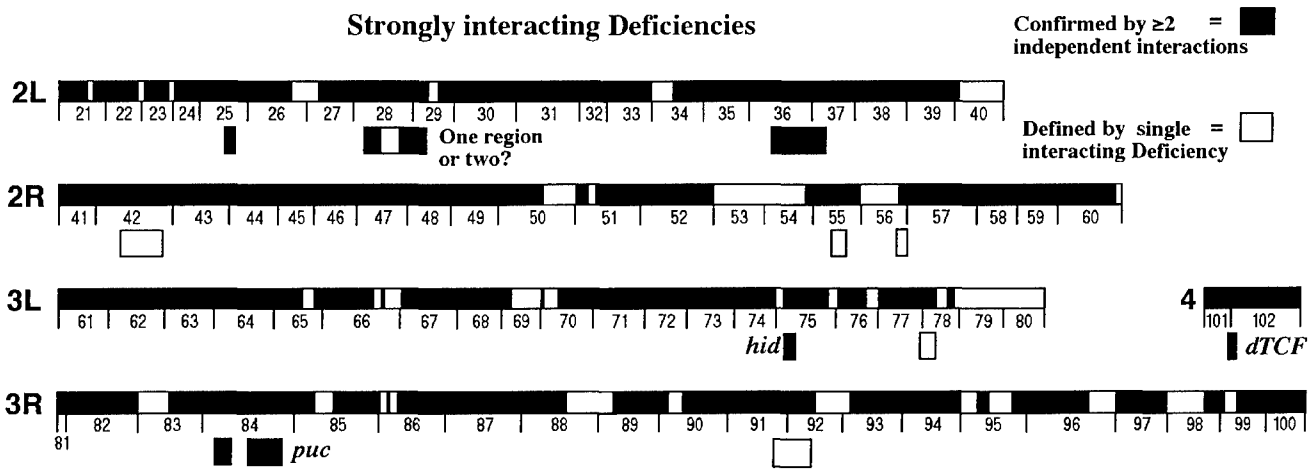

FIGURE 4.—Schematic summary of the screen. We estimate that ≥80% of the euchromatin of chromosomes 2, 3, and 4 were covered. Regions covered are represented by the black portions of the chromosomes; white portions are regions for which we were unable to find deficiencies. Black boxes below chromosomes represent regions containing putative suppressor(s) defined by the overlap between two or more deficiencies, or where an interacting gene was defined. White boxes represent regions defined by a single interacting Deficiency (see APPENDIX for details).

it complemented this Deficiency and was thus ruled out. Two deficiencies, *Df(2L)TE29* and *Df(2L)spd*, are in the vicinity of *wg*. While *wg* is a positively acting component of the pathway, our experience with dTCF made us cautious in ruling it out without a test. We found that: (1) *wg* complements *Df(2L)TE29* and (2) a *wg* null does not suppress *arm*. This ruled *wg* out, although *DWnt4*, which maps near *wg* (GRABA *et al.* 1995), remains a candidate. Finally, we tested alleles of two segment polarity genes that fell outside regions included in the Deficiencies in the kit: *hedgehog* and *teashirt*, which encodes a transcription factor that physically and functionally interacts with Arm (GALLET *et al.* 1998). Neither suppressed arm^{XP33}.

We also tested several genes with roles in cell-cell adhesion or cytoskeletal function. One was *DE-cadherin (shotgun)*, which we already knew could suppress *arm*. *Df(2)017* was suggested by its cytology to remove *DE-cadherin*, but both an allele of *DE-cadherin* and the small deficiency *Df(2)E2* that removes *DE-cadherin* (UEMURA *et al.* 1996) complement *Df(2)017*. Thus this interaction is due to a different gene. Three other genes that regulate the cytoskeleton, *enabled* (*ena*; GERTLER *et al.* 1995), *quail* (MAHAJAN-MIKLOS and COOLEY 1994), and *scraps* (SCHUPBACH and WIESCHAUS 1989), map to regions covered by interacting Deficiencies (56B5, 36C2-11, and 43E7, respectively). *ena* is an actin cytoskeleton regulator, *quail* encodes a vinculin-like protein thought to associate with actin, and *scraps* is required for the cytoskeletal events of cellularization. *ena* was included in interacting deficiency *Df(2R)PC4* by complementation (we did not test *quail* and *scraps* by complementation). However, when we tested alleles of all three genes, none suppressed arm^{XP33}. *18-wheeler*, a putative cell-adhesion molecule (ELDON *et al.* 1994) that maps in or near *Df(2R)017*, also did not suppress arm^{XP33}.

As a partial test of the effectiveness and completeness of the screen, we also tested a series of additional candidate genes, some of which fell outside Deficiencies in the kit and others of which were probably included in these Deficiencies but which we expected might physically or functionally interact with Arm. The vast majority did not show an interaction. We tested a variety of genes encoding components of other signal transduction pathways that pattern the dorsal or ventral epidermis: (1) the Hedgehog pathway, $hedgehog^{Ar}$; (2) the Dpp pathway, $decapentaplegic^{e87}$ and $screw^{J1}$; (3) the EGF receptor (EGFR) and other receptor tyrosine kinase pathways, $spitz^{2A14}$, $vein^{147-2}$, $argos^{257}$, $Egfr^{C18}$, $ras85D^{e1B}$, $rolled^{C18}$, yan^{XE-12}, and $torso^{1}$; and (4) the Jun N-terminal kinase pathway, *basket* and $Djun^{1}$. Of these, only $spitz^{2A14}$ interacted, and even in this case, only 3.8% fell into the weakest phenotypic categories, just above our cutoff for a weak interaction. We also tested five genes affecting the cytoskeleton or cuticle integrity: $krotzkopf\ verkehrt^{1}$, $myoblast\ city^{G1}$, $shroud^{1}$, $steamer\ duck^{3R-17}$, and $scraps^{8}$. None interacted. Finally, we tested one candidate among proteins that interact with mammalian β-catenin but for which the function of this interaction is not known. This was *Drosophila presenilin*, homolog of the mammalian presenilin family of transmembrane proteins (reviewed in HAASS and DE STROOPER 1999). Mammalian Presenilins bind mammalian β-catenin (ZHOU *et al.* 1997; MURAYAMA *et al.* 1998; YU *et al.* 1998; LEVESQUE *et al.* 1999). Further, misexpression and other experiments suggest that mammalian Presenilins may regulate Wnt signaling (MURAYAMA *et al.* 1998; ZHANG *et al.* 1998; KANG *et al.* 1999; NISHIMURA *et al.* 1999a). In contrast to the other candidates tested, *D. presenilin* showed a very strong interaction. Heterozygosity for *D-presenilin* strongly suppressed arm^{XP33} (14.6% with weakest phenotypes; Figure 3, A *vs.* C) and also suppressed the zygotic null *arm* allele, arm^{YD35} (Figure 3, E *vs.* *F*). A surprise from these results was that although *Dpresenilin* was removed by two of the Deficiencies tested, *Df(3L)ri-79c* and *Df(3L)rdgC-co2*, neither showed a significant interaction (percentage of suppressions = 1.8 and 1.5%, respectively). This suggests that some interactions are sensitive to genetic background, and thus not all potential haplo-insufficient interactors were identified in our screen.

P-element lethals that interacted: Our second approach to identifying genes responsible for an interaction was to use the collection of *P*-element-induced lethal mutations (hereafter called *P*-lethals) characterized by the Berkeley Drosophila Genome Project. These lethals are caused by *P*-element transposon insertions and are thus molecularly tagged, facilitating cloning. The available *P*-lethals are estimated to hit ~25% of essential genes (SPRADLING *et al.* 1999). One caveat to using these mutations to uncover a dose-sensitive suppressor is that there is no guarantee that the *P*-lethal will be a null allele, as is a Deficiency. *P*-transposons tend to insert either in the 5′ untranslated region or in introns, thus creating mutations that often are not null in phenotype and thus do not, when heterozygous, reduce gene function by 50%.

We obtained the *P*-lethals available from the Bloomington Stock Center (81 stocks) and the Kiss collection (73 stocks) in each of the interacting regions and tested their ability to suppress arm^{XP33}. A list of the *P*-lethal stocks tested is in a data supplement at http://www.genetics.org/cgi/content/full/155/4/1725/DC1. Of the *P*-lethals tested, we found two that suppressed arm^{XP33}. One of these, *l(3)A251.1*, mapped to region 84E. By examination of its homozygous phenotype and subsequent complementation tests, we learned that this is an allele of *puckered* (MARTIN-BLANCO *et al.* 1998). A detailed examination of the biology underlying this interaction is presented in MCEWEN *et al.* (2000).

The apoptosis-promoting gene *head involution defective* is a dose-sensitive suppressor of *arm*: The second *P*-lethal that interacted with *arm* was *l(3)05014*, which maps to 75C1-2 and gave as strong a suppression as either of the interacting deficiencies in this region.

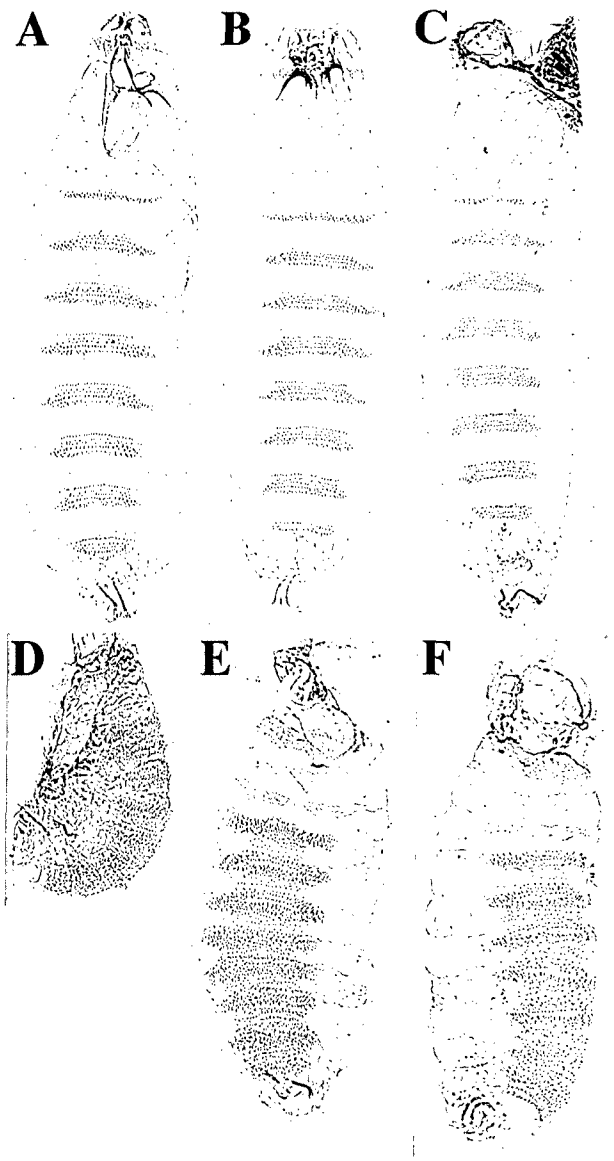

FIGURE 5.—Decreasing cell death suppresses *arm*. Wild type (A), hid^{05014} homozygotes (B), and *Df(3L)H99* homozygotes (C) have very similar cuticle phenotypes. hid^{05014} and *Df(3L)H99* homozygotes have head defects, but their segment polarity is normal. (D) arm^{XP33}/Y (E) arm^{XP33}/Y; hid^{05014}/+. Removing one copy of *hid* suppresses arm^{XP33}. (F) arm^{XP33}/Y; *armGAL4/UAS-p35*. Expression of the baculovirus antiapoptotic protein p35 in an arm^{XP33} mutant background also suppresses *arm*.

l(3)05014 is an allele of *head involution defective* (GRETHER *et al.* 1995). This allele is likely to be a null, as the *P*-element is inserted early in the protein-coding region. Null mutations in *hid* are embryonic lethal with defects in head involution during embryonic development (ABBOTT and LENGYEL 1991; Figure 5, A *vs.* B), although occasional escapers survive to adulthood. More recently, it was revealed that *hid* mutations affect programmed cell death.

The machinery that triggers PCD in Drosophila has been the subject of intense investigation (reviewed in ABRAMS 1999). This work was initiated by a screen for genomic regions required for PCD (WHITE *et al.* 1994). When chromosomal region 75C1-2 is deleted, in embryos homozygous for the small deficiency *Df(3)H99*, essentially all PCD in the embryo is eliminated (WHITE *et al.* 1994). Subsequent analysis revealed that this chromosomal region contains three genes involved in PCD: *hid*, *reaper*, and *grim* (reviewed in ABRAMS 1999). Ectopic expression of any of these will trigger PCD. However, loss-of-function mutations are only available for *hid*. In *hid* mutants, a subset of the cells that normally undergo PCD do not do so (GRETHER *et al.* 1995), resulting in defects in head development. In embryos homozygous for *Df(3L)H99*, which thus lack *hid*, *reaper*, and *grim*, all PCD is abolished (WHITE *et al.* 1994); these embryos have slightly stronger defects in head development (Figure 5C).

hid plays an important role in PCD. Ectopic expression of *hid* is sufficient to induce PCD in the eye, and this is completely suppressed by the baculovirus caspase inhibitor p35, suggesting *hid* acts upstream of caspases (GRETHER *et al.* 1995). *hid* has no clear homologs in other organisms; however, Hid overexpression triggers PCD in mammalian cells. Hid, Reaper, and Grim all share a short region of weak sequence similarity near their N termini. In Hid, this region is required for initiating cell death in mammalian tissue culture, while Hid's C terminus is required for localization to mitochondria, an organelle involved in PCD (HAINING *et al.* 1999). Recent work supports the idea that Hid functions by blocking interaction between Inhibitor-of-apoptosis (IAP) family caspase inhibitors and caspases (VUCIC *et al.* 1998; WANG *et al.* 1999).

Heterozygosity for hid^{05014} suppresses arm^{XP33} (Figure 5, D *vs.* E), as well as the zygotic null allele arm^{YD35} (data not shown). Heterozygosity for an X-ray-induced loss-of-function allele, hid^{WR+XI}, causes the same degree of suppression, further supporting the idea that *hid* is the gene responsible for the interaction. In addition, we generated revertants of the *P* element in hid^{05014} by mobilizing the *P* element and screening for viable stocks that lost the genetic marker carried by the *P* element. These revertant chromosomes fail to suppress arm^{XP33} (data not shown). Further reducing *hid* levels by making embryos homozygous for hid^{05014} does not increase the degree of suppression of arm^{XP33}. Likewise, either heterozygosity or homozygosity for the small deficiency *Df(3L)H99*, which removes *hid*, *grim*, and *reaper*, suppresses arm^{XP33} to the same degree as removal of one copy of *hid*.

The suppression by *hid* can be mimicked by blocking PCD: PCD is elevated in segment polarity mutants (MARTINEZ ARIAS 1985; KLINGENSMITH *et al.* 1989; PAZDERA *et al.* 1998). The dramatically shortened cuticle secreted by an *arm* mutant is presumably caused, at least in part, by loss of ventral epidermal cells via PCD. The suppression of arm^{XP33} by hid^{05014} could thus be due to Hid's role in PCD; alternately, it could be due to an unknown

function of Hid. To test if the *arm* suppression results from an effect on PCD, we reduced embryonic PCD by expressing the baculovirus antiapoptotic protein p35, which acts as a caspase inhibitor; p35 suppresses the PCD triggered by *hid* overexpression in the fly eye (GRETHER *et al.* 1995). We found that arm^{XP33} mutant embryos in which we ubiquitously expressed p35 using the GAL4-UAS system (BRAND and PERRIMON 1993) had a suppressed phenotype (Figure 5, F *vs.* D). The suppression by p35 was similar in degree to that resulting from *hid* heterozygosity (Figure 5E). This suggests that decreased PCD in the embryo can suppress *arm* and supported the idea that the interaction between *hid* and *arm* was due to *hid*'s role in PCD.

***hid* suppresses *wg* in a highly dose-sensitive fashion:** We next tested whether the effect was *arm* specific or whether reduction in PCD would suppress the phenotype caused by other reductions in Wg signaling. To do so, we examined whether reduction in PCD suppressed a null allele of *wg*, wg^{IG22}. wg^{IG22} mutant cuticles have a lawn of uniform, large denticles covering the ventral epidermis (NÜSSLEIN-VOLHARD and WIESCHAUS 1980; Figure 6A), and they are much smaller than wild type, but unlike *arm* mutant cuticles they are usually closed dorsally. We tested whether heterozygosity or homozygosity for either *hid* or for *Df(3L)H99* suppressed wg^{IG22}.

hid modified wg^{IG22} in a dose-sensitive fashion, but the nature of the phenotypic modification was different from that seen with *arm*. There was not any pronounced improvement in the *wg* segment polarity defect; in wg^{IG22}; hid^{05014} (Figure 6B) or wg^{IG22}; *Df(3L)H99* (Figure 6C) double mutants, all cells still secrete a uniform lawn of denticles, and the cuticle of the wg^{IG22}; *Df(3L)H99* double mutant remains much smaller than that secreted by a wild-type embryo, contrasting with the increase in cuticle size in *arm; Df(3L)H99* double mutants. However, we found a striking effect of *hid* dose on the number and size of the denticles on the ventral epidermis. The number of denticles is more than doubled in wg^{IG22}; *Df(3L)H99* compared to wg^{IG22} alone, and the denticles secreted by the double mutant are much smaller than those in the *wg* null (Figure 6, A *vs.* B and C; the change in denticle size may be less meaningful, as denticle size is also somewhat reduced in *Df(3L)H99* homozygotes that are wild type for *arm* and *wg*; Figure 5C).

wg^{IG22} is less sensitive to reduction in *hid* dose than *arm*, and thus the effect on wg^{IG22} is additive. Removal of one copy of *hid* in a wg^{IG22} background has only a subtle effect on cuticle pattern (data not shown), while removal of both copies of *hid* has a stronger effect (Figure 6, B *vs.* A). Removing one copy of the region covered by *Df(3L)H99* has a greater effect than removing both copies of *hid* (data not shown), suggesting that removing all three cell death genes results in a more pronounced interaction. The effect on cuticle pattern is thus most pronounced in wg^{IG22}; *Df(3L)H99* double mutants (Figure 6C), which have many more, much smaller denticles than does a wg^{IG22} single mutant (Figure 6A). To confirm this, we labeled embryos with phalloidin to visualize the filamentous actin in denticles and with TUNEL to identify embryos with cells undergoing PCD. Embryos homozygous for *Df(3L)H99* do not label with TUNEL, as they have no PCD, allowing us to unambiguously identify double mutants. The results matched the cuticle data: wg^{IG22} mutants showed the characteristic lawn of denticles (Figure 6F), while wg^{IG22}; *Df(3L)H99* double mutants (embryos without cells undergoing PCD as measured by TUNEL) had many more much smaller denticles (Figure 6E). In the course of this analysis, we also observed that *Df(3L)H99* mutants have significantly more epidermal tissue in the head (as was previously observed by GRETHER *et al.* 1995) and in the lateral epidermis (Figure 6, J *vs.* K), consistent with the idea that wild-type embryos reduce the number of epidermal cells via PCD. We also examined whether reduction in PCD suppressed a weaker *wg* heteroallelic combination, wg^{PE4}/*Df(2)DE*. We saw no noticeable suppression of the segment polarity phenotype and no noticeable increase in denticle number caused by either heterozygosity or homozygosity for *Df(3L)H99* (data not shown). This may not be surprising as this weaker *wg* phenotype likely primarily reflects changes in cell fate without significant ectopic cell death, as the cuticle is nearly wild type in length.

Blocking cell death in wg^{IG22} increases cell number but decreases cell size: The novel phenotype of wg^{IG22}; *Df(3L)H99* double mutants could have several causes. Extra denticles could result if individual cells secreted more denticles; alternately, they could result from an increased number of cells. To distinguish these possibilities, we examined the cell morphology of wild type, wg^{IG22}, and wg^{IG22}; *Df(3L)H99* double-mutant embryos, using antibodies to phosphotyrosine to outline ventral epidermal cells and to label developing denticles. In wild-type embryos (Figure 6G), ventral epidermal cells form a reiterated pattern of denticle-secreting cells, which are very narrow in the anterior/posterior (A/P) axis, and naked cuticle-secreting cells, which are much less narrow. There are, on average, 12 rows of cells per segment. In contrast, in *wg* mutants there are only 8 rows of cells per segment (Figure 6H; the segment boundary was determined by comparison of the denticle pattern in cuticles to the phosphotyrosine pattern). In the wg^{IG22}; *Df(3L)H99* double mutant, cell number is greatly increased relative to the wg^{IG22} single mutant. The double mutant has 12 to 14 rows of cells (Figure 6I), equaling or exceeding the number of cell rows in the wild type. Thus eliminating PCD in a wg^{IG22} mutant embryo increases cell number, as expected.

Blocking cell death in a wg^{IG22} mutant also had a second, unexpected consequence—cell size was significantly decreased. As mentioned above, in wild-type embryos anterior denticle-secreting cells are narrowed in the A/P axis, while posterior naked cuticle-secreting

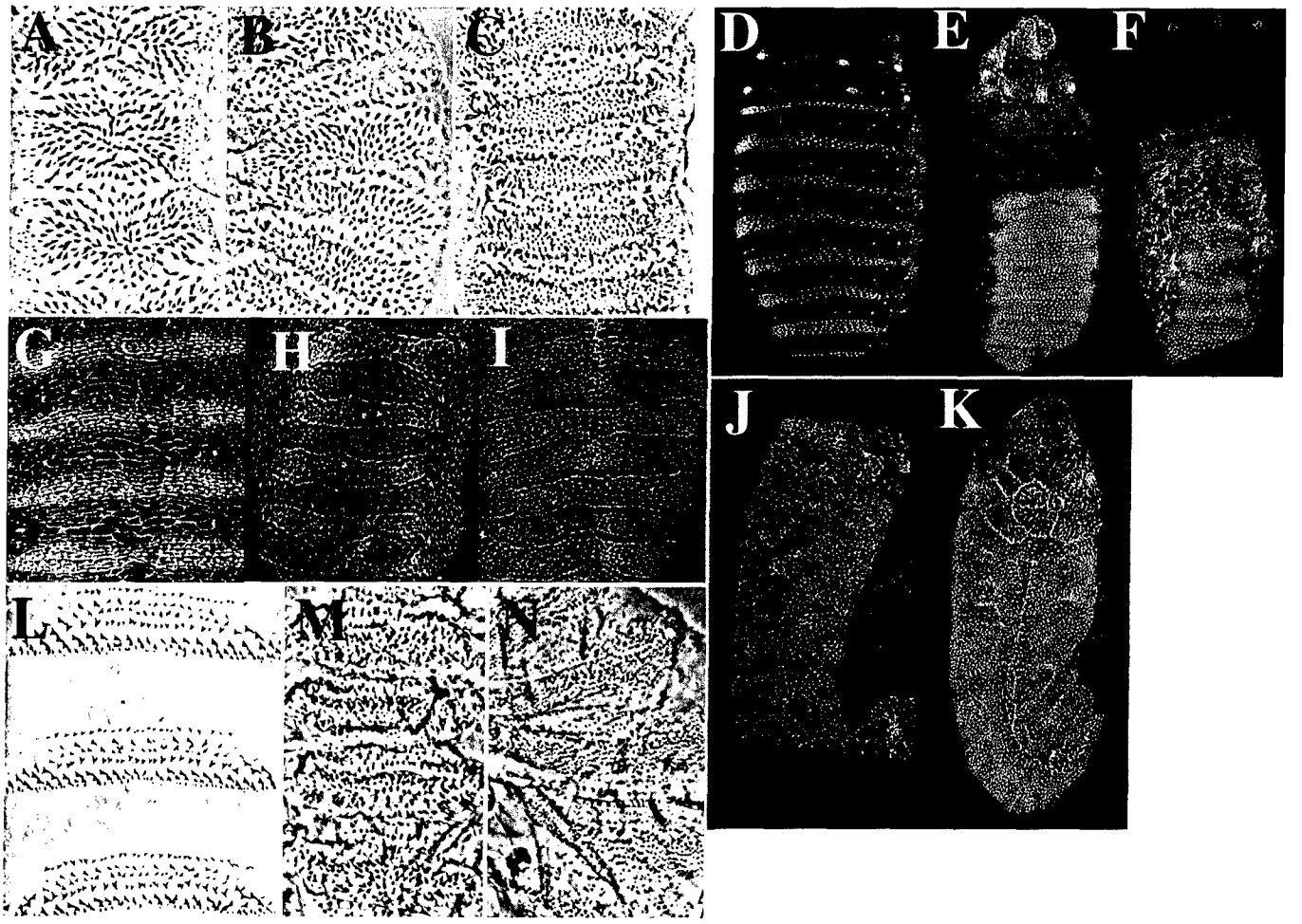

FIGURE 6.—Reducing PCD suppresses *wg* in a dose-sensitive fashion. (A–C) Cuticle preps. (D–F) Embryos labeled with phalloidin, which recognizes f-actin and thus highlights denticles. These embryos were also labeled via TUNEL (data not shown) to confirm their genotypes. (A, F) *wg* null mutants completely lack segment polarity and have only large, thick denticles. (B) wg^{IG22}; hid^{0501}. (C, E) wg^{IG22}; *Df(3L)H99*. (D) Wild type. In the double mutants, denticle number greatly increases. (G–K) Embryos stained with antiphosphotyrosine antibody to outline cells. (G) Wild type, showing reiterated groups of narrow cells, which will secrete denticles, and less narrow cells, which will secrete naked cuticle. There are 12 rows of cells per segment. (H) *wg* single mutants have fewer, larger cells. All cells are cuboidal, and there are about 8 rows of cells per segment. (I) *wg*; *Df(3L)H99* double mutants have many more ventral epidermal cells than *wg* single mutants—there are 12 to 14 rows of cells per segment. Cells in the double mutant are much smaller. (J) Lateral view of a wild-type embryo during germband retraction. (K) *Df(3L)H99* at the same stage, revealing an increased number of cells compared to wild type. Excess cells form a lateral fold and ectopic folds near the maxillary and labial segments and toward the posterior. (L) Wild-type cuticle. (M) arm^{XP33}. (N) arm^{XP33}; *UAS-dsh/VP16::armGAL4*. Expressing high levels of *dsh* in arm^{XP33} results in an increase in denticle number and reduction in denticle size, similar to that in *wg*; *Df(3L)H99* double mutants.

cells are not. In contrast, in a *wg* mutant all cells are both uniformly cuboidal (Figure 6H) and significantly larger than denticle-producing cells of a wild-type embryo. This increase in size likely reflects an increase in cell volume, because in optical cross sections wg^{IG22} and wild-type cells were the same height (data not shown). In contrast, cells of wg^{IG22}; *Df(3L)H99* double mutants are much smaller than those in *wg* single mutants (Figure 6I). Ventral cells of double mutants do resemble wg^{IG22} single mutants in several ways; most cells are cuboidal, the cells create a pattern of block-like pseudosegments (though with more rows of cells than in *wg* single mutants), and all cells secrete denticles. We do not have a good explanation for the qualitative difference in the effect of *hid* on the *arm* and wg^{IG22} phenotypes. We observed one other situation where manipulating Wg signaling resulted in an increased number of smaller denticles. Overexpression of *dsh* using the GAL4-UAS system in an arm^{XP33} mutant gives rise to a cuticle with many very small denticles, but with the length of an arm^{XP33} single mutant (Figure 6, M *vs.* N). Dsh is a positive effector of Wg signaling mapping upstream of Arm in the Wg pathway; we imagine that Dsh overexpression slightly augments the residual Wg signaling in an *arm* zygotic mutant.

Our comparison of wg^{IG22} and wg^{IG22}; *hid* suggests that

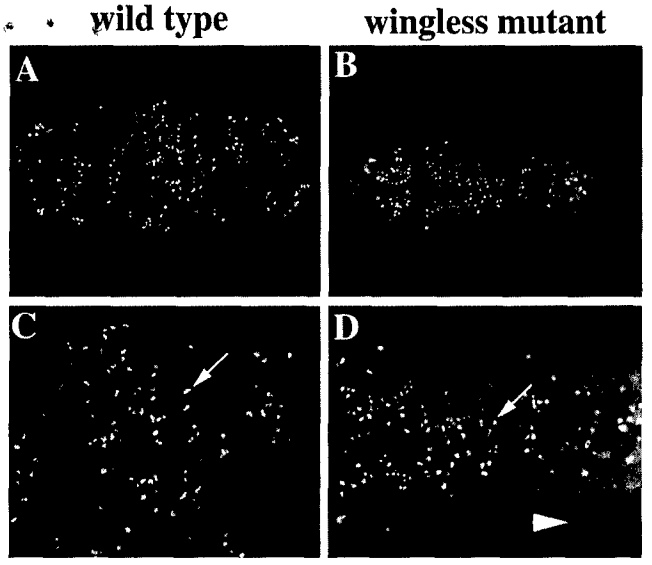

FIGURE 7.—*wg* mutants enter mitosis 16 in the ventral epidermis. Ventral views of representative wg^{IG22} (B, D) and phenotypically wild-type sibling (A, C) embryos stained with anti-phosphohistone H3 antibodies. The magnification in C and D is twice that of A and B. Arrows in C and D indicate condensed chromosomes of cells that were counted. Only mitotic figures in the epidermis were included in the counts; out of focus staining (*e.g.*, arrowhead) is from mitotic cells in the underlying central nervous system. Embryos were from a wg^{IG22}/*CyO ftz-lacZ* stock, allowing unambiguous identification of *wg* mutants by lack of β-galactosidase expression. *wg* mutants were also apparent due to defects in the normal segmental pattern of S phase and mitosis.

an increase in PCD contributes to the reduced number of ventral epidermal cells in *wg*, consistent with previous observations (PAZDERA *et al.* 1998). This might also explain the increased cell size in *wg* mutants, as epidermal cells have been observed engulfing dying neighbors (PAZDERA *et al.* 1998), thus potentially increasing their size. However, since Wnts are mitogens in certain cell types (*e.g.*, DICKINSON *et al.* 1994; NEUMANN and COHEN 1996), we also considered an alternate explanation that could explain both reduction in cell number and increase in cell size in wg^{IG22} mutants: a failure to complete the normal program of cell division. Since no growth occurs within the embryo, as cells divide they are reduced in size, and thus if wg^{IG22} mutant cells failed to complete one round of mitosis, they would be twice as large.

We thus assessed the pattern of cell division in wg^{IG22}. Ventral epidermal cells divide three times after the blastoderm stage and arrest in G1 of the 17th embryonic cell cycle (EDGAR and O'FARRELL 1989). Cell divisions can be visualized by pulse labeling with BrdU to detect replicating nuclei or with an antibody that specifically recognizes a phosphoisoform of histone H3 that only occurs during mitosis (Figure 7; SU *et al.* 1998). Condensed mitotic chromosomes can be easily identified in fixed tissues with this antibody (Figure 7, C and D). We analyzed embryos at a time (stage 12) when cells of the ventral epidermis normally complete their 16th cell cycle, to see if wg^{IG22} mutants fail to undergo this last cell division. BrdU labeling indicated that ventral epidermal cells replicate during S phase 16 in wg^{IG22} mutants (data not shown). In addition, mitotic figures are as readily apparent in the ventral epidermis of stage 12 wg^{IG22} mutant embryos as they are in wild type (Figure 7, A and B). Thus, lack of Wg activity does not cause inappropriate cell cycle arrest. To compare the mitotic index between wild type and wg^{IG22}, we counted the total number of phosphohistone H3 positive nuclei of the ventral surface of individual embryos (arrow in Figure 7, C and D). There was no significant difference between the average number of mitotic cells in wild-type (175 ± 75.7; $n = 7$) *vs.* wg^{IG22} mutant (232 ± 44.2; $n = 9$) embryos. The variance in the absolute numbers of mitotic cells from embryo to embryo can be attributed to at least two factors: First, the precise age of each embryo scored differs slightly, as stage 12 spans ~2.5 hr of development at 25°, and second, there is some cell cycle asynchrony among individual cells of a particular epidermal region that enter mitosis "together" (*i.e.*, mitotic domains). We conclude that wg^{IG22} mutant embryos complete the normal number of cell divisions in the ventral epidermis, supporting the idea that the reduction in cell number in this region of late stage wg^{IG22} embryos is primarily a consequence of elevated levels of PCD.

DISCUSSION

Drosophila Arm and its human homolog βcat are multifunctional proteins that play roles in cell-cell adherens junctions and in the transduction of Wg/Wnt signals. In both roles, Arm/βcat acts as a scaffold upon which a multiprotein complex is assembled. In addition to these well-documented roles, Arm/βcat associates with other proteins, such as the EGF receptor (HOSCHUETZKY *et al.* 1994), fascin (TAO *et al.* 1996), and Presenilin 1 (ZHOU *et al.* 1997). The biochemical function of these complexes is unknown.

We desire to learn more about the known roles of Arm in adherens junctions and in Wg signaling and also to begin to learn what Arm might do with its other partners. Genetics offers the opportunity to look for proteins that are functionally linked with Arm without assumptions as to their identity or biochemical role. Our initial goal in the screen was to identify novel proteins essential for adherens junction assembly or structure. However, as in all genetic screens, we had cast our net much wider. In the four cases where we proceeded from Deficiency to single gene, none encode new junctional proteins and each reveals a separate aspect of Arm biology. The fourth chromosome interactor dTCF revealed a previously unexpected role for a known component of the Wg pathway, providing evidence that dTCF not only activates Wg responsive genes but also, in the ab-

sence of Arm, represses them (Cavallo *et al.* 1998). Characterization of the interactor in 84E, Puckered, revealed a novel role for a known protein and led to data suggesting that the JNK and Arm pathways act in parallel both in dorsal closure and in ventral patterning (McEwen *et al.* 2000). The interaction with Dpresenilin suggests that the biochemical interaction observed in mammalian cells has impact on Arm function *in vivo*. The fourth interactor, Hid, demonstrated that altering a downstream consequence of the loss of Wg signaling, programmed cell death, could suppress *arm* and, as is discussed below, suggested that Wg may act as a survival factor by modulating Hid activity.

We were initially concerned about the amount of labor required to screen for suppressors reducing the severity of an embryonic lethal phenotype without restoring viability (we expected that suppression to viability was unlikely). In retrospect, the screen, while labor intensive, was quite straightforward and could be applied to other embryonic lethal genes with a clear cuticle phenotype (*arm*'s position on the X chromosome eased the effort). Use of the Deficiency kit reduced the number of stocks screened, although having completed the screen we now believe one could carry out such a screen using individual mutagenized lines. Others also recently screened for suppressors or enhancers of embryonic lethal phenotypes, suggesting that this approach may be widely applicable (Raftery *et al.* 1995; Hudson *et al.* 1998; A. Bejsovec, personal communication).

Our screen had several limitations that affected the spectrum of genes identified. First, for a gene to be identified, it had to affect the *arm* phenotype in a dose-sensitive way. Second, the effect on *arm* had to be consistent and substantial. Our arbitrary cutoff for degree of interaction likely eliminated genes in the desired categories in which mutations did not sufficiently suppress *arm*. For example, loss-of-function mutations of Drosophila *abelson* or Deficiencies that remove it suppress *arm*, but not to a sufficient degree to be scored positive in our screen (Loureiro and Peifer 1998). Third, due to the allele of *arm* we chose, we could not reliably score enhancement of the segment polarity phenotype, and likewise, potentially due to high levels of maternal Arm, we did not detect any interactor that produced defects in epithelial integrity. Fourth, since many *P*-element alleles are not null, our ability to move from Deficiency to single gene using these mutations was consequently limited. Finally, genetic background may obscure some interactions—for example, we saw a clear genetic interaction with two alleles of *Dpresenilin* but saw no significant interaction with two Deficiencies that remove it.

During preparation of this manuscript, an article appeared describing a different strategy for identifying genetic interactors with *arm*, which provides an interesting comparison. Greaves *et al.* (1999) expressed in the posterior compartment of the wing the intracellular domain of DE-cadherin, which they previously found could sequester Arm and thus block its signaling activity (Sanson *et al.* 1996). In parallel they overexpressed Arm in the same place. Each caused a reproducible wing phenotype, which appears to reflect reduction and elevation of Wg signaling, respectively. They then screened for modifiers of these phenotypes using, as we did, the Deficiency kit. Many of the deficiencies tested thus overlapped (though not all, as we did not test the X chromosome and they did not test the fourth chromosome).

We compared the spectrum of modifying Deficiencies obtained in our screen with the 59 interacting Deficiencies identified in their screen. The Deficiencies identified were quite different, likely reflecting the distinct methods used to examine interaction and the different tissues involved. These differences illustrate the benefit of taking a variety of genetic approaches to modifier screens and emphasize that no one screen will identify all or even most potential interactors. Most interacting Deficiencies identified in their screen did not interact in our screen; for 39 of their interacting deficiencies, the percentage of suppression in our screen was <3%. Eight of their interacting Deficiencies were weak interactors in our screen [*Df(2L)sc19-8*, *Df(2L)prd1.7*, *Df(2L)J32*, *Df(2L)H20*, *Df(3L)vin5*, *Df(3L)ZN47*, *Df(3R)crb87-5*, and *Df(3R)Hu*]. Four interacting Deficiencies from their screen, *Df(3L)Spd*, *Df(3L)Cat*, *Df(3R)D1-BX12*, and *Df(3R)p712*, were strong interactors in our screen. Within two of these latter regions we identified interactors: *hid* from *Df(3L)Cat* and *puc* from *Df(3R)p712*.

Even in cases where the two screens identified the same Deficiency, it is not clear that the same gene is responsible. First, in several cases different subsets of overlapping Deficiencies interacted in the two screens. Second, Greaves *et al.* (1999) identified interacting genes in many of their Deficiencies. In four cases, we also examined those candidates. Two were identified as interactors in our screen as well (*DE-cadherin* and *zw3*, used in our reconstruction experiments). In contrast, one of their interactors, *wg*, did not interact in our screen, even though a Deficiency that removes it, *Df(3L)Spd*, did interact. Likewise, components of the EGFR pathway interacted in their tests but not ours. Finally, in our hands *naked* complements *Df(3L)Cat*, thus ruling it out as our interactor in that region; in this region we identified *hid* as the interactor.

Hid activity, PCD, and the segment polarity phenotype: It has been known for more than a decade that PCD plays an important role in the segment polarity phenotype resulting from inactivation of either the Hedgehog or Wg pathways (Martinez-Arias 1985; Klingensmith *et al.* 1989). Recently, Minden and colleagues carried out a detailed analysis of this process, quantitating cell death in *wg*, *arm*, *gooseberry*, and *naked*. They found that the elevation in cell death affected particular cells (Pazdera *et al.* 1998). Since the first reports of cell death in segment polarity mutants, the

machinery that drives PCD in embryos has begun to be identified. Homozygosity for the small chromosomal Deficiency, *Df(3L)H99*, blocks essentially all PCD (White *et al.* 1994). Within this interval, three genes play roles in PCD: *grim*, *reaper*, and *hid* (reviewed in Abrams 1999). Ectopic expression of any of these can trigger PCD, but loss-of-function mutations are only available for *hid*.

Given the role of PCD in the segment polarity phenotype, it is perhaps not surprising that elimination of PCD would alter it. Several aspects of the effect of PCD reduction were unexpected, however. First, and most striking, the phenotypes of *arm* and *wg* mutants were very sensitive to relatively small changes in the dose of *hid* and the other cell-death promoters. For example, while heterozygosity for *hid* has no known effects on normal development, it strongly suppresses *arm*. Further reductions in the levels of *hid* or the other cell-death regulators had no additional effect on *arm*, suggesting that reducing the Hid dose by half eliminated the relevant ectopic PCD that occurs in an *arm* mutant. The *wg* phenotype was also suppressed in a highly dose-sensitive fashion, but in a different dosage range. A 50% reduction of *hid* caused slight but detectable effects, a 50% reduction in all three death promoters caused greater suppression, while homozygosity for the deletion removing all three genes resulted in the strongest *wg* suppression.

Recent observations regarding the role of Hid in PCD in the eye may explain this. Signaling through the ras/mitogen-activated protein kinase (MAPK) pathway promotes cell survival by antagonizing Hid (Bergmann *et al.* 1998; Kurada and White 1998). These authors suggested that Hid serves as a rheostat, with its levels determining the probability of PCD. They further suggest that Hid activity has to exceed a threshold to trigger PCD; the accumulation of *hid* mRNA in cells that are not programmed to die is consistent with this (Grether *et al.* 1995). Our observations further support this model. Wg signaling may normally antagonize Hid, potentially by regulating its expression. In embryos where Wg signaling is attenuated, elevated Hid activity may trigger PCD when it rises above a critical threshold. A threshold model could explain why the segment polarity phenotype is so sensitive to the dose of Hid and its partners.

Another surprise was the qualitative difference in the effect of cell death reduction on *wg* and *arm* mutants. While the resulting cell number was likely increased in both double-mutant genotypes in the *arm; hid* double mutant, the reduction in PCD restored an almost wild-type-length cuticle, while in the *wg; hid* double mutant, the increase in cell number was not reflected in an increase in cuticle length. The reason for this remains mysterious. One possible explanation for this discrepancy is the difference in the degree to which Wg signal is compromised in the two situations and the embryonic stage at which this disruption occurs. In the *wg* null, Wg signaling is totally eliminated from the beginning of development. In contrast, perdurance of maternal Arm substantially rescues early defects in Wg signaling in *arm* zygotic nulls (Klingensmith *et al.* 1989). *arm* mutants remain more normal in morphology than *wg* mutants through the onset of germband retraction and retain remnant denticle diversity. Thus when one eliminates PCD in an *arm* mutant a more normal pattern is restored. The difference in amount and timing of Wg signaling in the two backgrounds may also explain why *arm* mutants are affected by smaller alterations in Hid level. The remaining Wg signaling in an *arm* zygotic mutant may promote cell survival to some extent, meaning that a smaller reduction in Hid activity prevents ectopic PCD.

We were also surprised that reduction in cell death alleviated *arm*'s dorsal closure defect. We previously suspected that this defect was due solely to Arm's role as a catenin. However, recent data suggest that dorsal closure is promoted by Wg signaling (McEwen *et al.* 2000). We now suspect that defects in Wg signaling and catenin function combine to block dorsal closure in *arm* mutants. Restoring either rescues the *arm* dorsal closure defect. However, blocking PCD alone should not restore Wg signaling or catenin function. Perhaps the excess cell death in the head region or in the amnioserosa of an *arm* mutant contribute to its dorsal closure defect.

Presenilins and Arm function: While evaluating the effectiveness of our screen, we tested a variety of candidate genes, including some that mapped within noninteracting Deficiencies. Heterozygosity for one of these, *Dpresenilin*, strongly suppressed *arm*. Presenilins form a family of multipass transmembrane proteins that were first identified because missense mutations in two human Presenilins cause early onset familial Alzheimer disease (FAD; reviewed in Haass and De Strooper 1999; Nishimura *et al.* 1999b). The cell biological function of Presenilins and how dysfunction contributes to disease remain controversial. Genetic data in *Caenorhabditis elegans* and Drosophila implicate Presenilins in the function of Notch proteins, most likely via effects on protein processing. Likewise, human Presenilin mutations affect proteolytic processing of the plaque protein Aβ; this may lead to pathology (reviewed in Haass and De Stropper 1999). Recently, it was found that both βcat and other Arm repeat proteins such as δ-catenin associate with Presenilins *in vivo*. The function of this interaction remains confusing. Zhang *et al.* (1998) reported that wild-type Presenilin stabilizes βcat and that this is abrogated by missense mutations found in FAD patients, and Nishimura *et al.* (1999a) reported that *presenilin* missense mutant cells from FAD patients have less nuclear βcat. These data support a role for Presenilins as positive regulators of Wnt signaling via Arm/βcat. In contrast, both Muryama *et al.* (1998) and Kang *et al.* (1999) report that overexpression of wild-type Pre-

senilin destabilizes βcat; Kang *et al.* further show that βcat is stabilized in both *Presenilin1* null fibroblasts or if FAD mutants of *Presenilin1* are overexpressed, while Muryama *et al.* demonstrate that a Wnt-responsive promoter is downregulated by Presenilin overexpression. These data support a conclusion opposite from that above, in which wild-type Presenilins negatively regulate Wnt signaling. Finally, GEORGAKOPOULOS *et al.* (1999) suggest that the presenilin-βcat complex includes cadherins, in contravention of most other data. Our genetic data are most consistent with a model in which Presenilins negatively regulate Wg signaling (Figure 3) either directly or indirectly by binding Arm/βcat or by influencing adherens junction assembly. Clearly much work remains to differentiate between the different possible mechanisms.

We are very grateful to Clare Duffy, Tiernan Mennen, Joel Stein, Dave Roberts, and Christina Tuskey, who helped with the screen, to the Bloomington Drosophila Stock Center for patiently shipping and reshipping stocks, and to D. Curtis for providing the *Dpresenilin* alleles. We thank Susan Whitfield for her assistance with the figures. This work was supported by grants from the National Institutes of Health (NIH) to M.P. (GM-47857) and to R.J.D. (GM-57859). Work in the Duronio lab is also supported by the Cancer Research Fund of the Damon Runyon-Walter Winchell Foundation Award (DRS-10). R.T.C. was supported in part by NIH 5T32 GM-07092, D.G.M. and D.L.M. were supported in part by NIH 5T3 CA-09156 (D.G.M. and D.L.M.), National Research Service Award (NRSA) 1F32 GM19824 (D.G.M.), and NRSA 1F32 GM20019-01 (D.L.M.), and M.P. was supported in part by a Career Development Award from the U.S. Army Breast Cancer Research Program.

LITERATURE CITED

ABBOTT, M. K., and J. A. LENGYEL, 1991 Embryonic head involution and rotation of male terminalia require the Drosophila locus *head involution defective*. Genetics **129:** 783–789.

ABRAMS, J. M., 1999 An emerging blueprint for apoptosis in *Drosophila*. Trends Cell Biol. **9:** 435–440.

BERGMANN, A., J. AGAPITE, K. MCCALL and H. STELLER, 1998 The Drosophila gene hid is a direct molecular target of Ras-dependent survival signaling. Cell **95:** 331–341.

BRAND, A. H., and N. PERRIMON, 1993 Targeted gene expression as a means of altering cell fates and generating dominant phenotypes. Development **118:** 401–415.

CAVALLO, R. A., R. T. COX, M. M. MOLINE, J. ROOSE, G. A. POLEVOY *et al.*, 1998 *Drosophila* TCF and Groucho interact to repress Wingless signaling activity. Nature **395:** 604–608.

COX, R. T., C. KIRKPATRICK and M. PEIFER, 1996 Armadillo is required for adherens junction assembly, cell polarity, and morphogenesis during *Drosophila* embryogenesis. J. Cell Biol. **134:** 133–148.

DICKINSON, M. E., R. KRUMLAUF and A. P. MCMAHON, 1994 Evidence for a mitogenic effect of *Wnt-1* in the developing mammalian central nervous system. Development **120:** 1453–1471.

EDGAR, B. A., and P. H. O'FARRELL, 1989 Genetic control of cell division patterns in the *Drosophila* embryo. Cell **57:** 177–187.

ELDON, E., S. KOOYER, D. D'EVELYN, M. DUMAN, P. LAWINGER *et al.*, 1994 The Drosophila 18 wheeler is required for morphogenesis and has striking similarities to Toll. Development **120:** 885–899.

GALLET, A., A. ERKNER, B. CHARROUX, L. FASANO and S. KERRIDGE, 1998 Trunk-specific modulation of Wingless signaling in *Drosophila* by Teashirt binding to Armadillo. Curr. Biol. **8:** 893–902.

GEORGAKOPOULOS, A., P. MARAMBAUD, S. EFTHIMIOPOULOS, J. SHIOI, W. CUI *et al.*, 1999 Presenilin-1 forms complexes with the cadherin/catenin cell–cell adhesion system and is recruited to intercellular and synaptic contacts. Mol. Cell **4:** 893–902.

GERTLER, F. B., A. R. COMER, J. JUANG, S. M. AHERN, M. J. CLARK *et al.*, 1995 *enabled*, a dosage-sensitive suppressor of mutations in the *Drosophila* Abl tyrosine kinase, encodes an Abl substrate with SH3 domain-binding properties. Genes Dev. **9:** 521–533.

GRABA, Y., K. GIESELER, D. ARAGNOL, P. LAURENTI, M. C. MARIOL *et al.*, 1995 DWnt-4, a novel Drosophila Wnt gene acts downstream of homeotic complex genes in the visceral mesoderm. Development **121:** 209–218.

GREAVES, S., B. SANSON, P. WHITE and J.-P. VINCENT, 1999 A screen for genes interacting with Armadillo, the Drosophila homolog of β-catenin. Genetics **153:** 1753–1766.

GRETHER, M. E., J. M. ABRAMS, J. AGAPITE, K. WHITE and H. STELLER, 1995 The *head involution defective* gene of *Drosophila melanogaster* functions in programmed cell death. Genes Dev. **9:** 1694–1708.

HAASS, C., and B. DE STROOPER, 1999 The presenilins in Alzheimer's disease—proteolysis holds the key. Science **286:** 916–919.

HAINING, W. N., C. CARBOY-NEWCOMB, C. L. WEI and H. STELLER, 1999 The proapoptotic function of Drosophila Hid is conserved in mammalian cells. Proc. Natl. Acad. Sci. USA **96:** 4936–4941.

HAY, B. A., T. WOLFF and G. M. RUBIN, 1994 Expression of baculovirus P35 prevents cell death in *Drosophila*. Development **120:** 2121–2129.

HOSCHUETZKY, H., H. ABERLE and R. KEMLER, 1994 β-catenin mediates the interaction of the cadherin-catenin complex with epidermal growth factor receptor. J. Cell Biol. **127:** 1375–1380.

HUDSON, J. B., S. D. PODOS, K. KEITH, S. L. SIMPSON and E. L. FERGUSON, 1998 The *Drosophila Medea* gene is required downstream of dpp and encodes a functional homolog of human Smad4. Development **125:** 1407–1420.

KANG, D. E., S. SORIANO, M. P. FROSCH, T. COLLINS, S. NARUSE *et al.*, 1999 Presenilin 1 facilitates the constitutive turnover of beta-catenin: differential activity of Alzheimer's disease-linked PS1 mutants in the beta-catenin-signaling pathway. J. Neurosci. **19:** 4229–4237.

KLINGENSMITH, J., E. NOLL and N. PERRIMON, 1989 The segment polarity phenotype of *Drosophila* involves differential tendencies toward transformation and cell death. Dev. Biol. **134:** 130–145.

KURADA, K., and K. WHITE, 1998 Ras promotes cell survival in Drosophila by downregulating hid expression. Cell **95:** 319–329.

LEVESQUE, G., G. YU, M. NISHIMURA, D. M. ZHANG, L. LEVESQUE *et al.*, 1999 Presenilins interact with armadillo proteins including neural-specific plakophilin-related protein and beta-catenin. J. Neurochem. **72:** 999–1008.

LOUREIRO, J., and M. PEIFER, 1998 Roles of Armadillo, a *Drosophila* catenin, during central nervous system development. Curr. Biol. **8:** 622–632.

MAHAJAN-MIKLOS, S., and L. COOLEY, 1994 The villin-like protein encoded by the Drosophila quail gene is required for actin bundle assembly during oogenesis. Cell **78:** 291–301.

MARTIN-BLANCO, E., A. GAMPEL, J. RING, K. VIRDEE, N. KIROV *et al.*, 1998 *puckered* encodes a phosphatase that mediates a feedback loop regulating JNK activity during dorsal closure in *Drosophila*. Genes Dev. **12:** 557–570.

MARTINEZ ARIAS, A., 1985 The development of *fused-* embryos of *Drosophila melanogaster*. J. Embryol. Exp. Morph. **87:** 99–114.

MCEWEN, D. G., R. T. COX and M. PEIFER, 2000 The canonical Wnt and JNK cascades collaborate to promote both dorsal closure and ventral patterning. Development **127** (in press).

MÜLLER, H.-A. J., and E. WIESCHAUS, 1996 *armadillo, bazooka,* and *stardust* are critical for formation of the zonula adherens and maintenance of the polarized blastoderm epithelium in *Drosophila*. J. Cell Biol. **134:** 149–165.

MURAYAMA, M., S. TANAKA, J. PALACINO, O. MURAYAMA, T. HONDA *et al.*, 1998 Direct association of presenilin-1 with beta-catenin. FEBS Lett. **433:** 73–77.

NEUMANN, C. J., and S. M. COHEN, 1996 Distinct mitogenic and cell fate specification functions of wingless in different regions of the wing. Development **122:** 1781–1789.

NISHIMURA, M., G. YU, G. LEVESQUE, D. M. ZHANG, L. RUEL *et al.*, 1999a Presenilin mutations associated with Alzheimer disease cause defective intracellular trafficking of beta-catenin, a component of the presenilin protein complex. Nat. Med. **5:** 164–169.

NISHIMURA, M., G. YU and P. H. ST. GEORGE-HYSLOP, 1999b Biology of presenilins as causative molecules for Alzheimer disease. Clin. Genet. **55:** 219–225.

NÜSSLEIN-VOLHARD, C., and E. WIESCHAUS, 1980 Mutations affect-

ing segment number and polarity in *Drosophila*. Nature **287:** 795–801.

PAZDERA, T. M., P. JANARDHAN and J. S. MINDEN, 1998 Patterned epidermal cell death in wild-type and segment polarity mutant Drosophila embryos. Development **125:** 3427–3436.

PEIFER, M., D. SWEETON, M. CASEY and E. WIESCHAUS, 1994 *wingless* signal and Zeste-white 3 kinase trigger opposing changes in the intracellular distribution of Armadillo. Development **120:** 369–380.

POLAKIS, P., 1999 The oncogenic activation of β-catenin. Curr. Opin. Genet. Dev. **9:** 15–21.

PROVOST, E., and D. L. RIMM, 1999 Controversies at the cytoplasmic face of the cadherin-based adhesion complex. Curr. Opin. Cell Biol. **11:** 567–572.

RAFTERY, L. A., V. TWOMBLY, K. WHARTON and W. M. GELBART, 1995 Genetic screens to identify elements of the decapentaplegic signaling pathway in Drosophila. Genetics **139:** 241–254.

SANSON, B., P. WHITE and J.-P. VINCENT, 1996 Uncoupling cadherin-based adhesion from *wingless* signaling in *Drosophila*. Nature **383:** 627–630.

SCHUPBACH, T., and E. WIESCHAUS, 1989 Female sterile mutations on the second chromosome of *Drosophila melanogaster*. I. Maternal effect mutations. Genetics **121:** 101–117.

SPRADLING, A. C., D. STERN, A. BEATON, E. J. RHEM, T. LAVERTY *et al.*, 1999 The BDGP gene disruption project: single P element insertions mutating 25% of vital *Drosophila* genes. Genetics **153:** 135–177.

SU, T. T., F. SPRENGER, P. J. DIGREGORIO, S. D. CAMPBELL and P. H. O'FARRELL, 1998 Exit from mitosis in Drosophila syncytial embryos requires proteolysis and cyclin degradation, and is associated with localized dephosphorylation. Genes Dev. **12:** 1495–1503.

TAO, Y. S., R. A. EDWARDS, B. TUBB, S. WANG, J. BRYAN *et al.*, 1996 β-catenin associates with the actin-bundling protein fascin in a non-cadherin complex. J. Cell Biol. **134:** 1271–1282.

UEMURA, T., H. ODA, R. KRAUT, S. HATASHI, Y. KATAOKA *et al.*, 1996 Zygotic *D* E-cadherin expression is required for the processes of dynamic epithelial cell rearrangement in the *Drosophila* embryo. Genes Dev. **10:** 659–671.

VUCIC, D., W. J. KAISER and L. K. MILLER, 1998 Inhibitor of apoptosis proteins physically interact with and block apoptosis induced by Drosophila proteins HID and GRIM. Mol. Cell. Biol. **18:** 3300–3309.

WANG, S. L., C. J. HAWKINS, S. J. YOO, H.-A. J. MÜLLER and B. A. HAY, 1999 The *Drosophila* caspase inhibitor DIAP1 is essential for cell survival and is negatively regulated by HID. Cell **98:** 453–463.

WHITE, K., M. E. GRETHER, J. M. ABRAMS, L. YOUNG, K. FARREL *et al.*, 1994 Genetic control of programmed cell death in *Drosophila*. Science **264:** 677–683.

WIESCHAUS, E., and E. NOELL, 1986 Specificity of embryonic lethal mutations in *Drosophila* analyzed in germline clones. Roux's Arch. Dev. Biol. **195:** 63–73.

WIESCHAUS, E., and C. NÜSSLEIN-VOLHARD, 1986 Looking at embryos, pp. 199–228 in *Drosophila, A Practical Approach*, edited by D. B. ROBERTS. IRL Press, Oxford.

YU, G., F. CHEN, G. LEVESQUE, M. NISHIMURA, D. M. ZHANG *et al.*, 1998 The presenilin 1 protein is a component of a high molecular weight intracellular complex that contains beta-catenin. J. Biol. Chem. **273:** 16470–16475.

ZHANG, Z., H. HARTMANN, V. M. DO, D. ABRAMOWSKI, C. STURCHLER-PIERRAT *et al.*, 1998 Destabilization of beta-catenin by mutations in presenilin-1 potentiates neuronal apoptosis. Nature **395:** 698–702.

ZHOU, J., U. LIYANAGE, M. MEDINA, C. HO, A. D. SIMMONS *et al.*, 1997 Presenilin 1 interaction in the brain with a novel member of the Armadillo family. NeuroRep. **8:** 1489–1494.

Communicating editor: K. ANDERSON

APPENDIX A

Refining strongly interacting regions

Interacting deficiencies	Original region	Defining regions	Interaction
Df(2L)sc19-5; Dp(2;1)B19	25A4-5;25D5-7		Strong
Df(2L)sc19-8; Dp(2;1)B19		24C2-8;25C8-9	+Weak
Df(2L)cl-h3		25D2-4;26B2-5	+Weak
Df(2L)tkv2		25D2-4;25D6-E1	—
[a]**Df(2L)spd**	27D-E;28C		Strong
Df(2L)J136-H52		27C2-9;28B3-4	—
[a]**Df(2L) TE29Aa-11**	28E4-7;29B2-C1		Strong
Df(2L)TW137; Dp(2;2) M(2) m[+]	36C2-4;37B9-C1		Strong
Df(2L)H20		36A8-9;36E1-E2	+Weak
Df(2L)M36Fs5; Dp(2;2)M(2)m[+]		36D1-E1;36F1-37A1	+Weak
Df(2L)TW50		36E4-F1;38A67	—
Df(2R)ST1	42B3-5;43E15-18		Strong
Df(2R)cn9		42E;44C	—
Df(2R)PC4	55C1-3;55E2-4		Strong
Df(2R)P34		55E2-4;56C1-11	—
Df(2R)Pc111B		54F6-55A1;55C1-3	—
Df(2R)017	56F5;56F15; + In56D-E;58E-F		Strong
Df(2R)AA21		56F9-17;57D11-12	—
[b]**Df(3L)W10**	75A6-7;75C1-2	75B8;75F1	Strong
[b]**Df(3L)Cat**	75B8;75F1	75A6-7;75C1-2	Strong
Df(3L)Pc-MK	78A2;78C1-5		Strong
Df(3L)Pc		78C1-5;78C9-D3	—
[c]**Df(3R)Scr**	84A1-2;84B1-2		Strong
Df(3R)WIN11		83E1-2;84A4-5	+Weak
Df(3R)CA3		84F2;85A5-7	+Weak
Df(3R)Tpl10, Tp(3;3)Dfd[rv1]		83C1-2;84B1-2	—
Df(3R)MAP2		84A1-2;84A4-5	—
Df(3R)p712	84D4-6;85B6		Strong
Df(3R)D7		843-5;84F1-2	Strong
Df(3R)D1-BX12	91F1-2;92D3-6		Strong
Df(3R)Cha7		91A;91F5	—
C(4)RM	101-104		Strong
Df(4)M62f		101F1-102B	Strong

Boldface, original deficiency.
[a] These two deficiencies fail to complement.
[b] Narrowed each other.
[c] Interaction most likely more distal than original breakpoints.

APPENDIX B

Weakly interacting regions

Weak Interactors	Breakpoints	% supp.
Df(2L)a1	21B8-C1;21C8-D1	4.8
Df(2L)JS32	23C3-5;23D1-2	3.8
Df(2L)sc19-8; Dp(2;1)B19	24C2-8;25C8-9	3.0
Df(2L)N22-3	30A1-2;30D1-2	5.7
Df(2L)prd1.7	33B2-3;34A1-2	3.8
Df(2L)r10	35E1-2;36A6-7	5.4
Df(2L)H20	36A8-9;36E1-2	4.1
Df(2L)TW84	37F5-38A1;39D3-E1	3.8
Df(2R)M41A4	41A	3.6
In(2R)bw[VDe2L] Cy[R]/In(2LR)Gla	41A-B;42A2-3	3.0
Df(2R)vg135	49A-B;49D-E	3.7
Df(2R)Px2	60C5-6;60D9-10	3.1
Df(2R)ES1	60E6-8;60F1-2	3.0
Df(3L)ZN47	64C;65C	3.3
Df(3L)fz-GF3b	70C1-2;70D4-5	4.2
Df(3R)Hu	86A6-B1;86B3-6 + 84D4-5;84F1-2	4.2
Df(3R)crb87-5	95F7;96A17-18	3.6
Df(3R)B81	99C8;100F5	3.5